NUMERICAL AND EXPERIMENTAL INVESTIGATION OF HYDRAULIC TRANSIENT IN A PETROLEUM PIPELINE

BY

MUHAMMAD, Abba Bashir

PhD/SEET/2017/949

A THESIS SUBMITTED TO THE POSTGRADUATE SCHOOL FEDERAL UNIVERSITY OF TECHNOLOGY MINNA, NIGERIA IN PARTIAL FULFILMENT OF THE REQUIREMENTS FOR THE AWARD OF THE DEGREE OF DOCTOR OF PHILOSOPHY (PhD) OF ENGINEERING IN MECHANICAL ENGINEERING (THERMOFLUID AND POWER PLANT ENGINEERING OPTION)

FEBRUARY, 2022

ABSTRACT

Hydraulic transient (HT) is an important phenomenon that leads to unfavourable consequences in pipeline network system because of changes in operational status of flow control components such as pumps or valves. HT leads to the development of pressure surge in the pipeline that also results in damaging the pipeline components or total network failure. The aim of this research is to carry out numerical and experimental investigation of HT in a petroleum pipeline. The pipeline under investigation transports refined petroleum products namely; Automotive Gas Oil (AGO), Dual Purpose Kerosene (DPK) and Premium Motor Spirit (PMS). WANDA simulation software was used to carry out the numerical investigation of the HT in the pipeline and an experimental rig was used to carry out the experimental investigation of the HT in the pipeline. The pressure head and the velocity head of the petroleum pipeline network were analysed. Pressure heads of 0.117034 m, 0.115151 m, and 0.107164 m were recorded at the node just immediately after the pump for AGO, DPK and PMS respectively. This showed that the node just immediately after the pump experiences more load due to weight of the fluids. The research also revealed that the velocity head is high at the node just after the upstream tank and before the pump. The research also revealed that velocity head reduces along the downstream side of the network. The fluid particles at the nodes upstream of the pump require more energy to move down the downstream during steady state flow condition. The pressure surges developed due to sudden valve closure and pump failure were simulated for various calculated valve closure times using the simulation software for AGO, DPK and PMS. The result of the simulation analysis showed that worst case scenarios due to the sudden valve closures are the development of excessively high positive pressure and negative pressure of 1419kPa, - 98kPa (AGO), 1461kPa, -99kPa (DPK) and 1321kPa, -52kPa (DPK) were experienced at the node just before the flow control valve (node F) and the node just before the pump (node B) respectively against an operating pressure of 1034kPa of the nodal sets .In addition, the worst-case scenario experienced for pump failure is drop in pressure below atmospheric and below the vapour pressure of the fluids being transported at nodes just before the pump and the nodes just before and after the non-return valve for all the fluids. Hence, the formation of cavitation and column separation at these nodes. At the end of the research, a safe marginal valve closure rate (MVCR) range of 0.0006m/s to 0.0025m/s was established for a standard pipe of 0.3556 m (14 inches) diameter. In addition, experimental analysis was carried out using a transient test rig to validate the simulated results.

TABLE OF CONTENTS

LIST OF TABLES

LIST OF FIGURES

LIST OF PLATES

ABBREVIATIONS AND SYMBOLS

AGO   Automotive Gas Oil

ASME   American Society of Mechanical Engineers

ANSI   American National Standards Institute

ASTM   American Society of Testing Materials

API   American Petroleum Institute

APST   atmospheric pressure storage tanks

ATK   Aviation Turbine Kerosene

Bbl/d   blue barrel per day

CFD   computational fluid dynamics

DN   Nominal Diameter

DPK   Dual Purpose Kerosene

EFRT   External Floating Roof Tank

FDM   finite difference methods

FEM   finite element methods

H   Hydraulic

HT   Hydraulic Transient

IFRT	Internal Floating Roof Tank
IS	International standard
ISO	International standard organization
Km	kilometre
KPa	kilo Pascal
LPST	low pressure storage tanks
MAOP	Maximum Allowable Operating Pressure
MMSCF/D	Million Standard Cubic Feet Per Day
MOP	Maximum operating pressure
MOC	Method of characteristics
NNPC	Nigerian National Petroleum Company
NPS	Nominal Pipe Size
ODE	ordinary differential equations
PDE	partial differential equations
PMS	Premium Motor Spirit
Psi	pound per inch
RVP	Reid vapour pressure

RANS   Reynolds Average Navier-Stokes

STD   standard

SCADA   Supervisory Control and Data Acquisition

VCT   Valve closure time

WCM   Wave Characteristics Method

1D   Two Dimensions

2D   Two Dimensions

A   Cross sectional area of pipe, (m^2)

a   Acoustic wave speed, (m/s)

D   Pipe diameter, (m)

f   Friction factor

g   gravitational acceleration, (m/s^2)

H   dynamic head

h_f frictional head loss, (m)

K   Bulk Modulus of fluid, (N/m^2)

L   Pipe Length, (m)

N   Speed (rpm)

P	Pressure, (N/m^2)
Q	discharge
Re	Reynolds number R
t	thickness pipe, (m)
T	Temperature, (K)
V	Velocity, (m/

CHAPTER ONE

INTRODUCTION

1.1 Background of the Study

Petroleum, its products, and natural gas are predominantly transported across the globe via pipelines (Rukthong *et al.*, 2016). Transportation of fluids such as petroleum and its products via pipeline is considered as among the safest, surest, effective, and efficient methods of moving fluids from one location to another (Olugboji, 2011; Han *et al.*, 2016; Oluwole & Ojekunle, 2016). As in other countries, pipelines are used in Nigeria for transporting petroleum and its products across all the geographical spaces of the country. A pipeline network comprises of different components such as pumps, pipes, valves, and other nodal sets that are important in the daily operation of the fluid transporting pipelines (Mylapilli, 2015). A change in operational condition of either the pump or the valve will result in the development of an undesirable phenomenon known as hydraulic transient (HT) in the pipeline system (Abuiziah *et al.*, 2014). Change in operational conditions of the pump or the valve simply refers to a condition where the velocity as well as the pressure of the fluid being transported change quickly due to rapid valve closure or opening and pump failure (Mylapilli, 2015; Nerella & Rathnam, 2015 and Gómez, 2018). In addition, these changes in the operational condition are mostly caused by faulty pipeline components, improper actions of pump operators as well as poor maintenance (Twyman, 2018). Kelemen *et al.* (2011) reported that nodal sets are the weakest spots in a pipeline network and they are the most affected parts by HT in a pipeline system. Therefore, it has become imperative for Engineers to investigate the effects of HT on nodal sets. Fluid flow and its control form a vital part of

1

fluid transportation and management of the means of their transportation (pipeline system). Fluid flow and flow management activities such as pumping of fluids, closing of valves as well as the opening of the valves form the routine management schedules of operating a pipeline network system. In addition, abnormalities arising from the management and operation schedules can give birth to HT and this will bring failure and or destruction of the pipeline system. According to Vtorushinaa *et al.* (2017) pipeline system sometimes serves as a source of a larger number of dangers because of the numbers of welded and flanged nodes, control valves, environmental conditions, and the amounts of fluids conveyed by them. Also, transportation of hydrocarbons via pipeline experiences pulsation flow and shock waves, as such is a source of great danger (Vtorushinaa *et al.*, 2017). And the consequences of pipeline failure are pollutions, fire outbreaks and deaths.

HTs are also referred to as transient waves, pressure surges, fast transients, fluid transients, hydraulic hammers, water hammers, or oil hammers in the literature (Duan, 2017). According to a report by Akpan*et al.* (2015), HT can lead to the introduction of air bubbles in pipes, vibrations, valve movements, and slams. If HTs are not checked and attended to through suitable design and implementation, it can lead to serious catastrophic failures (Carlsson, 2016). Conducting HT analysis is of eminent importance. HT analyses are conducted in pipelines to authenticate whether the pipelines are working within the prescribed working pressures and also met the standards set out by the American Petroleum Institute (API), the American Society of Mechanical Engineers (ASME), the American Society of Testing Materials (ASTM) and other regulating agencies (Rodriguez& Pavel, 2016).Subani & Amin, (2015) reported that it is impracticable to get rid of HTs in fluid transporting systems, but its

consequences can be decreased. Therefore, it is very imperative to study the effects of HT as a result of either pump failure or sudden valve closure. The study will also assist in putting in place safer working strategies.

Fluid flow analysis is complex, due to its complexity, computational fluid dynamics (CFD) methods were employed to analyse the fluid flow conditions. Rikstad, (2016) reported that numerical approaches and algorithms are used by CFD to attend to fluid flow problems. One of the finest ways of analysing HT is by modelling and simulation methods. Akpan *et al.* (2015) reported that investigation of HT in pipelines using simulation techniques is a cost-effective and acceptable technique of evaluating HT or pressure surge in fluid pipelines. A simulation technique is a process of evaluating the workings of a system by imitating the performance of the real system under different settings of interest for over short or long periods of real-time employing a similar model or apparatus to get useful information easily (Yin & Mckay, 2018). Computer simulation is adopted when it is unfeasible, very costly or not viable to build a real system (Ashram, n.d).Unlike the analytical method, the simulation method is more steadfast, flexible and convenient in fluid flow and pipeline systems analysis (Abukhousa *et al*., 2014). Simulations are used before a fresh system is built or an old system is altered to meet design specifications, reduce the chances of failure, prevent over or underutilization of resources, optimize system performance and eliminate unforeseen bottlenecks (Olenev, n.d.).

1.2   Statement of the Problem

Fluids transportation pipeline networks are bedevilled by the problems of failures as a result of HT because of sudden valve closure or pump failures ((Twyman, 2018).

Predominantly such failures have devastating effects on the weak points of the pipeline such as nodes, welded points or corroded points. Pipe nodes being one of the weakest points in a pipeline system, they are more prone to the damages due to HT (Kelemen *et al.*, 2011), hence its consideration in this research. Therefore, to guarantee the safety of pipelines, product being transported as well as the workers, there is the need to carry out proper hazard identification and prevention analysis thus requiring a better CFD and experimental techniques.

1.3   Aim and Objectives of the Study

The aim of this research is to carry out numerical and experimental investigation of HT in a petroleum pipeline. The objectives of this research are to:

i.   evaluate pressure and velocity heads at nodes between two reservoirs

ii.   investigate pressure surge effects at pipe nodes due to sudden valve closure

iii.   investigate pressure surge effects at pipe nodes due to pump failure

iv.   experimental validation of simulated results

1.4   Justification

Nodes are one of the weak spots in a pipeline system and HTs are critical phenomena that normally and regularly exist in fluid pipeline systems with inherent devastating consequences.Therefore, it is of paramount importance for the pipeline crew to have a comprehensive knowledge of the capacities of a pipe node design. And most importantly due to the devastating nature of HT on the nodes, its analysis is enormously crucial in evaluating the effects of its magnitudes due to changes in operational status of the flow control devices such as pumps and valves, so as to establish design and maintenance criteria or methods for the pipeline system.

4

1.5   Scope and Limitations

This research is limited to investigating HT developed at the nodes of a low pressure petroleum pipeline transporting refined petroleum products namely; Premium motor spirit (PMS), Dual purpose Kerosene (DPK) and Automotive Gas Oil (AGO) using simulation and experimental techniques.

CHAPTER TWO

2.0   LITERATURE REVIEW

2.1   Hydraulic Transient in a Pipeline

Pipelines are designed for conveying fluids. During the flow of these fluids in the pipeline, change in pressure and velocity do occur. When these changes in pressures and velocities occurred rapidly, it will lead to the occurrence of hydraulic transient(HT). Figure 2.1 depicts graphical presentations of HT at the upstream end of a shut valve. In the Figure, pressure (P) is presented with respect to time (t). Also, the Figure depicts that the initiation of the HT is presented as P_i, the final pressure after the pressure wave oscillations is presented as P_f, the minimum pressure attained during the HT is denoted as P_{min} while P_{max} represents the maximum pressure attained by the fluid during the HT.
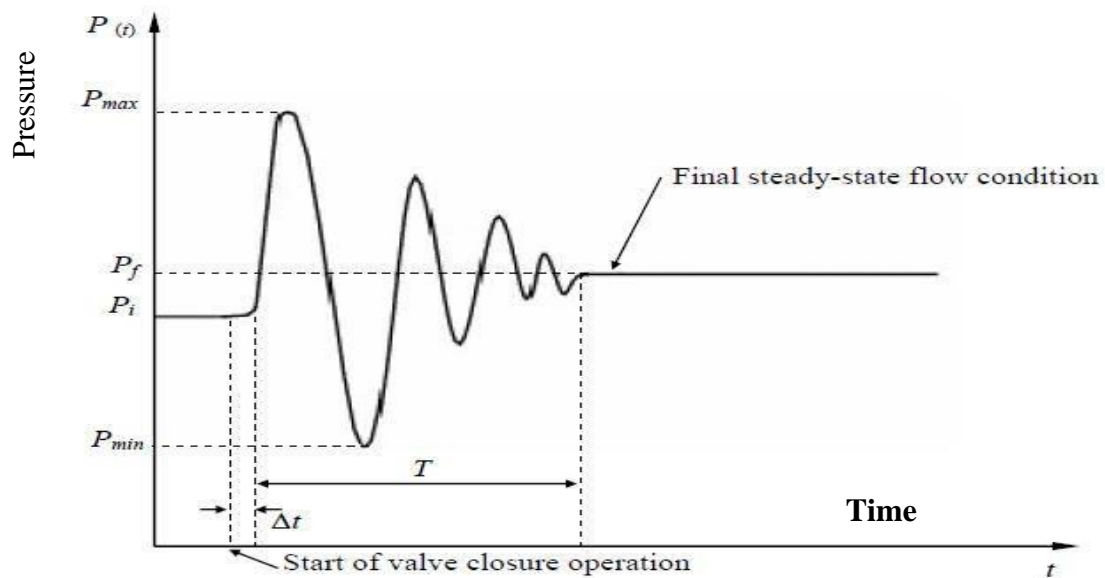
Figure 2.1: Transient state in a fluid pipeline (Shani and Gupta, 2017)

6

In the analysis of the forces acting on a flowing fluid at any time, the nature of the fluid flow must be considered. The steady state energy equation is to be used when analysing a steady state flow condition and the continuity and momentum equations are to be used when the nature of the flow is transient. The study of fluid flow in distribution pipelines include evaluation of the heads (pressure and velocity heads) as well as the discharges that comply with the laws of energy and mass conservations (Ammar, 2014).

2.1.1 Basic factors contributing to pressure transients

Many factors contribute to the occurrence of transient flow conditions across a pipeline network. These factors include pressure and flow control activities, sudden changes in flow, changes in demand (especially in water pipelines) and accidental or planned operational activities (manipulation of valves and pumps) (Rezaei *et al.*, 2015)

2.1.2 Consequences of hydraulic transient

The consequences of the occurrence of HT in a pipeline are the development of excessively high and low pressures in the pipeline system. These consequences can cause significant damages to the pipeline and flow control devices, disruption of fluid flow as well as incur expenses due to the damages, formation of local vacuum conditions that leads to cavitation at specific locations or devices, vibration of pipes or other devices and intrusion of contaminant at nodes and cracks (El-Turki, 2013). In addition, other types of failures that may occur due to HT are bends or elbow movement, joint or node rupture and failures such as buckling and implosions that are caused by excessively low pressures.

HT can lead to serious consequences in petroleum transporting pipeline systems if not correctly checked and addressed via suitable analysis, proper design and safe operational guidelines (Simão *et al.*, 2015).

Pipeline failures due to transients are generally categorized into two; namely:

i. Catastrophic failure: this is a kind of pipeline failure produced by a greater degree of pressure waves due to pump failure or sudden valve closure. This kind of failures mostly comes about in big pipeline.

ii. Fatigue-like failures: This is also a kind of failure that usually occur because of protracted recurring waves of smaller degree of pressure transients (Starczewska *et al.,* 2016).

2.1.3 Maximum pressure in a pipeline system

During transient events, the high pressure surges can cause damages in pipelines network system, tunnels or cause deformations of other equipment as well as cause cracks in internal linings of pipeline (Starczewska *et al*., 2016). Also pressure transients may lead to leakages in hydraulic systems even though no visible damage can be noticed (El-Turki *et al.,* 2013). Given that HT is regarded as an irregular force experienced in the pipeline system, the permissible rise in pressure is usually greater than the design pressure of the pipeline. The maximum allowable transient pressure (MATP) is the maximum gauge pressure permissible in the piping system under abnormal operating conditions; the MATP is not to exceed 110% of the rated maximum allowable operational pressure (MAOP) (Inno-bi solution, n. d). The MATP is sometime referred to as the maximum allowable surge pressure (Inno-bi solution, n. d).

8

2.1.4 Vacuum conditions and cavitations

Cavitation and vacuum formations are undesirable phenomenon that affects the operation and functions of pipeline system components such as pumps and other control devices. Cavitation or vacuum conditions come into being as a result of boiling of the transported fluid due to lowering of the fluid pressure. Boiling bubbles would be created when the pressure pipeline drops to a pressure lower than the fluid's vapour pressure, when these bubbles reach regions of higher pressure; they implode and generate pressure waves that lead to erosion. If cavitation or vacuum phenomenon lasted long, it may lead to serious mechanical failure (Cucit *et al.*, 2018).

2.1.5 Vapour pressure

The pressure and temperature at which a liquid tends to vaporise into its gaseous phase is called the vapour pressure (Satterfield, 2013). The vapour pressures of petroleum products are technically represented as the Reid vapour pressure (RVP) according to ASTM D323-99a. RVP is a critical factor considered in fluid pipeline designs. All petroleum pipelines should sustain their pressures greater than the RVP of the petroleum product they are transporting in order to keep the product in its liquid phase. The RVP of the petroleum products being transported must be constantly monitored (Miriti & Osiemo, 2012). When the internal pressure of a fully filled petroleum pipeline drops to a lower pressure than the RVP of the petroleum product at certain points like nodes or bends, cavitation will occur (Gseaa & Dekam, (2010).

2.1.6 Hydraulic vibrations

Mass oscillation of fluid through pipeline systems leads to the vibrations of the pipelines system. High or strong hydraulic vibrations also cause damages in pipelines and or pipeline system equipment. Prolong moderate pressure surges gradually lead to fatigue failure in pipeline network system. Therefore, the influences of mass oscillations and vibrations due to pressure surges must be taken into account at the design stage so as to evade damages to the pipeline network systems (El-Turki *et al.*, 2013).

2.1.7 Petroleum product quality

HT may affect the quality of petroleum or its product being transported via pipelines and can also result in serious health implications. Collapse or breakage of pipe as well as loosing of nodes or joints can lead to intrusion of dirties and other contaminants into the pipeline system. Negative or vacuum pressure pipelines pose a threat of bringing in contaminants into the pipeline system (Ammar, 2014). Also transients due to low-pressure can cause the adulteration of the transported fluid by the intrusion of contaminates through a leaky nodes or cracks into a pipe (Nnadi *et al.*, 2007).

2.1.8 Hydraulic transients and its causes

HT phenomenon is a flow disturbance that occurs as a result of operational and other unforeseen changes in a fluid flow system. The disturbances come into being because of abrupt changes in the flow and pressure of a moving fluid and the disturbance propagates as pressure waves that travel in the fluid medium at a speed of sound (Barros *et al.*, 2014). The fluid's compressibility and pipe's elasticity are determining factors of the speed (Jaya & Kolmetz, 2014). In a fluid flow system, some operational events like

10

pump start up or shutdown, sudden valve closure and opening, changes in the demand conditions can cause variation in transmission conditions. Twyman, (2018) reported that HTs are also caused by the actions of the pipeline operator, poorly selected pipeline components, mechanical failures as a result of poor maintenance or an external action.

2.1.9 Nigerian petroleum pipeline network

Nigeria is a leading producer of oil in Africa and occupies a top position in oil production globally. Oil is the backbone Nigeria's economy (Okoli & Orinya, 2013). Multi-product pipelines are used in transporting refined petroleum products to various depots and pump stations in Nigeria (Okoli & Orinya, 2013). The National Nigerian Petroleum Company (NNPC) has the largest pipeline network in Nigeria, about 5120 km interconnecting the refineries (located at Port-Harcourt, Kaduna, and Warri) with the 22 storage depots and as well connecting the jetties at Alas Cove, Okirika, Calabar, Escravos and Bonny. This is made up of 4315 km and 666 km of pipelines for refined products and crude oils respectively (Oyinloye *et al.*, 2017). Figure 2.2, shows a pictorial view of petroleum pipelines network across Nigeria.
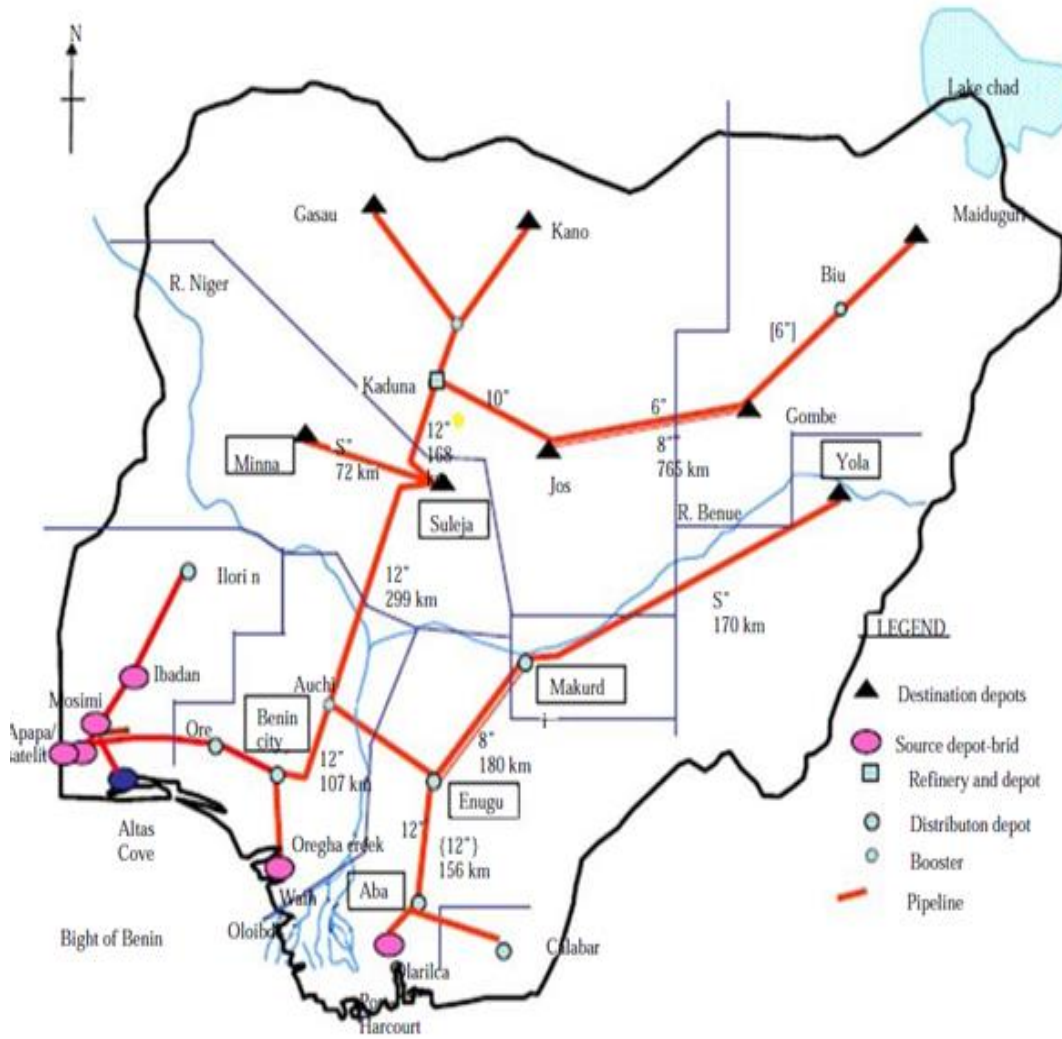
Figure 2.2: Nigerian petroleum pipeline network (Sani *et al.*, 2016)

The storage infrastructure at the 22 storage and loading depots are spread across the country. And they have a capacity of 1,266,890 (PMS), 1,007,90 (AGO); 676,400 (DPK) and 74,000 Aviation Turbine Kerosene (ATK) metric tonnes respectively and are linked by pipelines of different diameter ranges. Table 2.1 shows the areas covered by the pipeline network system in Nigeria.

Table 2.1: The petroleum pipeline distribution system in Nigeria

S/No.	System	Location
1.	System 2A	Warri-Benin-Ore-Mosimi
2.	System 2AX	Auchi-Benin
3.	System 2B	Atlas Cove- Mosimi-Ibadan-Ilori, Mosimi-Satelite (Eigbo in Lagos) and Mosimi-Ikeja
4.	System 2C	Excravos- Warri-Kaduna (Crude Lines)
5.	System 2D	Kaduna/Zaria-Kano-Zaria-Gusau and Kaduna-Jos-Gombe-Maiduguri
6.	System 2E	Port Harcourt- Aba-Enugu-Makurdi
7.	System 2EX	Port Harcourt- Aba-Enugu-Makurdi-Yola
8.	System 2CX	Enugu-Auchi, Auchi-Suleja-Kaduna, Suleja-Minna
9.	System 2DX	Jos-Gombe

(**Source:** Adeyemi, 2020)

In Nigeria, crude petroleum, refined petroleum products and gas are predominantly transported via pipelines. Nigerian petroleum pipeline networks are bedevilled by lots of challenges/problems such as oil spillage as a result of pipeline damage or rupture. According to reports by Aroh *et al.* (2010) and Achebe *et al.* (2012) the major causes of oil spill includes operational human error, human and natural hazards, pressure surges, structural and machine failures, ageing, welding defects and sabotage. The rates of petroleum pipeline failures or ruptures in Nigeria are high when compared with other developed nations. Records of NNPC have showed that in 2007 more than twenty (20) cases of petroleum pipeline failures were recorded. The rate of failure had grown to more than thirty (30) in the year 2008 due to different causes (Achebe *et al.*, 2012).

According to a report by Nnadi *et al*. (2007) many of the pipeline failures are caused by accidents that happen as a result of mechanical failure (pressure surge, welding defects and vibrations). The mechanical failure constitutes about 42%, corrosion constitutes 18%, third party activity constitutes (vandalism) 24% while operational error and natural hazards such as flooding constitutes 10% and 6% respectively.

Also, according to a report by Dawotola, (2012) about 73% of Nigerian petroleum pipelines are older than 20 years and about 41% of the total network length were over 30 years, and the reliability rating of pipelines are 46% and 21% for pipes having service life of less than 20 years and above 30 years respectively. Every fluid-transporting pipeline network has its own special characteristic that makes it different from other networks. Rukthong *et al.* (2016) reported that due to varying geographical and geological characteristics, the transportation profile might differ from one petroleum product to another. Therefore, it is important to study the nature and behaviour of different pipeline networks under varying working conditions to identify the nature and severity of the destruction due to HT, so as to design and maintain fluid pipelines working properly.

2.1.10 Hydraulic transient analysis governing equations

The transient nature of flow in a pipe is described numerically by continuity and momentum equations (Partial differential equations (PDE), this is because the velocity and pressure in transient flow depends on time and distance. Governing equations for the transient flows were obtained from mass and energy conservation laws. These governing equations are the continuity and momentum equations and are they are one

14

dimensional incompressible fluid flow analysis equations (Carvajal & Bohorquez, 2018, Ammar, 2014).

2.1.11 Hydraulic transient analysis methods

Different methods are used in the analysis of HT, the methods ranges from numerical, experimental and analytical methods (Elbashir *et al.*, 2007; Muhammad *et al.*, 2019). There are different numerical methods employed in resolving the governing equations. These methods comprises of method of characteristics (MOC), wave characteristics method (WCM), finite difference method (FDM), and finite element methods (FEM) (Carlsson, 2016 and Malppan & Sumam, 2015). According to Larock *et al.* (2000) the condition under which HT analysis can be performed can be further grouped as rigid column methods (RCM) or elastic method. Also Muhammad*et al*. (2019) reported that there are other means of analysing the sets of the PDE in HT analysis in a pipeline. These are further divided into graphical (Salmanzadeh, 2013), analytical (Lebele-alawa & Oparadike, (2015) and experimental methods (Simão *et al.*, (2014). Traditional HT models typically fall within the time domain analysis spectrum and rely on unidirectional analysis. These models are two quasi-linear hyperbolic PDEs (dynamic and continuity equations). The numerical solutions to these equations generally fall into MOC, WCM, FDM and FEM (Radulj, 2010).

2.1.12 Elastic method

Elastic method is a process of solving HTs that involves PDEs. The process includes calculating the acoustic wave pressure. Also, rapid changes in velocity and pressure, the pipe's elasticity and compressibility are all considered and included in the analysis (Abuiziah *et al.*, 2013).

2.1.13 Rigid column method (RCM)

Rigid column theory is a surge analysis process that usually includes numerical or mathematical solution of simple a PDE. In transient analysis using RCM, the fluids properties such as the compressibility as well as the elasticity of the conduit are all neglected and also the entire fluid's column is considered to move as a rigid body (Abuiziah *et al.*, 2013). RCM is used in the wave plan method. In RCM, the effects of frictions between the fluid and the pipeline wall are not considered in calculating the variations in pressure as well as the flow rate because of HT and this might not produce the correct results.

2.1.14 Method of characteristics (MOC)

MOC is the most outstanding and commonly employed numerical approach used for one dimensional (1D) analysis for HT in fluid pipelines (Delgado, 2013). Bhattarai *et al.* (2019)reported that MOC is good, especially for capturing the location of steep wave fronts (for a constant wave speed). MOC gives a simpler numerical treatment to the PDEs that were used for modelling the HT in pipes. Its power lies in its capability of converting the two PDEs of continuity and momentum equations into four ODEs that can be solved numerically by using FDM. The equations are expressed in infinite difference form, using time steps intervals and then the resolutions are done with computers (Abuiziah *et al.*, 2014; Carmona-Paredes, *et al.*, 2019; Wood, 2011). MOC are used to investigate HT in pipelines with varying pipe properties such as different diameters, with and without booster stations, valves (throttling, relief) and surge control devices (Carmona-Paredes *et al.*, 2019).

2.1.15 Finite difference methods (FDM)

FDM is a method used to analyze HT (Rathore *et al.*, 2015). In general, FDMs are broadly categorised into explicit and implicit schemes (Lee, 2015). The explicit schemes are easy to program and solve but have a problem of numerical stability that needs the use of small time steps. While, the implicit methods are generally numerically stable that permits the use of larger time steps, but these are achieved at a high computational cost (El-Turki, 2013). In this method, ODEs are replaced by approximations known as finite difference approximations, where known parameters at the commencement of the time intervals are expressed as functions of unknown quantities at the termination of the time intervals. If errors linked with the numerical approximation are bounded in time, then the method is considered to be numerically steady but the method is called unstable and the results obtained from unstable scheme is not accurate and are meaningless when there is exponential increase in error (El-Turki, 2013). One of the short coming of FDM is that there are non-linear variables in the governing equations, as such significant computing times are required for the iterative techniques (Nerella & Rathnam, 2015).

2.1.16 Wave plan method (WPM)

WPM is like MOC because both methods clearly combine wave lane in the resolution process. It is based on rigid column theory. A fine discretisation is required for this method to achieve accurate solutions (Ghidaoui*et al.,* 2005). Rigid column theory is a process of HT analysis which usually includes solving ODEs mathematically or numerically. In this method, fluid's compressibility and the pipe's elasticity are ignored. In wave plan method, the effects of friction are not taken into consideration while

calculating flow rate variations and pressure and this in turn might affect the actual result (Nerella & Rathnam, 2015).

2.1.17 Graphical method

Graphical method is one of the methods used for solving water-hammer problems. It is first of the transient analysis methods where friction conditions are incorporated into the PDEs. The process is also used to determine flow situations at any point in the pipeline. This technique solves HT problems assuming quasi-steady friction model and a correction term that takes care of the dynamic effects. Despite the fact that the method is fast in producing results, the accuracy of the results obtained from this method is low for later stages of HT except for the first wave period (Shani & Gupta, 2017).

2.1.18 Finite element method (FEM)

FEM is a technique used to solve PDEs numerically. It is important for at least two reasons. First, FEM is able to solve PDEs on almost any arbitrarily shaped region. Second, the method is well suited for use on a large class of PDEs. While it is almost always possible to conceive better methods for a specific PDE on a specific region, the FEM performs quite well for a large class of PDEs. In summary, FEM is important since it can deal with arbitrarily shaped regions and a large class of PDEs. One of the shortcomings of FEM is that large amount of data is required as input for the meshing in terms of nodal connectivity depending on the problem at hand (Ques10, n. d).

2.1.19 Simulation software

In this research work, commercial software known as WANDA simulation software was used in carrying out the simulation of the flows of PMS, DPK and AGO in a

pipelines system. WANDA simulation software is among the excellent software used in the study of fluid flow and heat transfer in pipeline systems (Jalut & Ikheneifer, 2010). WANDA is made up of three different modules of control, engineering and transient. Experimental data are usually used to validate various components of WANDA for reliability (Tukker, 2012). WANDA Transient simulation software is a product of Deltares of Netherlands. WANDA was formulated for the design, analysis and optimization of hydraulic systems such as hydrocarbon and water transportation pipelines. WANDA is equipped with a user-friendly interface that makes the user carry out hydraulic simulation and analysis with ease and efficiently. There are two modes in which WANDA can be operated; these are the steady state and the transient modes.

2.1.20 WANDA steady state mode

This mode is used for the design and analysis of pipeline system working under steady state condition of flow. This is the mode in which only steady state (constant time and all other variables are constant) calculations were done in the WANDA software. Incompressible fluids are handled in the steady state and transient flow condition modes. WANDA steady state mode was developed to analyse most common actions in the design of hydraulic piping systems. Some of the capabilities of WANDA engineering mode are:

  i.   Design of hydraulic networks using different types of available hydraulic components.

  ii. Fast design using flow-specifying components (valves and pumps.). Calculating losses, pump speeds, valve positions as well as balancing fluid flow and pressure.

  iii. Design of reliable hydraulic systems using customised components parameters.

iv. Evaluation of pipe parameters such as pipe diameters, discharge, flow velocities and hydraulic gradients.

v. Calculation of the system characteristics that assist in pump selection.

vi. Calculation of pumping efficiency and energy consumption in pumping station

2.1.21 WANDA transient mode

The transient mode: this mode is used to carry out the design and analysis of pipeline system operated under transient flow condition (WANDA 4.2, 2013). The WANDA transient mode is used for the analysis and investigations of unsteady flow conditions. WANDA transient mode is used for computing different kinds of transients (unsteady) phenomena and cavitation. Transition from steady to unsteady states involves changes in behaviour of the pipeline components. WANDA transient mode is used for calculating water hammer and other fluid flow problems such as cavitation and column separations. In the transient mode, the hydraulic fluids in the pipes are considered as incompressible that results in an infinite wave speed.

2.1.22 General petroleum pipeline design considerations

Pharris & Kolpa (2007) reported that the essential pipeline performance goals and engineering design factors are the main steps considered in the design as well as operation of petroleum pipelines and the components involved in the design of pipeline system are as follows;

i. The petroleum products throughput required (usually volume per unit time),

ii. The distance the petroleum product will travel,

iii. The product's properties like density, viscosity and compressibility.

20

iv.   The topographical nature of the pipeline route,

v.   The operational pressure and the maximum permissible operating pressure of the network,

vi.   Required diameter of the pipes, yield strengths and wall thickness,

vii.   Number of pump stations required and the distance between them, and

viii.   The power rating of the pump station.

2.1.23 Maximum allowable operating pressure (MAOP)

MAOP is the peak pressure at which pipelines are certified to operate. The MAOP is less than the design pressure of the pipeline. MAOP are set up by regulatory bodies that supply pipes, compressed gas pressure vessels and storage tanks. Barlow's formula is used for determining the value of MAOP of a pipeline. This takes into account the pipe wall thickness, pipe diameter, allowable stress and safety factor(Chandra & Dutta, 2014).

2.1.24 Pipelines

Steel pipes are predominantly used in most pipelines in the transportation of petroleum products. The pipes are produced according to international standard organisation (ISO) specifications. Petroleum pipelines can be small or large in diameter; some are short while others are long up to 1,500 km or more. Some of the pipeline networks are simple while others are complex in nature (Miriti & Osiemo, 2012).

2.1.24.1   *Pipelines network elements*

Pipeline network is made up of many elements that are interconnected together to form the system. These elements are; storage tanks, pipes, valves, pumps and nodal sets.

2.1.24.2 *Storage tanks*

Storage tanks are usually used for storing different types of fluid. Hydrocarbons are generally stored in tanks that are made of steel. Storage tanks are produced in conformity with American Petroleum Institute API 650, API 620 and IS 803 standards as well as the guidelines of the Department of Petroleum Resources (DPR) (Agho *et al.*, 2017). According to a report by Samanody & Noaman, (2017) the operational pressure of the greater part of tanks is atmospheric and based on API 620 standard the maximum allowable pressure (MAP) for hydrocarbon storage tanks is 15 psi. Selection of the type of tank to be used usually depends on the product to be handled and ambient conditions. Singh *et al.* (2012) reported that storage tanks are categorised into low-pressure storage tanks (LPST) and atmospheric pressure storage tanks (APST).

2.1.24.3 *Low pressure storage tanks (LPST)*

LPST are the type of tanks that operates at pressures in its gas or vapour spaces greater than those allowed in API STD 650. These types of tanks are designed according to API 620 standards. LPST are sub-divided into three categories:

i. External Floating Roof Tank (EFRT)
ii. Fixed Roof Tank
iii. Internal Floating Roof Tank (IFRT)

2.1.24.4 *Atmospheric pressure storage tanks (APST)*

APST are the types of storage tanks designed according to API 650 standards or its equivalents. These types of tanks are designed to operate in the gas and vapour spaces

of the stored fluid at an internal pressure almost equal to atmospheric pressure. APST are sub-divided into two categories:

i.   Atmospheric storage tanks with open vent to atmosphere

ii.   Atmospheric storage tanks with blanketing facilities

2.1.24.5   *Pipes*

Pipes are structural members used in transporting fluid and are characterized by some parameters such as diameter, mass flow rates, length, roughness coefficient as well as velocity (Dawidowicz, 2018). Pipes are conduits used in many industrial and domestic applications such as in conveyance of portable water, transportation of crude oil, refined petroleum products, gasses and other types of fluids (Hirani & Kiran, 2013). Pipes used for the transportation of fluids are usually of circular cross-section as shown in Plate I. There are different types of line pipes used in the petroleum industry. Steel pipes are the commonly used types of pipe in pipeline networks for conveying hydrocarbons. These pipelines are produced according to standard specifications set out by API as stipulated by ISO 3183 (Nnadi *et al.*, 2007 and Kiefner & Rosenfeld, 2012). API spells out pipes specifications in conjunction with the ASME, ASTM and ANSI. These specifications are created in order to offer standards suitable for transporting fluids of different nature (Egbe *et al.*, 2017). The most popular API specification in use in the area of petroleum transportation is the API 5L.

It includes both welded as well as seamless steel pipes suitable in transporting fluids (petroleum and its products, gas and water). Grades under this specification are A25, A, B, X42, X46, X52, X56, X60, X65, X70 and X80. A25 pipes have minimum yield strength of 25,000 pounds per square inch (psi), A30 line pipes have minimum yield

strength of 30,000 psi while Grade B line pipes have a minimum yield strength of 35,000 psi. For the other categories of grades used in offshore and high-pressure oil and gas pipelines, the two digits in thousands of psi indicate their minimum yield strengths.

Plate I: Circular carbon steel pipes (Tycoon, n. d)

Hydrocarbon pipelines are categorised into three main types (Economides & Kappos, n.d.)

i.   Flow lines

ii.   Trunk lines

iii. Finished product pipelines

2.1.24.6   *Flow lines*

These are type of pipeline networks used for crude gathering in the production areas by moving crude oil from wells to collation (central storage point) storage and treatment

centres. Generally, these types of pipelines are small in diameter (2 and 4 inches) and also operate at a low pressure (below 100 psi) (Pharris & Kolpa, 2007).

2.1.24.7 *Petroleum trunk lines*

Trunk lines are used for moving crude petroleum products from storage reservoirs to another reservoir over a long distance or to refineries. The operational pressures of trunk lines are higher than the operational pressures of flow lines. The pipes diameter varies in size; it ranges from 6 inches to as big as 4 feet (Pharris & Kolpa, 2007, Egbe *et al.*, 2017).

2.1.24.8 *Product pipelines*

Product pipelines are used to transport refined petroleum products at their liquid phase at ambient temperatures. Such pipelines are operated at pressures that are not excessively high in order to keep the petroleum product in its liquid state. But petroleum products that vaporise at ambient temperature are transported at higher pressures. The diameter of refined petroleum product pipelines are usually from 12 to 24 inches (Pharris & Kolpa, 2007). Product pipelines are in general used for transporting a range of petroleum products all together in a batch manner. Petroleum products that are chemically stable when mixed with one another but having different physical properties with one another were always transported together. Mode of operation of the pipeline allows for reducing the interface between the products. The mixtures of two products are separated from one another at the terminals. Such mixtures are handled as products of lower quality compared to the original petroleum products (Pharris & Kolpa, 2007). The distribution pipes used for the transportation of petroleum products operates at low pressures of 200 psi (1379 kPa) to high pressure of 1200 psi (8,273 kPa) (Natgas, 2013).

According to the Nigerian law of oil pipeline of 1990, API 5L Grade B and ASTM A 106 Grade B are the most recommended class of pipes to be used for a range of low pressure high working pressure or pipelines with large diameter as specified by DPR (DPR, 2007). The Maximum allowable operating pressure of carbon steel grade B pipes - ASTM A53M, A106M, API 5L, Seamless (355.6 mm ID and 16mm thick) operating at a temperature range of -23 to $+38$ is 4,400 kPa (Pearson, 2021).

2.1.24.9   *Valves*

Valves are protective mechanisms used to control the flow of fluid by closing, opening or partially obstructing flow passageways (Woodford, 2020).   Among the main functions of valves are starting and stopping the flow of fluid, reducing the amount of fluid flow, regulating process pressure as well as relieving piping over pressure (Twyman, 2018).   Valves are commonly used in everyday life as a protective device during normal as well as emergency operations (Bhatia, n.d.-a). Valves are of different design, they are technically considered pipe fittings in pipeline networks, and each of the different valve designs has its own merits and demerits (Lebele-alawa & Oparadike, 2015).   There are different types of valves available made from different materials with variety of shapes, styles, sizes and connections.

Valves are selected based on the primary task they are to accomplish, the service conditions as well as the characteristics of load to be applied to it (Bhatia, n.d-a).

2.1.24.10   *General classification of valves*

Valves are generally defined by their stalk which moves to stop, allow or throttle the fluid's flow. Based on the movement of the stem, valves are classified into rotary motion valves and quarter turn valves (Twyman, 2018).

2.1.24.11   *Linear motion valves*

These are types of valves characterized by the linear movement of their stem in order to stop, allow or throttle the flow of fluid; such valves includes gate and globe valves (Twyman, 2018).

2.1.24.12   *Rotary motion valves*

These are classes of valves characterized by the angular or circular path movement of their stem. Butterfly and ball valves are the types of valves that fall under this class (Kolmetz *et al.*, 2020).

2.1.24.13   *Quarter turn valves*

Quarter turn valves are types of valves that their stems requires approximately about a quarter turn ($0°$ through $90°$) to completely close from a completely opened position. example of such valves are butterfly and ball valves (Beckman *et al.*, 2009).

2.1.24.14   *Basic types of valve*

The common types of valves utilised in pipeline networks are; (Bhatia, n.d-a).

   i.   Gate valve

  ii.   Ball valves

iii.   Butterfly valves

iv.   Globe valves

v.   Check Valve

2.1.24.15   *Gate valve*

Gate valves are type of valves that use linear stem movement for the closing and opening. They use wedge or parallel shaped discs for the closure so as to provide tight sealing as shown in Figure 2.3. Gate valves are suitable for air, non-condensing gases, steam, heavy liquids, abrasive, corrosive liquids, oil and gas. Their available sizes range from as small as 2 inches up to more than 100 inches. Gate valves used in low pressure petroleum pipelines are rated at 150 psi (1,034 kPa) and they correspond to standard ASME 125/150 bolting pattern configurations. Gate valves have advantages of high capacity, low cost and tight shutoff (Sutton, 2017).
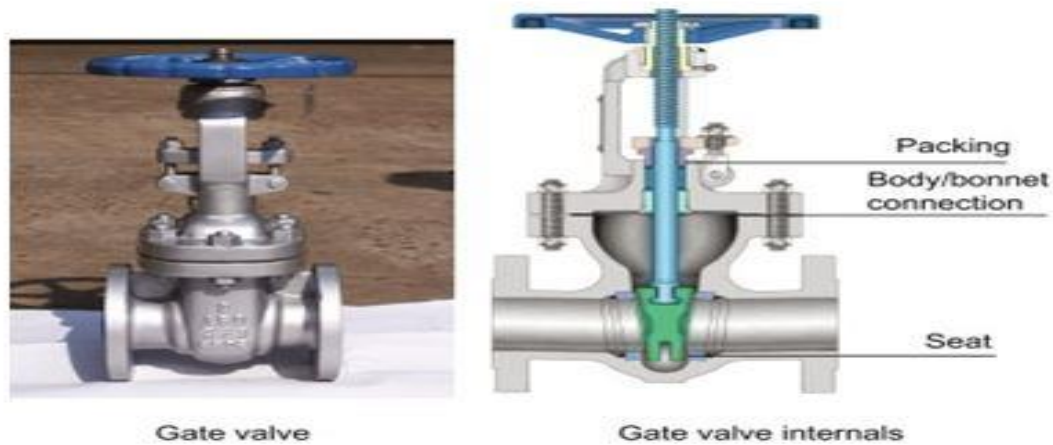
Figure 2.3: Gate valve and its sectional view (Stewart, 2016)

2.1.24.16 *Butterfly valves*

Butterfly valves are type of control valves that has a circular disc having the same diameter with the valve's internal diameter. The disc is used for opening and closing the fluid flow passages; the disc is rotated to either open or close the fluid passage as shown in Figure 2.4 (Pullinger, 2011).
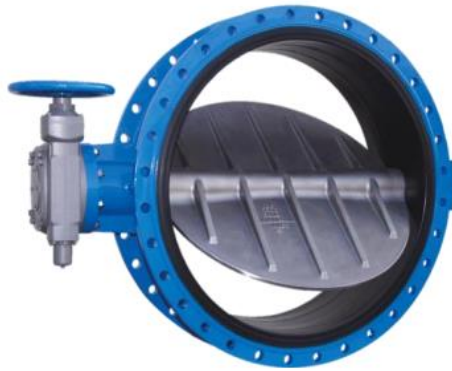
Figure 2.4: Butterfly valve (Nikodijević *et al.*, 2018)

2.1.24.17 *Ball valve*

Ball valve also known as spherical valve, it consists of a spherical plug that has a passage diameter equal to the pipe diameter as shown in Figure 2.5. When in open position, the passage will be in line with the conduit and by turning the sphere to a 90°, the passage will be eliminated (closed) as shown in Figure 2.5. Ball valves are largely used for fluid shutoff in both onshore and offshore as well as the upstream sector of oil and gas production facilities (Stewart, 2016).

Figure 2.5: Ball valves (Stewart, 2016)

2.1.24.18   *Check valve*

The check valve is one of the vital components of a hydraulic system. Check valve restricts fluid's flow in only one direction and stop reverse flow. Check valves are also installed in pipeline systems in order to control the HT produced by pump failure (Himr *et al.*, 2017). Figure 2.6 shows a typical type of swing check valve.
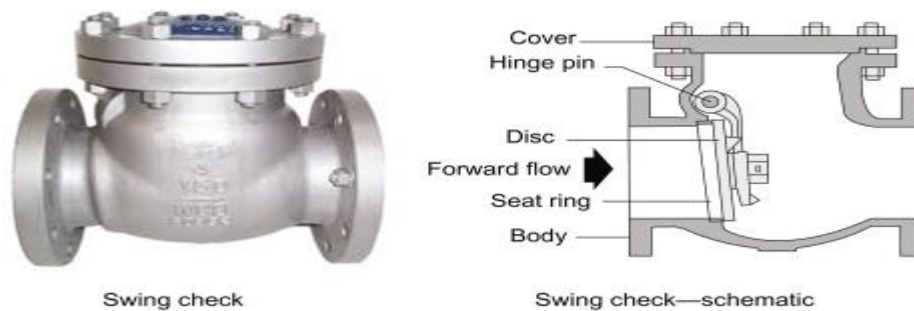
Figure 2.6: Swing check valves (Barker, 2018)

2.1.24.19   *Flanges*

Flanges are commonly employed to provide a strong non-permanent joint without permanently welding the pipe sections together as shown in Figure 2.7. It is used to

connect pipe, pumps, valves and or tanks in a pipeline network and it is found both at the inlet and the outlet of valves, pumps, flow meters, safety devices and other fittings of steel pipes. Flanges are used in conjunction with gaskets and seals (Jones *et al.*, 2017). According to the pressure ratings for ASME B16.5 NPS 1/2 flanges are classified according to pressure classes, this classes includes class 150, 300, 400, 600, 900, 1,500 and 2,500 (B16.5, 2013). According to ASME B16.5 the 150 class flanges have pressure rating of 230 psi (1586 kPa gauge) (Bhatia, n.d.).
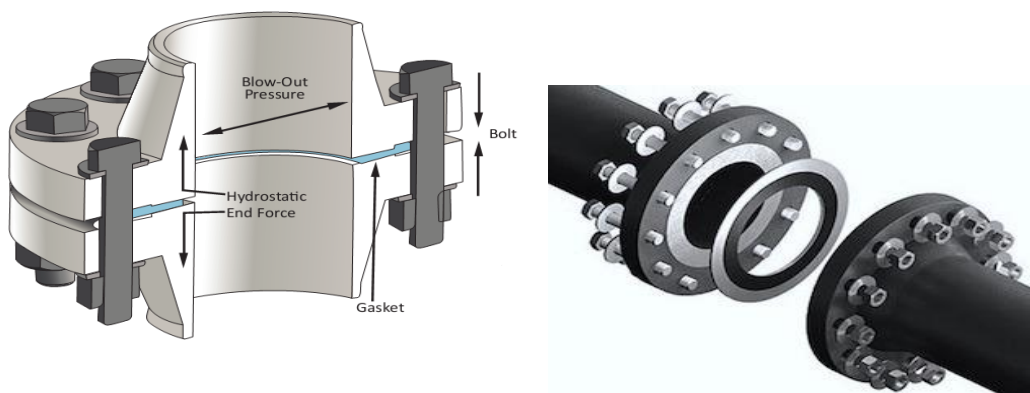
Figure 2.7: Flange connection and flange connection section (Metallic-steel, 2018)

2.1.24.20   *Gaskets*

A gasket is a compressible material made from engineering material or blend of materials which when tightened between two stationary members such as flanges, it will eliminate leakages (Aibada *et al.*, 2017). Gaskets are conventionally employed to provide seal between flanged nodes (Jones *et al.*, 2017). ASME grouped gaskets into two, these are metallic gaskets (for example spiral wound) and non-metallic gaskets (Jones *et al.*, 2017). The choice of a gasket and gasket material must be done by taking into consideration that it can withstand the pressure applied to the gasket, the type of fluid in use and the working temperature of the fluid (Aibada *et al.*, 2017). Four

different types of pressures are considered in gasket selection in flanged applications, and these pressures are the system design, working, hydro test and operating pressures respectively (Jones *et al.*, 2017). Spiral wound gaskets are the type of gaskets used in petroleum pipelines transporting refined petroleum products. Figure 2.8 depicts a typical type of spiral wound gasket.

Figure 2.8: Spiral wound gasket (Gambit-Group, n. d).

2.1.24.21   *Pumps*

Pump is a mechanical device that supply energy to a fluid to move; it increases the kinetic or pressure energy of a fluid (Rajput, 2013). Pumps are basically classified as rotodynamic and positive displacement pumps (centrifugal pump is the most common type of rotodynamic pump in use) (Moran, 2016). Figure 2.9 shows a centrifugal pump. Positive displacement pumps are made up of reciprocating and rotary types of pumps (Kothandaraman & Rudramoorthy, 2007).
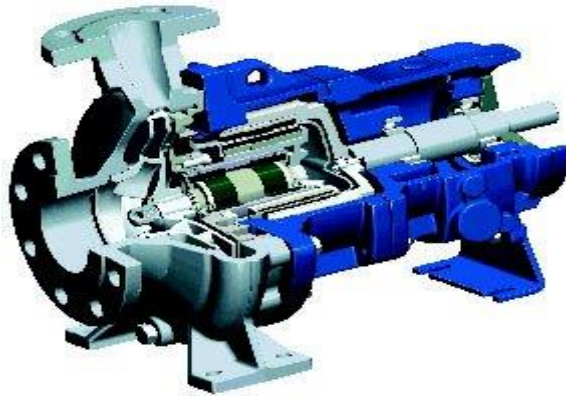
Figure 2.9: A centrifugal pump (James, 2012)

2.1.24.22 *Leakages in pipelines*

There are many connections, nodes and valves in a pipeline system between the pipes and the tanks. These connection nodes and valves are supposed to be air tight in order to avoid leakages. Leakage is a common phenomena that occur in pipelines due to HT as a result of human operational errors, third parties interference, damages because of sudden pressure changes, geological disasters like earthquake, human errors during operation, faulty workmanship and or destructions caused by fatigue in pipes (Sousa & Romero, 2017). Therefore, there is the need to study and investigate the vulnerability of nodes in the pipeline network and the effects of HT on these nodes.

2.2   Brief Review of Hydraulic Transient Analysis

The study of HT phenomena in simple and complex pipeline networks has been an area of investigation and research for long. Many investigators and scholars have undertaken researches and studies on HT phenomenon using different methods. These methods range from analytical to numerical methods as well as experimental methods (Elbashir *et al*., 2007). The review of some of the researches and studies conducted by different scholars are presented as follows.

33

Maryono *et al.* (2013) conducted a study on experimental investigation of water hammer in a micro hydropower turbine in order to find means of minimizing the effects of HT in a water distribution network. A laboratory scale test rig was used in the studies; a camera and a manometer were used to observe the changes in pressure within the pipeline as a result of variations in valve closure times (VCTs). The VCTs were varied gradually during the experiment from 1 second until it reached 10 seconds. The study revealed the lesser the valve closure rate, the higher the pressure surge, According to the study, highest pressure occurred at VCTs of 1, 2 and 3 seconds. For a VCT of 10 seconds, the peak pressure decreased by 68.3% at a point just before the turbine (point A), while point B (a point 25 cm before point A) recorded a decrease of 75.6% and point C (a point 25 cm away from point B) and point D (a point 50 cm away from point B) recorded 60 and 60.3% respectively. The study revealed that camera scheme is excellent in capturing HT in pipeline. It can trace HT from their starting to end points.

Wang *et al.* (2014) carried out a research on methods of assessing pipe rupture. Classification maps and pipe rupture prediction models were used as technical guides for the pipeline design, operation and maintenance. For the transient analysis in the system, both experimental and simulation approaches were used. In the experimental investigation, transient phenomenon was created in a laboratory facility and different transient scenarios were tested. For the simulation, a CFD based model was developed using the FEM to study and analyse the structural behaviour of the pipeline system under pressure transients. The study revealed four (4) aspects of water hammer hazards and these are: excessively high pressures bursting pipes, the vacuum flattening pipes as a result of negative pressure leading to water pollution, pipes and pump impellers damages due cavitations and mass oscillations as well as loosening of pipe joints due

34

vibrations caused by transient force. The study concluded that fluid flow behaviours and pipeline structural characteristics can be studied as a whole.

Simão *et al.* (2014) conducted a research on fluid and pipe structure interaction using real and CFD approach. A CFD model was developed using FEM to study the structural vibrations induced by unsteady flow phenomenon in a hydrodynamic system. Two domains (fluid and pipe structure domains) were created in a simulation interface in order to study and analyse the resulting the consequences of displacement caused by different fluid loads and on pipe supports. The research found that the fluid motion induced by perturbation tends to raise the pressure magnitude in the hydrodynamics system and this will eventually lead to structural deformation. Also the research reveals that simulations based on CFD analyses is a better way or method of analysing and understanding the hydrodynamic and pipe structure interaction phenomena than analytical method.

Transient phenomena in fluid transporting pipeline network was studied using modelling and simulating approach by Abuiziah *et al.* (2014). In this research, the flow governing equations (dynamic and continuity equations) were analyzed using RCM and MOC methods. The investigation reported that RCM reduces its calculations complication by successfully shunning interpolation error that takes place in MOC. The authors also stated that despite the fact the two methods produce identical results, the use of full elastic method for transient analysis is recommended because the full elastic method takes into consideration all factors that take part in developing transients. The results of the research showed that the model is an effective tool for the analysis of HT. The study also suggests that the use of open surge tank will minimize the negative effects of HT.

Naik & Shreenivas (2015) investigated the effects of active stress and HT. The authors used simulation method to determine the stresses and the highest pressure that come about in a pipeline network using *Flownex*. According to the authors, numerical analysis based CFD tool will yield accurate prediction results for the stresses that may occur due to sudden or gradual closure of valves. Both experimental and simulation methods were used to determine the highest pressure in the main pipeline as well as at the bends for steady state flow as well as for abrupt and gradual valve closures respectively. Finally, it was found that features like length of the pipe, VCT, pressures, pipe materials, pipe diameter as well as the fluid's velocity can influence HT. In addition, the study recommended that water hammer effect can be reduced slightly by the introduction of an accumulator into the pipeline network system but it cannot eliminate it.

Henclik (2015) adopted a numerical process to build up a model of HT with fluid-structure interaction for a straight pipe controlled by fourteen (14) hyperbolic PDEs. The fourteen (14) hyperbolic PDEs were transformed into compatibility equations with the use of unified variables (velocities and loads). The algorithms were executed using computer codes, and the results were validated with experimental data from the laboratory. The author formulated a numerical model that can be used in the analysis of hydraulic transient by using coupling matrix and the new mark method.

Simão *et al.* (2015)investigated and presented a fluid–structure interaction and structural dynamic. Numerical and experimental processes were employed to conduct the analysis of HT, fluid- structure interaction and the resulting vibrations of the pipes due to the transients. At the end of the study, the developed models were validated through experimental tests. CFD models were used to predict and simulate the fluid-structure

interaction in relation to the types of anchored supports types, the rigidity and geometry of the pipes as well as the resulting pressure transients and dynamic forces acting in whole of the system. The study concluded that fluid-structure interaction phenomenon is a way of finding the structural behaviour in relation to the propagation of the pressure waves.

Chaichan & Al-zubaidi (2015) investigated HT as well as means of controlling the effects of HT in water distribution pipelines and its pumping system. A study was conducted on pumping station possessed by Iraqi General Company for execution and irrigation (Badra – pumping station number five) and pipeline network of about 7500 m. HT analysis software (Surge2012) was used to investigate the transient potentials in the pipelines. The analysis was conducted for the pipeline system with and without any protection devices. The water flow inside the pipeline network system as well as the positive and negative pressure waves inside pipeline were analysed and compared. Several momentum disturbance scenarios were tested in the HT analysis due to abrupt stoppage of one or all of the pumps. The investigation showed that the worst incidence would occur when all the working pumps stopped abruptly while running the system with no protection devices. The study further revealed that a very high pressure (429.3 m) which can damage the system can be created as a result of the pump failures. The study found that Installation of $2x14m^3$ closed surge tanks will minimize the danger of water hammer.

Rukthong *et al.* (2016)investigated the consequence of crude oil properties such as mass density, dynamic viscosity and thermal conductivity on HT. The influences of these physical properties were analysed using design of experiment based on 24 factorials. In addition, a CFD model was developed and simulation of a viscous liquid phase flowing

in a straight pipeline was conducted using the CFD model and the results obtained were validated with ANSYS FLUENT and theoretical transport phenomena concept. Sixteen (16) runs of simulation were carried out based on the experimental design. The study revealed that in all the sixteen (16) simulations, flow distributions were quite similar in trends. The results of all 16 simulations or responses were analysed using ANOVA and the result showed a confidence level of 95%.

Akpan *et al.* (2015) carried out investigation of transient flow conditions due to sudden change in fluid flow velocity in pipelines. The authors used modelling and simulation techniques in studying the causes and effects of the HT in water pipeline. In the study, WANDA HT analysis software was applied to perform the pressure surge analysis in two separate pipeline systems for different flow parameters (miniature system and a simple main water riser system). For the simulation of the model, data obtained from laboratory experiments and system parameters were used. The results of the simulation on air performance in air vessel employed as a safety device of the pipeline are in conformity with the results of numerical analysis obtained using RCM. The authors declared that the nature of the results gotten from the two systems were in agreement with the previously recognized knowledge of effects of polytropic index values and initial air volume as well as rigid column assumptions on the actions of air vessel during HT and how it protects pipelines.

Victor & Shi-yi (2015) researched processes of developing a unique process in HT analysis for better examination of flow regimes in petroleum and gas wells. A new statistical approach was created for detecting HT in shut-in and flowing conditions. To ensure the reliability of the developed model, the model was tested with constant flow rate conditions, constant pressure as well as in high water producing wells. And the

outcome of the test revealed that the developed model demonstrated a unique radial flow fingerprint with high level of accuracy. The study further revealed that the statistical approach gives superior reading of flow scheme and the model aid to detect reservoir flow scheme for description.

Malppan & Sumam (2015) carried out a study to investigate the dangers in pipe network. In this research work, water distribution network of Adat panchayat in India was chosen as case study, because there is likelihood of HT in the pipeline system due to its undulating topography. The water supply system is made up of 250mm diameter pipe having length of 1765m with 24l/s capacity. A transient analysis commercial software known as Surge 2000 was used in this study to analyse the flow regimes and assess transient risks in the water pipeline system. A digital pipeline network was created in an interface called ArcMap 10 and then the created pipeline network model was transferred and modelled in Surge 2000 for both steady state and transient state conditions. In this study, transient analyses of the system due to pump trip or shut down as well as valve operations were carried out. In addition, the pipe failure threat factors for highest, lowest and HT forces were also created and the failure threat factors with protection devices were determined in order to find a system in which the failure threat of the system is entirely removed or reduced. The investigation concluded that Surge 2000 software could be used to carry out fluid flow analysis of complex networks. The study also found that pump trip is the dangerous scenario in the HT analysis of the pumping main. The study further revealed that one of the most effective ways of mitigating the risk in the pumping main is incorporating surge tanks near the pumps.

Oyedeko & Balogun (2015) investigated how to locate leaks in hydrocarbon pipelines, contain it and ascertaining its flow rate using numerical approaches. MATLAB was

used to develop the numerical model. Experimental data (flow pressure, volumetric flow rate and temperature) of the pipeline were used to formulate the model. A horizontal pipeline of about 2,000 m length and 0.3556 m diameter transporting petroleum was used for this study. When the model was applied for detecting leakages in the pipeline, a crude oil leakage incident was detected at a location about 1,433.5 m from the upstream end and the leaking rate is estimated to be 12.09456 kg/s, but the location detected by the model was about 18.5 m away from the actual leak location. The study revealed that pressure decline along the length of the pipeline has greater effect on the leak. At the end of the research, the following recommendations were made among others; Supervisory Control and Data Acquisition (SCADA) and an accurate alarming system should be employed in monitoring and surveillance of all complex pipeline networks for security and data gathering.

Waltrich *et al.* (2016) studied the behaviour of vertical two-phase high velocity fluid flows in big pipes. A two-phase (air–water) test rig (experimental) for flow analysis was built at Louisiana State University. Pipes with internal diameters of 2, 4, 8, and 12 inches were used. In addition, a gas and liquids with high injection rates were used for the experimental analysis. The changes in pressure along a 20 feet pipe of the test rig were measured using pressure transducers. Experimental data were obtained for ranges of water flow rates between 216 bbl/d and 27,429 bbl/d, and airflow rates between 0.006 MMSCF/D and 2.4 MMSCF/D. Three different flow rates from different centrifugal pumps were used for the experiments. The water pressure, temperature and the water holdup were measured using an acquisition system at a sampling rate of 1 Hz. It was found that the measured experimental data for 2-inch diameter pipe are inconsistent with the information from the literature for similar pipes and other flow

parameters but the information produced for pipe diameters (4, 8, and 12) are in agreement with other data available in the literature. The research concluded that there were huge variations between the results obtained via experimental and numerical analysis.

Starczewska *et al.* (2016) investigated the generation of HT in a water supply pipeline system. The study was aimed at exploring the occurrence of pressure surges in operational water distribution pipelines and studying the characteristics of specific sites that may correlate and dissipates effects of network properties. The study also found better methods of presenting and quantifying the pressure transient response of a water distribution schemes. Ten (10) samples of pressures were collected from ten separate locations and were analysed in this study. Statistical (Histogram) method was used to study the rate of change of pressure and exhibition of data on the different HT characteristics between the sites. The investigation found that the data obtained displays differences in the HT measured in each pipeline.

According to a study carried out by Nerella & Rathnam (2015) HT analysis of fluid pipeline is of greater importance than steady state operation analysis which engineers normally use in the design of pipelines. The authors investigated HT and wave transmission because of flow differences due to quick valve closure at the downstream of a pipeline. MOC model was used for the analysis. A pipeline system having decreasing diameter (from 305 mm to 153 mm) was used for this study. HT was found to be the reason for changes in the flow rates and as a result of valve closure. The investigation found that the flow rates and the pressure head were found to be oscillating due to un-damped wave propagation. When the valve was closed suddenly,

the fluid velocity decreases to zero while the pressure rose. The authors recommended that HT conditions should be considered in pipeline design.

Jayakumar*et al.* (2015) studied flow through transverse corrugated pipes using CFD methods. The authors reported that unlike fluid flow through a round or circular pipes, the flow pattern through corrugated pipes are different due to the varying geometry of the pipes. Experimental and simulation techniques were used for the study and analysis. The pipe geometry was modelled with solid works while ANSYS FLUENT was employed as solver for the numerical simulation of the pipeline. Simulations were carried out for both smooth wall and rough wall conditions. The flow patterns in the corrugated pipes give rise to the difference in behaviour of these pipes compared to normal pipes. The study revealed that pressure contours of the analysis showed that at the regions where the internal diameter is low, there is a strong interaction among the fluid and the pipe wall, and the friction factor for the corrugated pipes tend to be constantly high. The study further revealed experimental values are in significant agreement with the estimation of the smooth wall and also reducing the vortex shedding frequency will lead to the reduction in pressure loss and whistling condition. The study suggested further studies into the variation of vortex shedding frequency inside the corrugated pipe.

Adamkowski *et al.* (2016) investigated the impact of pipe supports on transient flow parameters of fluid using experimental approach. An experimental rig was developed at Gdansk's institute of fluid flow machinery of the polish academy of sciences for the experimental analysis. Pipeline pressures, vibrations, strains, flow, velocity and temperatures of the test rig were, measured and analysed for different stiffness of supports during the experiments. Water hammer runs were carried out for two different

values of initial pressures (P =1.12 MPa and P = 0.72 MPa) of water-air pressure vessel. Ten values of initial velocities from 0.06 m/s up to 2.0 m/s were used. These tests were conducted with the purpose of generating free vibrations in the pipeline system as a result of mechanical shock generated due to valve closure so as to observe the transients in the pipeline. The experimental results were collected, analysed and compared with numerical and theoretical results. High frequency oscillations were seen at the water hammer peak because of mechanical vibrations due to valve closure. The study revealed that the stabilization of the pressure oscillations and fluctuations were not regular at the beginning of the experimental run. The study concluded that lowering the stiffness of the pipeline supports leads to the reduction of water hammer and pressure oscillations because of damping effect. The study further showed that lowering of the stiffness of the pipeline support could be considered efficient as a result of generating high vibrations in the pipeline and superior energy distribution and dissipation at the pipeline. In addition, it was found that pressure transient mitigation and fast vanishing of the column separation effects are caused by lower stiffness of the supports.

Zhang (2016)investigated HT due to pump shut-down in a hydropower plant pipeline. A hydroelectric company based in Zurich (Oberhasli Hydroelectric Power Company) was taken as the case study area. CFD and experimental methods were adopted in this research work. The flow velocity and the pressure head in pipeline network were established as a product of time and the axis along the pipe. The analysis of the data was carried out using Microsoft Excel program. The study revealed that pressure transient at any location can be tracked at each time step due to restricted value of the acoustic speed in the water. Also, the authors revealed that transmission of the HT leads to the

generation of wave reflection and wave propagation. The study found that the wave tracking method is good in analysing HTs and produces accurate results.

Puntorieri *et al.* (2017) studied transient flow associated with cavitation in a copper pipe using experimental techniques with the aim of studying the steady and dynamic behaviours of a pipeline system as a result of valve closure. A laboratory test rig at Instituto Superior Técnico, Lisbon, Portugal was used for the experiment. The behaviour of the pipeline rig in steady state and various valve closures were analysed for different transient events. The authors carried out seventeen tests for different initial discharges. Water hammer was generated in the system by abrupt valve closure at the downstream of the pipeline system. The results obtained from the transient tests analysis, includes discharges and their corresponding piezometric head variations as well as experimental celerity values. In addition, other parameters determined in this research include theoretical celerity value, relative differences between the experimental and theoretical Joukowsky overpressure. Water hammer phenomenon with and without cavitation were also studied. The experimental results revealed and confirmed that water hammer theory is not always justifiable. The authors reported that sudden drop in transient pressure as well as cavitation only occurs on high flow rates. The authors also recommended that a modern transient analysis technique be used by Engineers to deal with water hammer adequately.

Yang *et al.* (2017) investigated pressure wave generation in HT using experimental as well as numerical methods. For the investigation of the wave generating process and pressure wave's characteristics, ICEM CFD 14.5 software was employed to generate the frame work of the parts and the CFD analysis was done with ANSYS Fluent 14.5. Realizable k–ε turbulence model was used in the simulation of the pressure wave

characteristics. The pressure wave generating process in pipe flows were simulated, the amplitude and frequency characteristics of the pressure waves generated were obtained. The study revealed that the pressure waves produced at the downstream and upstream ends are similar. The validation of the result showed that the amplitude of the pressure wave increases with the speed frequency at the beginning of the pressure wave generation but at lower speed, the pressure wave diminishes. The authors recommended further study into practical investigation of flow transition with high speed frequency.

Chuka *et al.* (2016) investigated leakage in oil pipelines using transient model and localization method. A pipeline transporting crude oil was used as a case study. The aim of the study is to develop a leak detection model to supervise the operations of the pipelines. The parameters used in the development of the model are the flow parameters such as fluid pressure, flow velocity and temperature. The developed model was able to locate a leak incident at 1088.12 m from the inlet of a horizontal pipeline having length and diameter of 2000 m and 0.3556 m respectively. But the developed model detected the leakage at a point behind the actual leak position of 1100 m. The developed model is neat but the accuracy of the leak detection is weak. The authors suggested that more works are needed to improve the model.

Urbanowicz (2017) investigated water hammer in hydraulic equipment of ships. The author investigated the effect of calculating wall shear stress using MOC. Simplified process was employed in evaluating shear forces in the internal nodes. The study compared the results of the simplified way of modelling the hydraulic resistance, simplified effective weighting functions, and found that to accurately model the analysed transient conditions, the simple two-terms weighting functions are the most effective. In addition, the solutions presented boosted the rate of the calculations

without concession of the accuracy for calculating the HT. The author recommended that the accuracy of the model used needs improvements; as such, the model needs modifications by the inclusion of gas cavitation.

Jablonska & Kozubkova (2017)investigated the characteristics of flow of water in a long pipeline using mathematical modelling and experimental techniques. The authors stated that despite the fact water hammer or pressure transients in pipelines are serious problems in technical practice, they can be analyzed by using either mathematical modelling or experimental measurement techniques. The authors investigated HT at multiphase flow of water and air. MATLAB Sim Hydraulics and ANSYS FLUENT software were used in the study. Simulation method was used to test the developed mathematical model and verified by experimental measurements. The results showed that there is agreement between the simulated and the experimental results periods and the amplitudes of the static pressure.

Yousif & Kalaf (2017) conducted a research with the aims of experimentally investigating the dynamics of a surge tank after sudden opening and closure of a valve. The research also takes into consideration the effects of friction factor via theoretical analysis. The experimental analysis was conducted using water hummer test rig from Armfield Company; UK, with a simple surge tank with 0.044 m diameter, constant head reservoir height of 0.881 m and a water pipeline with a diameter of 0.0202 m were used for the investigations. The experiment was carried out by drawing water from a tank by a centrifugal pump and transported through a pipe into a tank having a diameter and constant water level of 0.044 m and 0.881 m respectively. A stainless steel pipe with a diameter of 0.0202 m and a length of 3 m was used for transporting the water from the constant head tank. Flow meter was employed to measure the volumetric flow rate of

the water. When the VCT is t = 0, the water height in the surge tank rises from the initial 0.086 m exceeding the constant head tank of 0.75 m and reaching a peak of 0.0952 m after 4 s. This rise in water level was as a result of conversion of kinetic head to the wave pressure in the pipeline. When the water level begins to move, the water level continues to oscillate with attenuated amplitude. The experimental results were compared with the theoretical results of the surge tank dynamics by assuming that the system is frictionless. And the comparison showed that the oscillation was sinusoidal in nature and also stable at higher amplitude of 0.4028 m causing flooding while the time is found to be 7.5 s. The results of the investigation revealed that sudden closure of the downstream valve will lead to under damping but stable oscillation in the surge tank. Experimental responses are in good agreement with results obtained via theoretical approach when the friction factor is taken to be variable. The research further revealed that there is no significant effect on the level of stability by increasing the surge tank area.

Bergant*et al.* (2017) investigated the effects of cavitation caused by valves closure at the end of a pipeline using experimental and numerical approaches. The authors reported that a small-scale water hammer analysis rig was used for the experimental investigations. Two different experiments were run on the test apparatus; in the first experiment only the effects of a single valve closure were investigated; while in the second experiment the effects of the closure of two valves suddenly and with a time delay of 9.5*L*/*a* were investigated. In addition, for the numerical analysis, discrete gas cavity model was used for the simulation and analysis. The experimental investigation at the single valve found that due to sudden valve closure, severe repeated column separation events were generated at the valve in the downstream. The first rapid valve

closure at downstream generates rise in pressure head and but delayed valve closure leads to drop in the pressure head. The authors concluded that the dynamic response for long term pressure pounding is less aggressive compared to the reaction of a similar column separation case with the downstream end valve closure only. Also the investigation stated that several valve closures drastically increases the magnitude of column separation and causes fluctuations in the pipeline. The simulation predictions from the numerical analysis and the measured results for the single and multiple valve closures were in significant agreement.

Jiang *et al.* (2018) investigated HT with cavitation in water pipelines. According to the authors, due to the difference in HT pressure dynamics in upstream and downstream ends of pipelines, FDM was chosen to handle steady and frequency-dependent unsteady frictions as well as pressure transients with and without cavitation. A transient model was built to investigate the features of cavitation and the degree of HT generated at upstream and downstream of a water pipeline. The study found that because of rapid valve closure at the downstream, a negative pressure wave will transmit towards the downstream tank. Furthermore, the positive pressure wave travels back to the valve due to its reflection from the downstream tank and it eventually leads to the first positive pressure peak. The study found that cavitation volumes and durations are larger and longer respectively on the downstream side of the valve. The study further showed that the likelihood of the occurrence of cavitation at the downstream side of the valve is very clear.

Wéber & Hős (2018), investigated HT in the presence of air valve using simulation and experimental processes. In order to have clear visual access of the mechanical characteristics of the fluid inside the pipeline, a Plexiglas material was used in building

the experimental test rig. Pressure transducers were used to measure pressure at several points of the pipeline. A commercial CFD software (ANSYS CFX) was used for the simulation. The research found that liquids and gases are immiscible in the pipeline; their mixtures behave as two distinct phases in the pipeline. The experimental study revealed that the air valve has the capacity to protect a pipeline from considerable vacuum but it also triggers positive pressure surges at the downstream of the valve. The study further revealed that the CFD simulations can be adopted as techniques for calculating the effects of air valve in a fluid carrying pipeline.

Garg & Kumar (2018) investigated HT in a reservoir-pipeline-valve set up of a hydro power plant. The degree of water hammer at several locations on the hydro power plant pipeline was examined. MOC was used in MATLAB environment to analyze the continuity and momentum equations. It was found that the degree of the HT was highest (around 285 m) at the valve but it continues to diminish along the network. The study further revealed that both positive and negative pressure transients' events are present in the penstock and if these pressure transients are not controlled it might lead to destruction of civil and mechanical infrastructures of a hydropower plant. The authors concluded that penstock must be designed to withstand pressure variations, otherwise buckling penstock, rupture, leakage, wear and tear as well as whole system failure may takes place.

Research on experimental investigation of cavitation and pressure pulsations in a low pressure water pipeline was carried out by Jiang *et al.* (2019). An experimental test rig was used to conduct the research. The cavitation, pressure pulsations and as well as growth and collapse of gas bubbles were recorded by pressure transducers and high speed cameras in the pipeline network under two different experimental conditions.

Piezoelectric pressure sensors were used to measure the pressure pulsations in the test rig pipeline; while the high speed video camera was used to capture the increase and breakdown of both cavitation and gas bubbles because of abrupt valve closure in the pipeline. The results of the pressure pulse showed that the pressure in the pipeline jumps to its peak value and then drop to its vapour pressure and stay at this transient condition for a small period of time. Between 0 and 0.2 s, there were about six pressure peaks. But after 0.2 s, the pressure pulsations take the shape of an attenuated sinusoidal wave. Also the high speed video shots of the pressure transients showed that the pressure pulse will propagate from the valve to the reservoir once it was generated. The research further showed that when the pressure declines down to the vapour pressure, some vaporous cavities and bubbles are created at some points.

Bhattarai *et al.* (2019) conducted a research on analysis during extreme cases of HT in a high-head hydropower station. A system that consists of a constant-head upstream reservoir, headrace tunnel, orifice and surge tank was used for the research. Gradual valve closure during the highest water level in the reservoir and major HT behaviors in the system were studied using MOC. The authors reported that VCT has significant effects on the pressure changes within the penstock pipe and the tunnels. And the effects are considerably low in the surge tank.

2.3   Research Gap

Many researchers have carried out researches on HT in pipelines networks conveying different types of fluids. But there was no enough information on HT experienced at hydraulic nodes of a petroleum pipeline transporting refined petroleum products (such as PMS, DPK and AGO) due to sudden valve closure or pump failure.

CHAPTER THREE

3.0   **MATERIALS AND METHODS**

3.1   **Materials**

This chapter provides the information (description and specifications) of a petroleum pipeline network adopted in this research, the materials used, the methods adopted as well as the detailed layout of the simulation and experimental procedures used. Simulation analysis and laboratory experimental test approaches were adopted in this research work because it is almost impossible to use the real pipeline network to carry out the analysis due to security reasons. The use of computational fluid dynamics (CFD) tool will reduce cost as well as the time required to analyse the hydraulic effect than the practical method (Lahane *et al.,* 2015). Also, CFD-based simulations are generally adopted for analyses to better understand the dynamic trend (Simão *et al*., 2015). A hypothetical petroleum pipeline network was used in this research; the pipeline network is made up of upstream and downstream tanks, steel pipes, a centrifugal pump, gate and non-return valves. Experimental and field data obtained from the literature, Nigerian National Petroleum Company (NNPC) archives, and field work were also used (Chuka *et al.*, 2016; Oyedeko & Balogun, 2015)

3.2   **Materials and Equipment Used in this Research Work**

    I.   WANDA 4.5.5 simulation software

   II.   Transient test rig

 III.   Stopwatch

 IV.   Automotive Gas Oil (AGO)

V.   Dual Purpose Kerosene (DPK)

VI.   Premium Motor Spirit (PMS)

3.2.1   WANDA 4.5.5 simulation software

Commercial software known as WANDA simulation software was used in carrying out the simulation analysis of the flows of AGO, DPK, and PMS as well as the pressures developed because of abrupt valve closure or pump failure in this research. WANDA is primarily used in the study and analysis of fluid flow through a pressure pipeline system. In fluid flow analysis, the pressure and the volumetric flow rates are the two most important quantities of interest while other related quantities such as flow velocity and the pipes cross-sectional areas can be obtained from these two quantities (Huijzer, 2018). The simulation software can be employed for both steady and transient flow analysis as shown in the simulation flow chart in Figure 3.1. In the design of fluid pipelines, Engineers usually use the steady-state flow condition of a pipeline to design instead of using both steady state and transient flow conditions, and the steady-state flow condition does not account for any unforeseen scenarios. WANDA have the shortcoming of slightly over predicted the maximum pressure surges and slightly under predicting the minimum pressures surges. The simulation results of the software generally show larger fluctuations than reality.
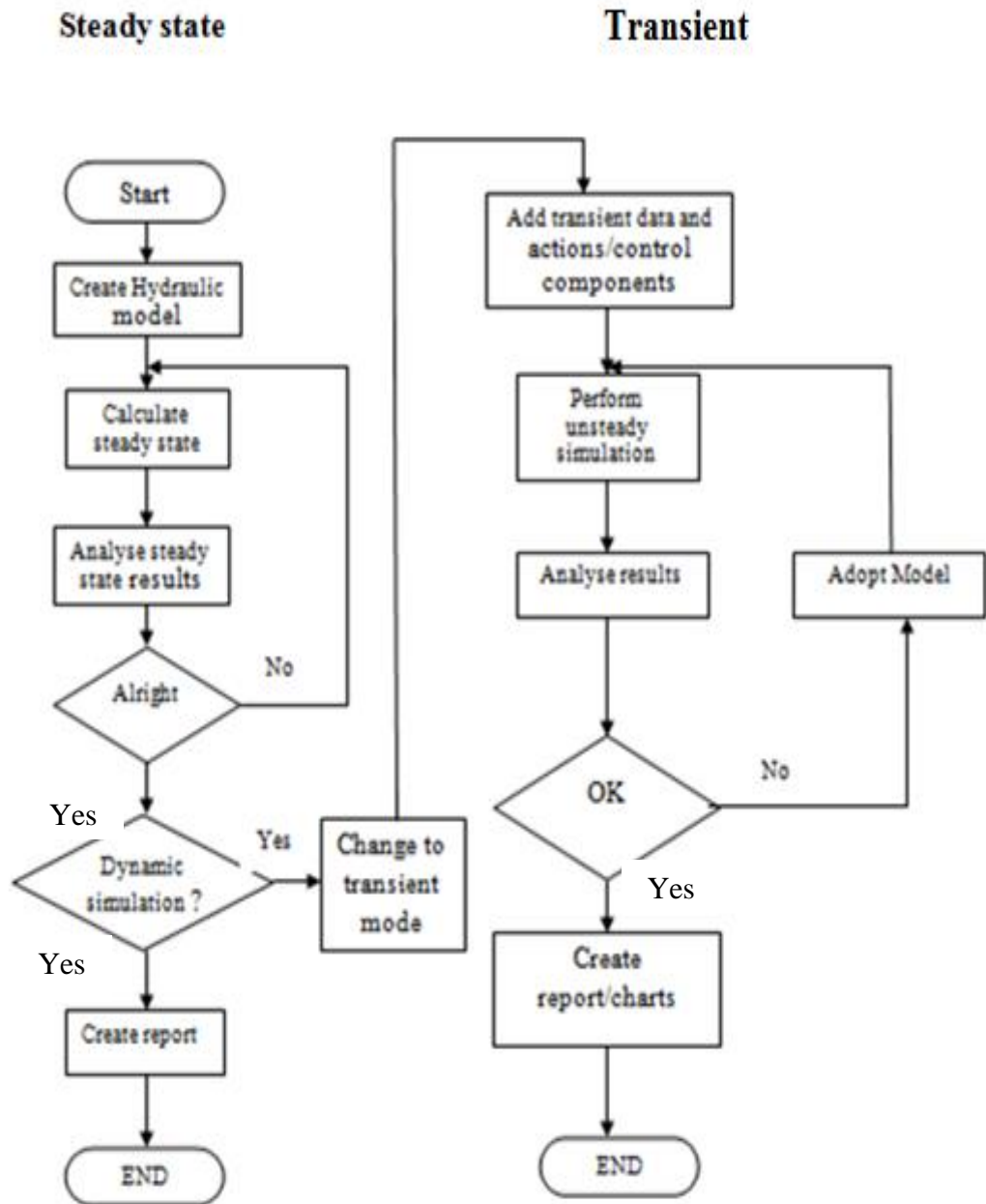
Figure 3.1: Flow chart for the simulation analysis using WANDA software

3.2.2 Transient test rig

For validation of the simulated results, experimental analysis of the HT was carried out using transient test rig situated at the University of Maiduguri. Plates II and III shows the upstream and downstream sides of the test rig. The rig consists of two reservoirs

(upstream and downstream reservoirs), pipes (P1=1 m, P2=10 m, P3=10 m, and P4=1 m), check and gate valves, a centrifugal pump and pressure gauges. The upstream tank has a volume of 0.0512 m^3. The fluid flows from the upstream to the downstream tank via a pipeline of a constant diameter of 0.3556 m. The pressure gauges were installed at various at joints where a pipe is connected to a pump, valve or any other pipeline component (nodes) along the pipeline to measure the pressure transients. The check valve and a gate valve were installed at the downstream side of the pipeline.

Plate II: Upstream and downstream sides of experimental test rig

Plate III: Pressure gauges on the experimental test rig

3.2.3 Stopwatch

Plate IV shows a stop watch used for measuring VCTs. A stopwatch is a device used to measure the time intervals of an activity or event. The digital stopwatch also has a precision of 1/10 of a second. Stopwatches are also called chronometers as they are used to measure short (fractions of times) accurately. There are two types of stopwatches used in scientific analysis, these are; digital and analogue stopwatches. Stopwatches are usually used for timing a particular activity; they can be started or stopped at will for accurate timing (Ox-science, 2020).

Plate IV: A digital stopwatch (Ox-science, 2020)

3.2.4 Automotive gas oil

AGO is also popularly called diesel. It is a compound blend of hydrocarbons produced by blending fractions of crude oil products with additives to improve performance. Middle distillates of about 40% with changeable percentages of straight-run gas oil, light vacuum distillates, light heat-cracked distillates, and light distillates are blended to obtain the AGO. It has a characteristic odour under normal conditions. AGO is used for powering heavy-duty electricity generators and vehicles (Profound-Energy, 2018).

3.2.5   Dual purpose kerosene

DPK is an inflammable colourless or light yellow petroleum distillate oil fraction with a characteristic odour. It has intermediate volatility (between PMS and AGO). It is generated from crude oil via distillation. DPK is a versatile petroleum product. DPK is used as a source of energy in jet engines and rockets and as such it is called Aviation Turbine Kerosene (ATK). It is also used as a source of energy in homes as a fuel for stoves, lamps, and cookers and hence it is called Household Kerosene (HHK). When kerosene is adopted as a source of energy in both domestic and jet or rocket engines, it is then referred to as Dual Purpose Kerosene (DPK) (J-Gold, n. d.).

3.2.6   Premium Motor Spirit

PMS is also called gasoline or petrol. PMS is generated from crude oil through distillation, it is a blend of organic mixtures and additives that improves the performance of engines, and it is orange in colour with a merchantable odour. It is mostly used in internal combustion engines as a source of energy (Total-Energies, n. d.).

3.3   Methods Used in this Research Work

CFD simulation and experimental methods were adopted in this research. The relations used in the research work are presented according to the objectives of the research.

3.3.1   Equations for pressure and velocity heads analysis

Fluid dynamics equations were used in this research in analyzing some of the basic transient flow fundamentals. The basic concept of fluid dynamics or engineering concept that represents the bulk motion of a fluid is called velocity head. The velocity

and pressure heads of the flowing fluids were calculated using Equations (3.1) and (3.2) respectively.

$$h = \frac{v^2}{2g}$$
(3.1)

Equation (3.2) is used in the evaluation of pressure head in conduits

$$Ph = \frac{P}{\rho g}$$
(3.2)

where, h is the velocity head, v is the velocity of the following fluid, g is the gravitational force, Ph is the pressure head, P is the pressure of the fluid and ρ is the mass density of the fluid under consideration.

Equation (3.3) was used in determining the acoustic wave speed in pipelines for transient flow conditions as reported by (Nerella & Rathnam, 2015; Yang *et al.,* 2017)

$$a = \sqrt{\frac{\frac{k}{\rho}}{1 + \left(\frac{k}{E}\right)\left(\frac{D}{e}\right)(C)}}$$
(3.3)

where, K is the bulk modulus of elasticity of the fluid, ρ is the mass density of the fluid, E is the Young's modulus of elasticity of the pipe material, e is the pipe wall thickness, D is the diameter of the pipe while C is movement restrain constant (full pipe restraint from axial movement, $C = 1-\mu^2$, μ = 0.30 m for steels).

El-Turki (2013) reported that whenever a pressure surge is generated in a conduit, the pressure wave will propagate and reflect back towards the valve at a time of t = 2L/a seconds. The reflection time required by the increase in pressure to travel from beginning of the pipe to the end is given by Equation (3.4).

57

$$T = \frac{2L}{a} \tag{3.4}$$

where T is the reflection time in seconds, L is the length of the pipe, and a is the wave speed.

Calculating the maximum safe pressure of a pipeline is one of the vital ways of assessing the pipeline residual strength (Li & He, 2015). B31G criterion is usually used for the assessment of pipelines; the Equation is expressed as Equation (3.5),

$$P = \frac{2SMYS}{D} \times F \times e \tag{3.5}$$

Where P is the maximum allowable design pressure, SMYS is the specified minimum yield strength, F is a design factor, which is normally 0.72 and e is the thickness of the pipe wall and D is the pipe diameter.

3.3.2   Computational method

The computational Fluid Dynamics (CFD) method was used in carrying out the numerical simulation of the petroleum pipeline system in this research. WANDA simulation software compiled with one-dimensional continuity and momentum equations was used in this research work. Therefore, one-dimensional transient model equations were used to investigate the effects of HT at the pipe nodes when either the valve was closed suddenly or the pump fails in this research as was used by other researchers in the literature. Al-Muntasser & Dekam (2019) reported that WANDA uses two types of transient flows in simulating transient flow conditions, the models were used to solve quasi-steady and true transient flow problems. Quasi-steady flow is a type of flow in which there was a gradual variation of pressure and discharges with time. The flow seems to be steady over a small time interval. While true transient flow is a type of

flow in which the effects of fluids compressibility, inertia, and elasticity of pipes are vital factors in the flow performance.

According to Kim (2012), the following assumptions were adopted for numerical analyses for transient pipe flows by many researchers.

I. The fluid pressure and velocity are uniform and averaged (one-dimensional).

II. The fluid is slightly compressible.

III. During HT, the pipe remains full.

IV. The wall of the pipe is considered elastic and slightly deformable.

V. Negligible free gas content in the liquid (constant acoustic speed).

These assumptions were also adopted in this research to simplify the analysis process. The governing equations under these assumptions were expressed by the continuity and momentum equations (Kim, 2012). These equations were presented in the form of PDEs and were solved numerically by using MOC and these equations are solved simultaneously with the use of a computer (Ammar, 2014). One-dimensional momentum and continuity mathematical equations were used in this research analysis. The two Equations are presented as reported by (Abuiziah *et al.*, 2013, Rathore, 2015, Carvajal & Bohorquez, 2018).

3.3.3 Wanda transient flow governing equations

WANDA uses sets of PDEs of momentum and continuity Equations as governing equations to calculate the transient flows in a closed conduit. The fluid flows were considered to be one-dimensional. The momentum and continuity Equations are presented as Equations (3.6) and (3.7).

$$\frac{\partial V}{\partial t} + g\frac{\partial H}{\partial s} + \frac{fV|V|}{2D} = 0 \qquad (3.6)$$

$$\frac{\rho_f g}{K_f} + \frac{\partial H}{\partial t} + \frac{\partial V}{\partial s} + \frac{2}{R}\frac{\partial UR}{\partial t} = 0 \qquad (3.7)$$

The value of H (head) was computed using Equation (3.8)

$$H = \frac{P}{\rho_f g} + \frac{V^2}{2g} + h \qquad (3.8)$$

where, D is the diameter of the pipe, A is the pipe's cross sectional area, f is the Darcy-Weisbach friction factor, ρ is the mass density of the fluid, K is the fluid's bulk modulus, g is the acceleration due to gravity, t is time, V is the mean flow velocity of the fluid, S is the axial point along the pipeline and UR is the radial displacement of pipe wall.

A dimensionless parameter known as Reynolds number was used to classify a fluid flow through a pipeline as laminar, transitional, or turbulent, depending on the value of the Reynolds number. The fluid's properties, pipeline diameter, and fluid flow velocity are the factors upon which the Reynolds number depends (Adamu, 2017). A relation used by WANDA that defines a Reynolds number is presented as Equation (3.9).

$$Re = \frac{QD}{VA_f} \qquad (3.9)$$

where Q is the flow discharge, D is the pipe diameter; A_f is the pipe's cross sectional area and v is the average fluid velocity.

Also Darcy-Weisbach equation was used by the software to calculate the pressure drops across the pipeline and the Equation is presented as Equation (3.10).

$$H_2 - H_1 = \frac{fL}{D} + \sum_I \xi \frac{Q|Q|}{2gA_f^2} \tag{3.10}$$

In calculating the friction factor of turbulent flows (where Reynolds Number is greater than 4000), the Colebrook-White Equation was used and it is presented as Equation (3.11).

$$\frac{1}{\sqrt{f}} = -2log\left(\frac{K/D}{3.7} + \frac{2.51}{Re\sqrt{f}}\right) = 0 \tag{3.11}$$

3.3.4 Boundary conditions

Flow speed, pressure, discharge, and temperature are common boundary conditions for a fluid pumping system and the best method is to describe the boundary condition as they will be in the existing system (Garcia-Hernandez *et al.*, 2010). To solve the set of the system equations, it is required to apply boundary conditions on the case study; the boundary conditions adopted for this research work were selected according to thumb rule of the petroleum transportation pipelines and they are as follows;

  I.   The constant fluid velocity of 1 m/s at the inlet section.

 II.   Constant product velocity of 1 m/s at the outlet section.

III.   Atmospheric pressure of 101.4 kPa at the inlet section.

IV.   Atmospheric pressure of 101.4 kPa at the outlet section.

 V.   Constant operational temperature of 37°C.

VI.   Fixed wall and no-slip condition at the solid-wall zone (0 m/s)

VII.   Constant product flow-rate of 160 m^3/h at the inlet section

VIII. Constant product flow rate of160 m^3/h at the outlet section

IX.   Initial operational pressure of 120 kPa

Figure 3.2 presents the pipeline network indicating some of the physical boundary conditions used in the research work.
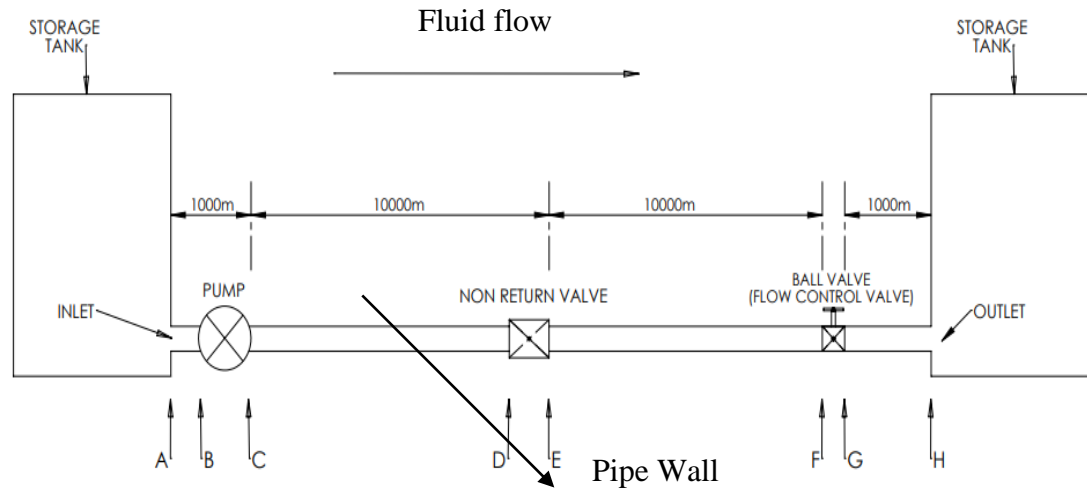
Figure 3.2: Physical boundary conditions of the petroleum pipeline network

3.4   Pipeline network simulation procedures using WANDA

The followings are the steps followed to carry out the simulation process:

I.   Data collection/determination of flow rate

II.   Creation of the hydraulic model in the WANDA graphic user interface

III.   Specification of the pipeline system components

IV.   Specification of hydraulica actions that will trigger the transient mode of flow

V.   Preparation and entering of the pump and valve characteristics tables

VI.   Simulation/calculation of steady state and transient state flow conditions

VII.   Reporting of results

3.4.1   Determination of flow rate and pressure

The first step in the simulation process was the collection of relevant available data (pieces of information such as flow rate and pressure as well as the temperature of the fluid in real-life operations) from the field that will be used in setting up the system. In this research, petroleum pipeline network parameters that are made up of the product type (AGO, DPK, and AGO), size and geometries of pipes (diameter and length), pumps and valves were used as input data in the simulations. The area of the pipe conduit used for the transportation was calculated using Equation (3.12) and the flow rate of the petroleum products in the pipeline was determined using Equation (3.13) as reported by Lebele-Alawa and Oparadike, (2015).

$$A = \frac{\pi d^2}{4} \tag{3.12}$$

$$(A = \frac{\pi \times 0.3556^2}{4} = A = 0.0993 m^2)$$

$$Q = VA \tag{3.13}$$

$$(Q = 1 \times 0.0993 = 0.0993 \, m^3/s)$$

Velocity of the fluid was taken as 1m/s because according to thumb rule, the flow of fluid in low pressure petroleum pipelines ranges between $1 - 2$ m/s. Equation (3.14) depicts the relation used to calculate the pipe flow velocity.

$$V = \frac{Q}{A} \tag{3.14}$$

where A is the pipe's cross-sectional area, and V is the velocity of the fluid while d is the pipe's internal diameter.

3.4.2   Creation of the hydraulic model

The second step was the creation of the schematic diagram of the pipeline network system (hydraulic model) on the software graphic user interface. The hydraulic model was drawn/created using lines and other symbols from the palette of the software having symbols representing various elements of the network and all the components were connected via nodes. The pipeline model is made up of four carbon steel pipes labelled P1, P2, P3 and P4 respectively. The pipeline model also have upstream tank (B1) and downstream tank (B2) as well as pump (P), non-return valve (NR) and gate valve (GV) respectively. The joint where P1 was connected to the upstream tank is called node A and also the joint where P1was also connected to the pump is called node B. The joint where the P2 was connected to the pump is called node C, while the joint where P2 was connected to the check valve is called node D. Node E is the joint where P3 was connected to the non-return valve and the joint where P3 was connected to the gate valve is called node F. The gate valve was connected to P4 at a joint called node G and node H is the point where P4 was connected to the downstream tank as shown in Figure 3.3.
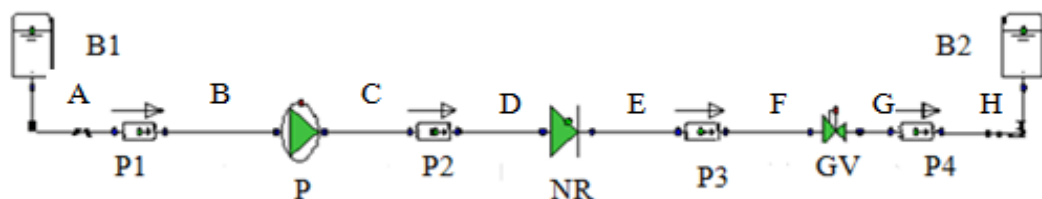
Figure 3.3: Model of pipeline network layout

3.4.3 Specification of the pipeline system components

After the creation of the hydraulic model, the dimensions and other specifications of components such as the geometry, size, and other characteristics as well as locations of all the components of the network were specified and were entered into the software via the property windows. The units of the various parameters were also specified. Physical constants under which the real system operates such as gravitational force and fluid temperature were also specified. The pipeline network has four standard carbon steel pipes of diameters of 0.3356 m used in transporting petroleum products with a thickness of 0.016 m, and surface roughness of 0.045 mm. All the pipes were connected in series between the upstream tank (B1) and the downstream tank (B2). The upstream end of the first pipe, (P1) with a length of 1m was connected to the upstream tank via node A. While its downstream end is connected to the pump at node B. Pipe 2 (P2) has a length of 10m, it is the second pipe in the series, its upstream end is connected to the pump at node C and its downstream end is connected to the check valve at node D. The third pipe in the series is pipe 3 (P3) with a length of 10m, P3 is also connected to the check valve at its upstream end at node E while at the downstream end is connected to the gate valve at node F. The last pipe in the series is pipe 4 (P), which has a length of 1m, the upstream end of P4 is connected to the gate valve at node G while its downstream end is connected to the downstream tank at node H.

3.4.4 Specifications of hydraulic actions

Next, after the steady-state simulation analysis, the simulation model was changed from steady state mode to transient mode using the mode and options menu and then the hydraulic actions were activated. In the hydraulic actions, things such as manipulation

of valves (specification of the calculated VCTs), pump running and trips, pump speeds, as well as heads and delivery rates adopted from the literature were all specified in the property window. In this research, the various VCTs adopted were specified, entered, and executed under this window. Action tables were used to specify the hydraulic actions. The action tables were only accessible in transient mode.

3.4.5 Preparation and entering of pump and valve characteristics tables

The characteristics tables for both the pump and valves were prepared separately and the input data were entered into the software via the menu property window. The input data specified in the pump table includes the pump head, the fluid discharge, pump speed, and efficiency as well as the power required for the operation of the pump concerning the other operating parameters. While input data entered for the valves includes valve size (diameter of 0.3556 m). The valve with this diameter was chosen because is the size that can tally with the standard 0.3556 m diameter pipes used, valve type, the VCT, and the flow rate through the valves. At this stage, the physical properties and configuration of the pump and the valves were defined and entered into the software via the property window.

3.4.6 Calculate steady-state and transient state flow conditions

The next step of the simulation process was the calculation of the steady-state and transient flow conditions under engineering and transient modes. Calculate steady is a command used in WANDA to calculate the steady-state flow condition in the pipeline network system. The steady-state flow condition was calculated by the software during the first run of the simulation process. WANDA computes the steady-state flow and the

results were used as the initial conditions for the computation of the unsteady state. For steady-state flow calculation, it is required to set the minimum sets of iterations in order to obtain a fulfilled and totally converged solution. To avert the program from looping if convergence was obtained, the highest number of iterations were instituted.

After the steady-state flow condition calculations, the next step is running the simulation for the calculation of the transient state flow conditions. WANDA computes the transient state condition by automatically using the values of the results obtained through steady-state flow conditions as input data for the computation of the transient state flow conditions. After the initial calculation of the steady-state flow condition, the VCTs, as well as the transient calculation mode, were activated at the property window, and then without changing any data the transient mode calculation was carried out. Wanda calculates all the various kinds of unsteady conditions. In calculating transient behaviours of the fluid pressure, it is required to change the operational status of one or more of the pipeline components (either valve closure or pump failure). WANDA starts the calculation with initialisation and authentication of the input data. Once the input data is authenticated, then the simulation analysis will commence. After the convergence of the steady-state flow calculation, a transient calculation can be carried out. Both the steady and transient calculations are executed in SI units.

In WANDA, when carrying out HT analysis in transient mode, each pipe is broken into elements of the same length based on acoustic wave speed and time step. Transient means that the fluid flow is time varying. Time derivatives are approximated by finite differences in time, this finite difference is presented as $\frac{\partial v}{\partial t}$. Then the time step is the ∂t that comes from the time discretization of the pipe length as well as the fluid property.

Then time step is the incremental adjustment in time for which the governing equations are solved. It is recommended that time-step size should be small in order to account for all the flow oscillations. A large time-step usually reduces computation time, but produces weak results while choosing a small time step produces more accurate results. The choice of the time step has to be established on pipe's properties and the type as well as nature of fluid considered in the system. In WANDA the element length of free surface pipes is computed from the time step. Therefore, the user must specify clearly a maximum element length, which is used in engineering mode; the element length is calculated from the time step (Zhu & Zhang, n. d.).

The WANDA calculation starts with initialization and validation of the input. Initialization is the process of locating and using the defined values for variable data that is used by software. Once the input is validated (checking and confirming that the positions of the pipeline components are correct), the steady calculation commences.

In steady state analysis, a start vector is build to start the iteration process. The start vector contains values of the core variables estimated from the input. The friction in all pipes is updated at each iteration. Linearization is a method for assessing the local stability of an equilibrium point of a system of nonlinear differential equations or discrete dynamical systems. Important information about how the system behaves in the neighbourhood of equilibrium points is obtained at this step (whether the point is stable or unstable, or moves away from the equilibrium point).

From a computational point of view the main difference between steady state and transient mode is the compressibility of the fluid. As no time-effects are included in

steady state mode, the fluid is considered incompressible and the complete hydraulic set is solved as one big system of equations.

For steady-state flow calculation, it is required to set the minimum sets of iterations in order to obtain a fulfilled and totally converged solution. To avert the program from looping if convergence was obtained, the highest number of iterations were instituted.

After the steady state calculation has obtained convergence, an unsteady calculation can be performed (transient). All calculations are performed in SI-units. Control evaluation is the preliminary evaluation. As well as verification if the controls proposed in the pipeline are adequate and the expected effect is emerging and if so, be able to take measures

Component dynamics is the state of the various pipeline components in terms of forces acting on them and their equilibrium presented by the differential equations. Here the differential equations are checked for linearization.

Post-processing involves processing of the output of the simulation analysis (results) especially the conversion of output into a visual form (graphs) or a form readable (tables). Post processing and conversion to the unit system chosen by the user are part of the graphical user interface (GUI) and take place after the calculation of steady (engineering) or the last time step of unsteady (transient) (WANDA 4.2, 2013). Figure 3.4 schematically presents the steady and transient flow condition calculation procedures of WANDA.
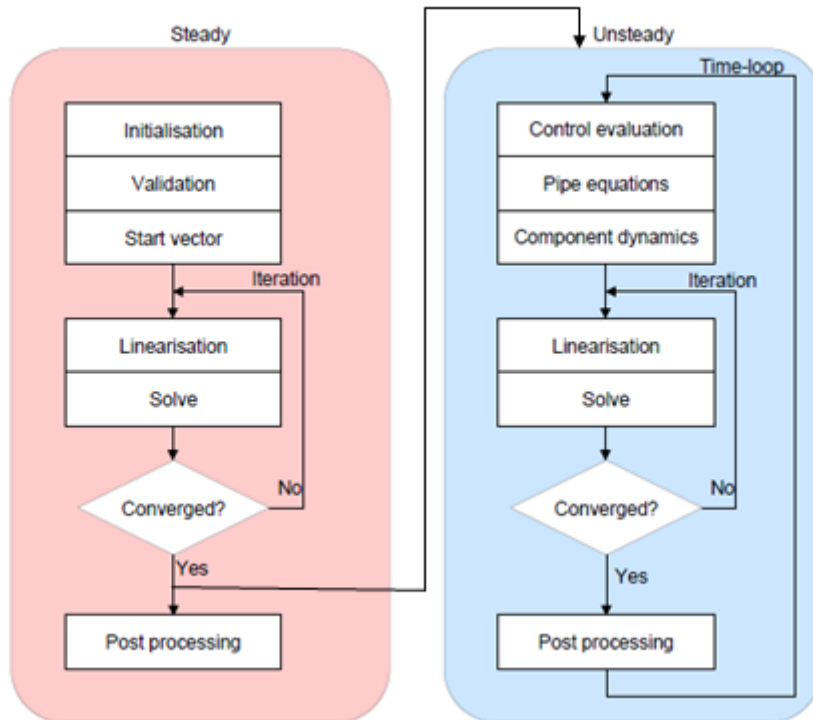
Figure 3.4: Steady and transient flow condition calculation procedures of WANDA

(WANDA 4.2, 2013)

3.4.7   Results

At this step, the simulation results were retrieved from the output window of the software. After running the simulation, there is the need by the user for the full report of the simulation actions. The reports menu is an interface that allows the user to have access, save, and edit all data (input and output) of the hydraulic model. The software (WANDA) generates the reports in a compressed spreadsheet format after a fruitful calculation. The results were obtained in Tables and graphic form for further analysis.

3.5 Experimental Setup and Procedure

The experimental analysis was carried out using a transient test rig located at the University of Maiduguri between 21st July and 30th, 2021. The following are the steps for experimental analysis.

I. The first step of the experimental analysis is verification of the calibration state of the test rig and it was found to be in good working condition.

II. The second step in the experimental analysis was the introduction of the fluid AGO into the upstream tank up to the required level.

III. Thirdly, all the valves were checked and ensured that they were fully opened.

IV. All the pressure gauges were ensured that they were rightly connected.

V. The experiment was started by witching on the pump to ensure the flow of the fluid from the upstream to the downstream without any interruption.

VI. After the flow of fluid for some time and after establishing a steady-state flow condition, then the valve was closed suddenly at different calculated VCTs of 4.75 s, 9.5 s, 19 s, 38 s, 76 s, 152 s, 304 s and 608 s.

VII. The nature and magnitude of pressure surge developed at the various hydraulic nodes due to the sudden valve closure were observed and recorded.

VIII. Next, the valve was opened and another experiment was conducted, but this time around, the pump was deliberately switched off with the valve open, and then the nature and magnitude of pressure surge developed due to the pump stoppage viewed from the pressure gauge and recorded.

IX. Next, steps I-VII were repeated for DPK using VCTs of 4.4 s, 8.5 s, 17 s, 34 s, 70 s, 140 s. 280 s and 560s.

X.   Next, also steps I-VII were repeated for PMS using different VCTs of 4.5 s, 9 s,
      18 s, 36 s, 72 s, 144 s, 288 s and 576 s.

Table 3.1 presents some of the fluid flow parameters selected for the simulation and
experimental analysis. The fluids are transported at an average temperature of 37°C and
a velocity of 1m/s was adopted (thumb for petroleum pipeline flow velocity is 1-2 m/s)
(Smith, (n. d.). According to Chuka (2016), the inlet pressure of petroleum products
from storage reservoirs with air vents is 120 kPa. Also according to ASTM D1298 the
densities of PMS, DPK and AGO are 720 kg/m^3, 810 kg/m^3, and 870 kg/m^3
respectively.

Table 3.1: Fluid flow parameters selected for the simulation and the experiment

Temperature (°C)	Pressure (kPa)	Flow velocity (m/s)	Material (Fluid type)	Dynamic viscosity (Pa)	Density (kg/m^3)
37	120	1	PMS	1.2463	720
37	120	1	DPK	0.0022	810
37	120	1	AGO	0.0249	870

Table 3.2 presents the pipeline parameters used as input variables into the WANDA
software. The pipeline parameters presented in Table 3.2 were obtained from the
literature as reported by (Oyedeko and Balogun, 2015) and these are standard values for
a standard petroleum pipe with 0.3556 m diameter.

Table 3.2: Pipe properties

Pipe	Diameter (m)	Length (m)	Thickness (m)	Roughness (m)
1	0.3556	1	0.016	0.0045
2	0.3556	10	0.016	0.0045
3	0.3556	10	0.016	0.0045
4	0.3556	1	0.016	0.0045

Table 3.3 presents the design pressure rating of the pipeline components such as pipes, flow control devices and the nodal sets of the petroleum pipeline under investigation.

Table 3.3: Pipeline components design pressure specifications

Component	Specifications
Pipes	1,379 kPa – 4,400 kPa
Flanges	Class 150 (1,586 kPa)
Valves	Class 150 (1,034 kPa)
Gaskets	Class 150 (1,034 kPa)

(**Source:** Bhatia, n.d.-b**)**

Table 3.4 present the values of atmospheric constants used and under which the simulation and experimental analysis in this research were carried out at an ambient temperature of 37° C.

Table 3.4: Physical constant parameters

Physical constants	Values
Atmospheric pressure	101.4 (kPa)
Gravitational acceleration	9.810 (m/s^2)
Ambient temperature	37.00 (°C)

Table 3.5 presents the properties of AGO that were used during the simulation and the experimental investigation of HT in this research. AGO has an acoustic speed of 1,226 m/s as a result of its density of 817.0 kg/m^3.

Table 3.5: AGO properties

Liquid name	AGO
Density	871.0 (kg/m^3)
Bulk modulus	$1.477e^9$ (N/m^2)
Vapour pressure	1.100 (kPa)
Kinematic viscosity	$2.860e^{-5}$ (m^2/s)
Acoustic wave speed	1,226 (m/s)

(**Source:** Curl and O'Donnell, 1977)

Table 3.6 presents the properties of DPK that were used during the simulation and the experimental investigation of HT in this research. DPK has an acoustic speed of 1,193 m/s as a result of its density of 810.0 kg/m^3.

Table 3.6: DPK properties

Liquid name	DPK
Density	810.0 (kg/m^3)
Bulk modulus	1.300e^9 (N/m^2)
Vapour pressure	0.5000 (kPa)
Kinematic viscosity	2.710e^{-6} (m^2/s)
Acoustic wave speed	1,193 (m/s)

(**Source:** Curl and O'Donnell, 1977)

Table 3.7 presents the properties of PMS that were used during the simulation and the experimental investigation of HT in this research. PMS has an acoustic speed of 1,160 m/s as a result of its density of 780.0 kg/m^3.

Table 3.7: PMS properties

Liquid name	PMS
Density	780.0 (kg/m^3)
Bulk modulus	1.070e9 (N/m^2)
Vapour pressure	48.00 (kPa)
Kinematic viscosity	0.001731 (m^2/s)
Acoustic wave speed	1,160 (m/s)

(**Source:** Curl and O'Donnell, 1977)

Table 3.8 present the various calculated VTCs for AGO, DPK and PMS adopted for analysis in this research work. AGO, PMS and DPK have the initial VCTs of 3.8 s, 3.6 s and 3.4 s respectively.

Table 3.8: VCTs for AGO, DPK and PMS

Fluid	T=2L/a	T_1 (s)	T_2 (s)	T_3 (s)	T_4 (s)	T_5 (s)	T_6 (s)	T_7 (s)	T_8 (s)
AGO	38	4.75	9.5	19	38	76	152	304	608
DPK	34	4.38	8.5	17	34	68	136	272	544
PMS	36	4.5	9	18	36	72	144	288	576

CHAPTER FOUR

4.0   **RESULTS AND DISCUSSION**

According to Nerella & Rathnam, (2015) it is conventional to examine the maximum values of pressure in transient flow analysis. Furthermore, the pressure together with the flow rate is capable of providing adequate information about the other flow parameters that are mutually dependant. In this chapter, the results obtained for the sudden valve closure and pump failure analysis are presented.

4.1   Pressure and Velocity Head Evaluation at the Various Hydraulic Nodes

4.1.1   Pressure heads evaluation results

Figure 4.1 shows the nature of the pressure head across various nodes of the pipeline network. Figure 4.1 depicts the pattern of pressure head characteristics in the pipeline network under investigation with node C (a node just upstream of the pump) having the highest pressure heads among all the nodes. The pressure heads developed at node C due to the flow of AGO was 0.117034 m, due to the flow of DPK was 0.115151 m, and due to the flow of PMS was 0.107164 m. The study showed that there was a rise in pressure head at node C. The pressure head at node C rises from 0.0140 m to 0.117034 m for AGO, 0.0151 m to 0.115151 m for DPK and 0.0156 m to 0.107164 m for PMS. Node C experiences rise in pressure head because that is the node where more pressure or energy is being added to the flowing fluid by the pump and low at node B, because node B is a node where fluids were extracted from the system. The points that experience high-pressure heads were subjected to high pressure in terms of the weight of the fluid and pressure of the fluid under normal working conditions; therefore there is

the need to ensure that the pipe flanges at these points (node C) are made to be thicker and stronger in order to withstand the high-pressure heads. The study also showed that the density of fluid plays a very vital role in the magnitude of pressure head developed (because denser fluids are heavier than less dense fluids), hence the reason why AGO is having the highest-pressure head at the node.
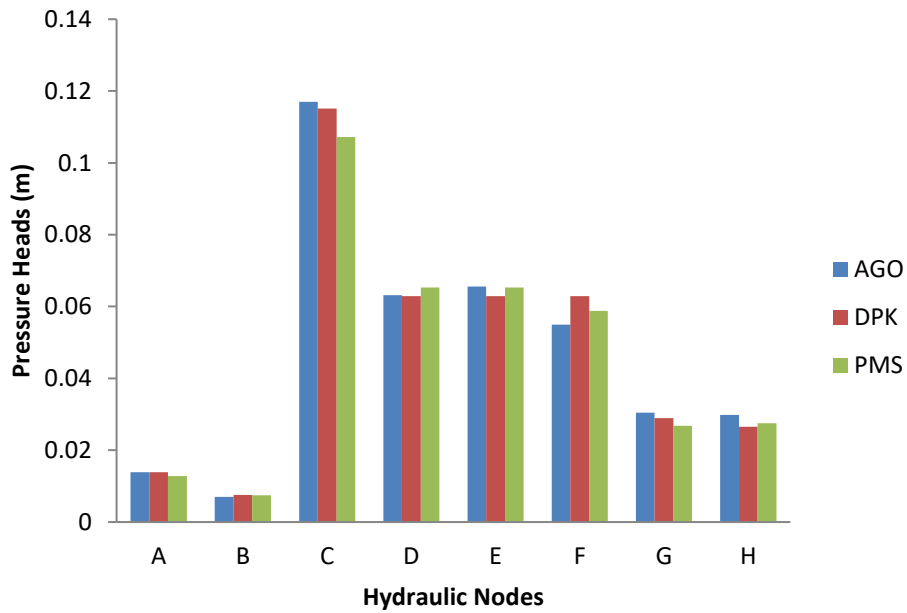
Figure 4.1: Pressure heads at various hydraulic nodes of the pipeline

4.1.2   Velocity head evaluation results

Figure 4.2 depicts the nature and pattern of the velocity head along the pipeline network for all the fluids (AGO, DPK, and PMS). As the Figure depicts, the velocity head in the pipeline network is high at nodes upstream of the pump (nodes A and B). This is because the fluids at these nodes need more energy to travel from the upstream to the downstream end. The Figure depicted that the velocity head is reducing along the downstream side of the network.
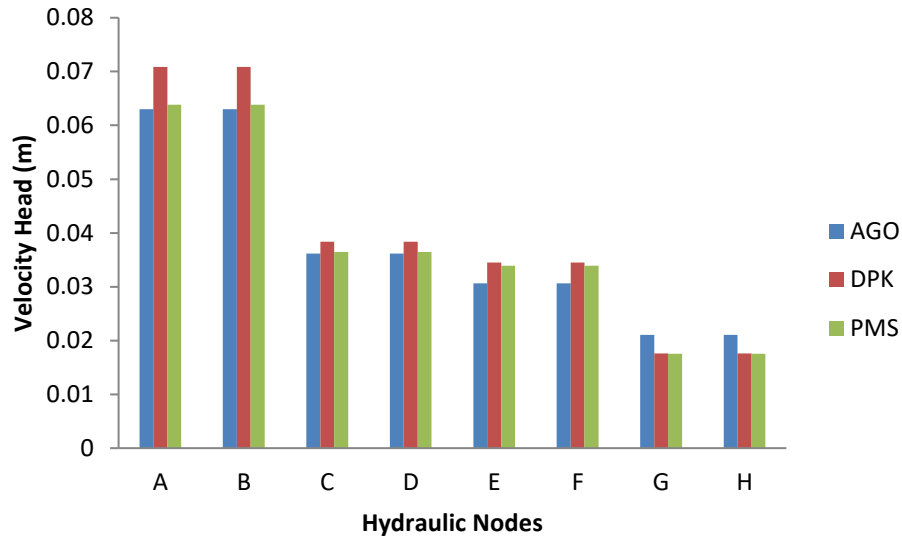
Figure 4.2: Velocity heads at various hydraulic nodes of the pipeline

4.2   Simulation Results

Simulation results of HT due to sudden VCTs and due to sudden pump failures in a refined petroleum product pipeline transporting AGO, DPK, and PMS are presented in this section.

4.2.1   Convergence study

The convergence is a parameter used for establishing the end of the iteration process for solving the non-linear hydraulic model equations in the steady-state flow conditions and at the boundary conditions of the transient state. If the comparative difference for each component between the last calculation of vector and the previous solution (iteration) is less than the specified convergence standard, the solution is presumed to have converged. In WANDA software, for the calculation of steady-state flow condition, it is necessary to set the minimum number of iterations to obtain a completely converged and satisfied solution. Time steps are used for a transient state flow where the properties

of the flow change with time, the time between each iteration is specified. The solver will start solving the equations based on the time steps (it will start at time 0), then it will proceeds until the specified final time is reached or convergence is achieved. In this research, a time step of 0.1 s was used and a simulation time of 100 s for all the fluids. Also, for all the simulation run, it converged after 1,001 iterations. The software has a convergence criterion relative error of $1.000e^{-6}$.

4.2.2   Simulation results of sudden valve closure for AGO, DPK and PMS

The initial operational pressure and flow rate use in this research for AGO, DPK and PMS were 120 kPa and 160 m^3/hr respectively. However, due to sudden valve closure, the pressure of the fluid fluctuates between a minimum and maximum pressure before stabilization.

4.2.2.1 *Simulation results of AGO for different VCTs*

Figures 4.3 present results of pressure surges developed due to VCT of 4.75s. The Figure depicts that positive and negative pressure surges would be experienced at nodes F and B of the pipeline. A positive peak pressure surge of 1,419 kPa and a least negative pressure surge of –98 kPa will developed at nodes F and B respectively. The Figure also depicts that the pressure surges fluctuate at various times between maximum and minimum pressure values until stabilities were established at an operational pressure of about 1,200 kPa.

Figure 4.3: Pressure transients at H-nodes for a VCT of 4.75 s in AGO pipeline

Figure 4.4 present results of pressure surges developed due to VCT of 9.5s. The Figure depicts that positive and negative pressure surges would be experienced at nodes F and B of the pipeline. A positive peak pressure surge of 1,392 kPa and a least negative pressure surge of –98 kPa will developed at nodes F and B respectively. The Figure also depicts that the pressure surges fluctuate at various times between maximum and minimum pressure values until stabilities were established at an operational pressure of about 1,200 kPa.

Figure 4.4: Pressure transients at H-nodes for a VCT of 9.5 s in AGO pipeline

Figure 4.5 present results of pressure surges developed due to VCT of 19s. The Figure depicts that positive and negative pressure surges would be experienced at nodes F and B of the pipeline. A positive peak pressure surge of 1,373 kPa and a least negative pressure surge of –98 kPa will developed at nodes F and B respectively. The Figure also depicts that the pressure surges fluctuate at various times between maximum and minimum pressure values until stabilities were established at an operational pressure of about 1,200 kPa.
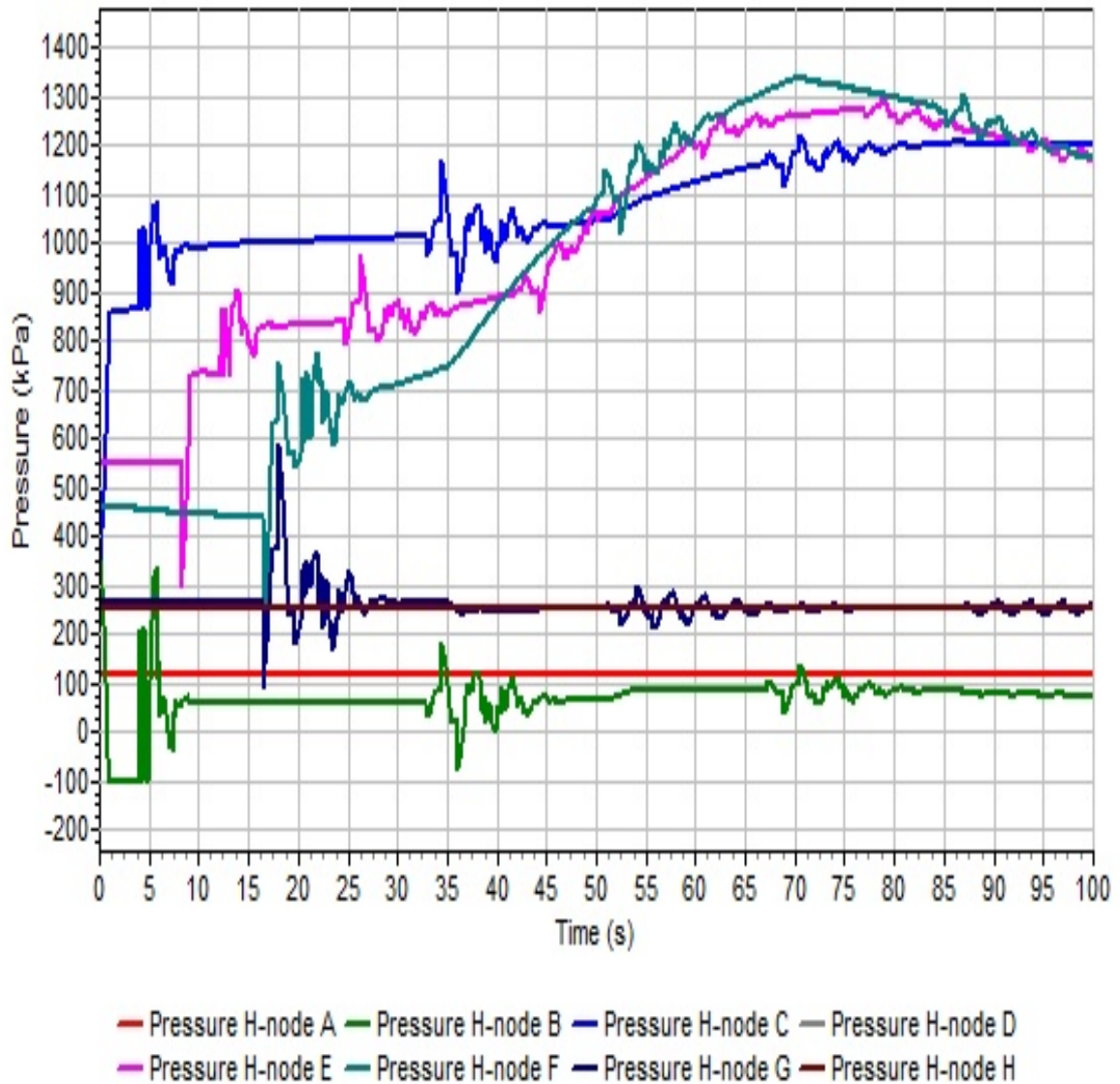
Figure 4.5: Pressure transients at H-nodes for a VCT of 19 s in AGO pipeline

Figure 4.6 present results of pressure surges developed due to VCT of 38s. The Figure depicts that positive and negative pressure surges would be experienced at nodes F and B of the pipeline. A positive peak pressure surge of 1,336 kPa and a least negative pressure surge of –98 kPa will developed at nodes F and B respectively. The Figure also depicts that the pressure surges fluctuate at various times between maximum and minimum pressure values until stabilities were established at an operational pressure of about 1,200 kPa.
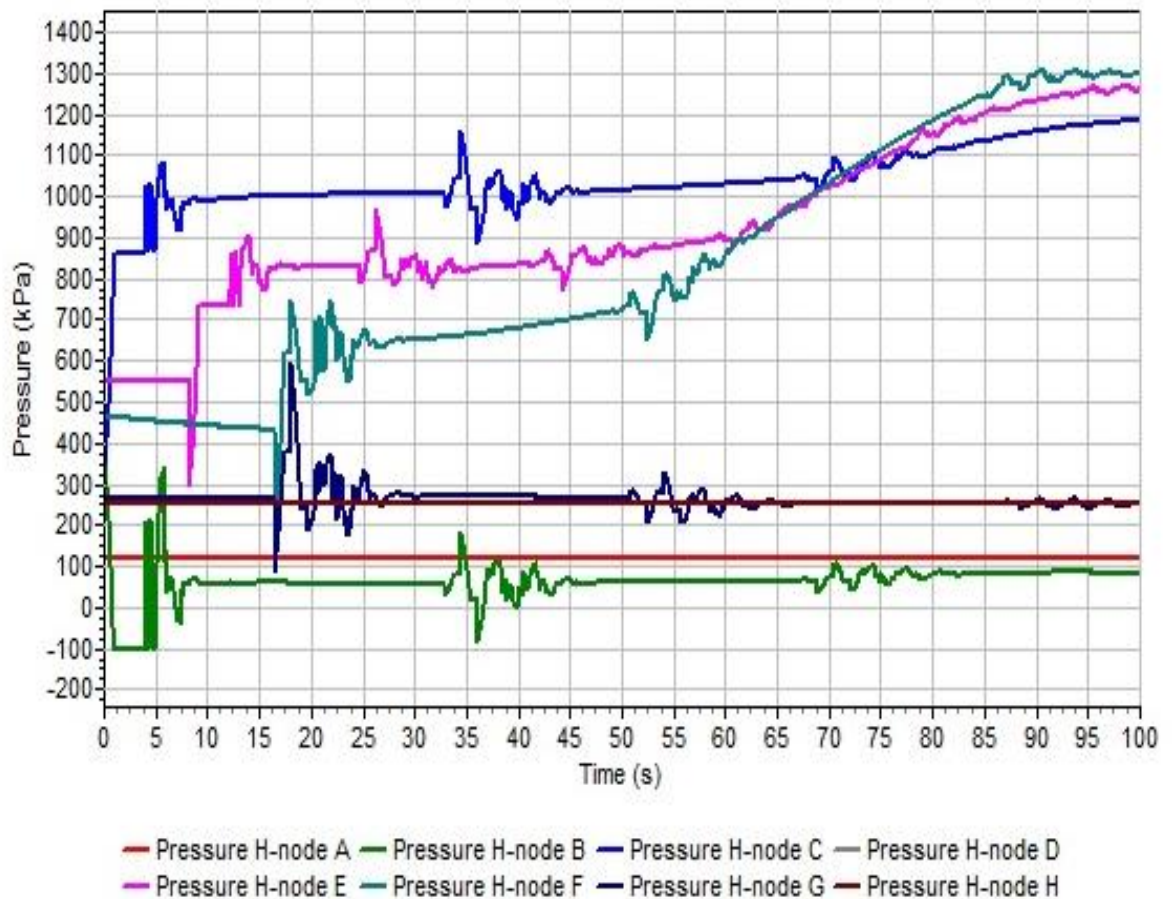
Figure 4.6: Pressure transients at H-nodes for a VCT of 38 s in AGO pipeline

Figure 4.7 present results of pressure surges developed due to VCT of 76s. The Figure depicts that positive and negative pressure surges would be experienced at nodes F and B of the pipeline. A positive peak pressure surge of 1,311 kPa and a least negative pressure surge of –98 kPa will developed at nodes F and B respectively. The Figure also depicts that the pressure surges fluctuate at various times between maximum and minimum pressure values until stabilities were established at an operational pressure of about 1,200 kPa.
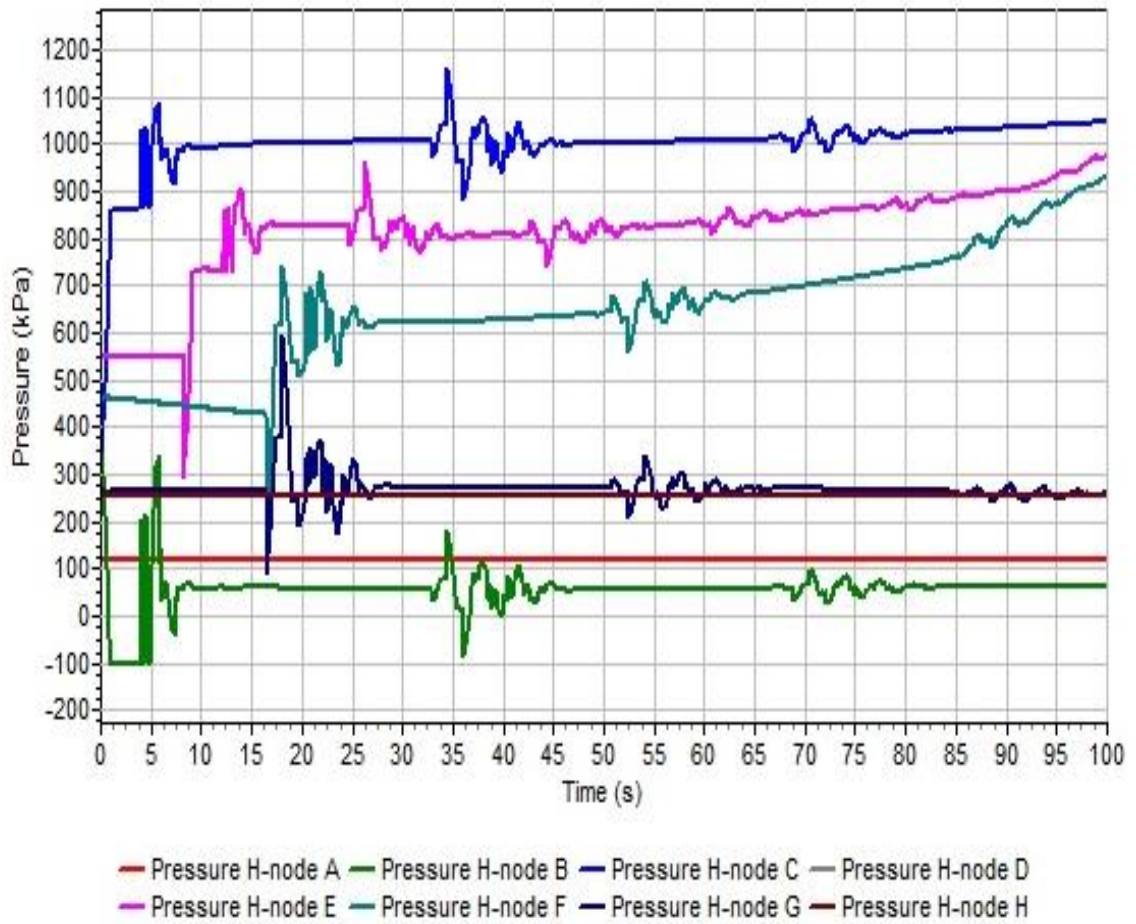
Figure 4.7: Pressure transients at H-nodes for a VCT of 76 s in AGO pipeline

Figure 4.8 present results of pressure surges developed due to VCT of 152 s. The Figure depicts that positive and negative pressure surges would be experienced at nodes F and B of the pipeline. A positive peak pressure surge of 1,272 kPa and a least negative pressure surge of –98 kPa will developed at nodes F and B respectively. The Figure also depicts that the pressure surges fluctuate at various times between maximum and minimum pressure values until stabilities were established at an operational pressure of about 1,200 kPa.
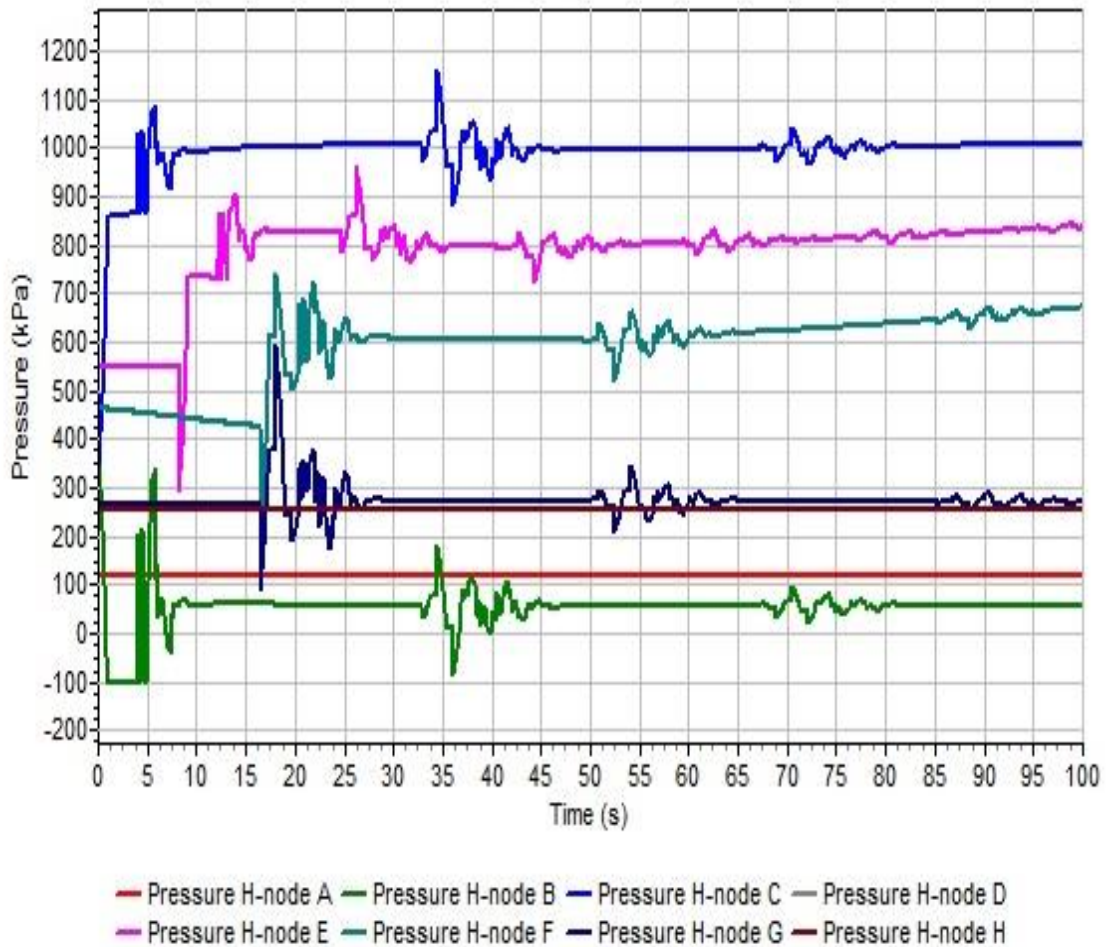
Figure 4.8: Pressure transients at H-nodes for a VCT of 152 s in AGO pipeline

Figure 4.9 present results of pressure surges developed due to VCT of 308s. The Figure depicts that positive and negative pressure surges would be experienced at nodes F and B of the pipeline. A positive peak pressure surge of 1,267 kPa and a least negative pressure surge of –98 kPa will developed at nodes F and B respectively. The Figure also depicts that the pressure surges fluctuate at various times between maximum and minimum pressure values until stabilities were established at an operational pressure of about 1,200 kPa.
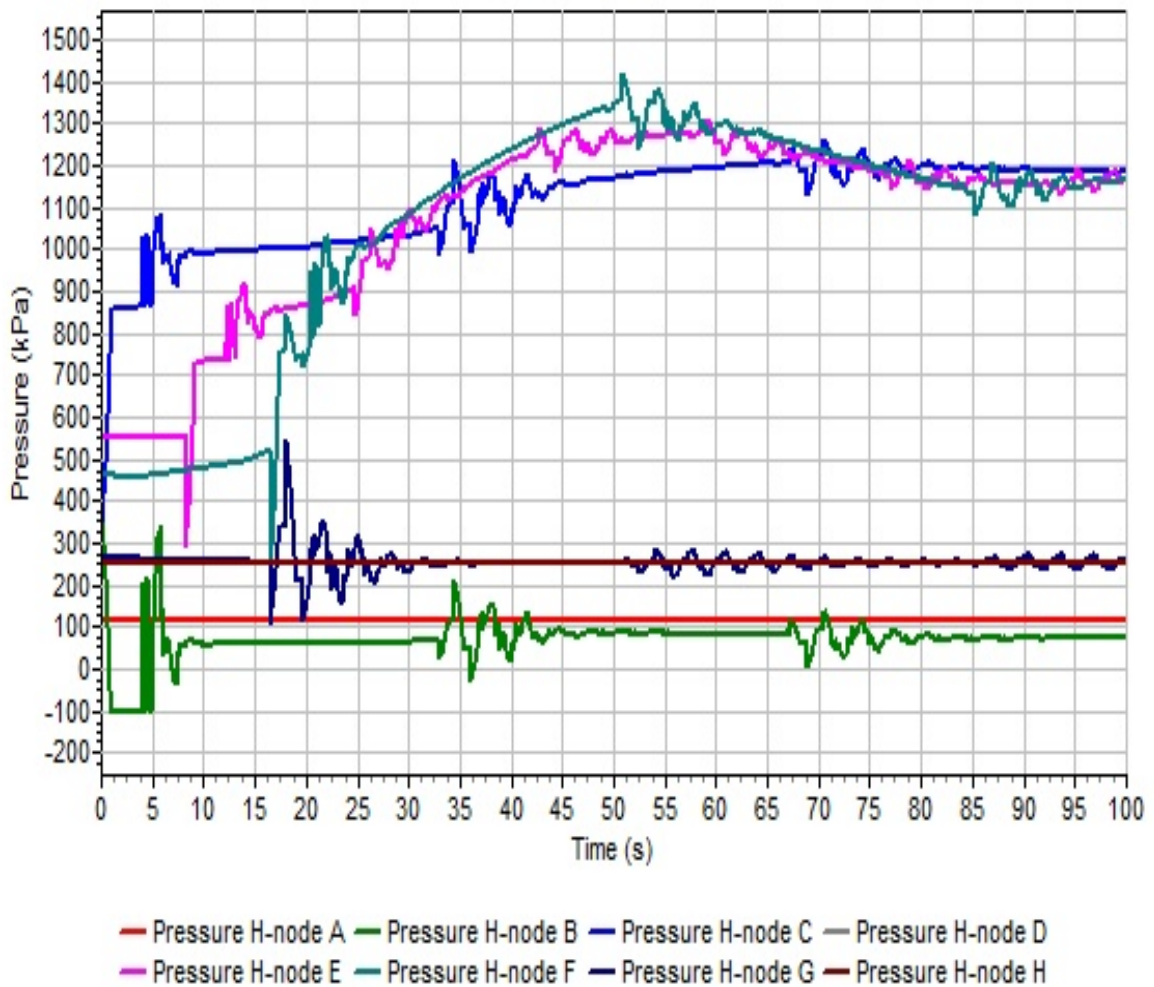
Figure 4.9: Pressure transients at H-nodes for a VCT of 304 s in AGO pipeline

Figure 4.10 present results of pressure surges developed due to VCT of 608s. The Figure depicts that positive and negative pressure surges would be experienced at nodes F and B of the pipeline. A positive peak pressure surge of 1,269 kPa and a least negative pressure surge of –98 kPa will developed at nodes F and B respectively. The Figure also depicts that the pressure surges fluctuate at various times between maximum and minimum pressure values until stabilities were established at an operational pressure of about 1,200 kPa.
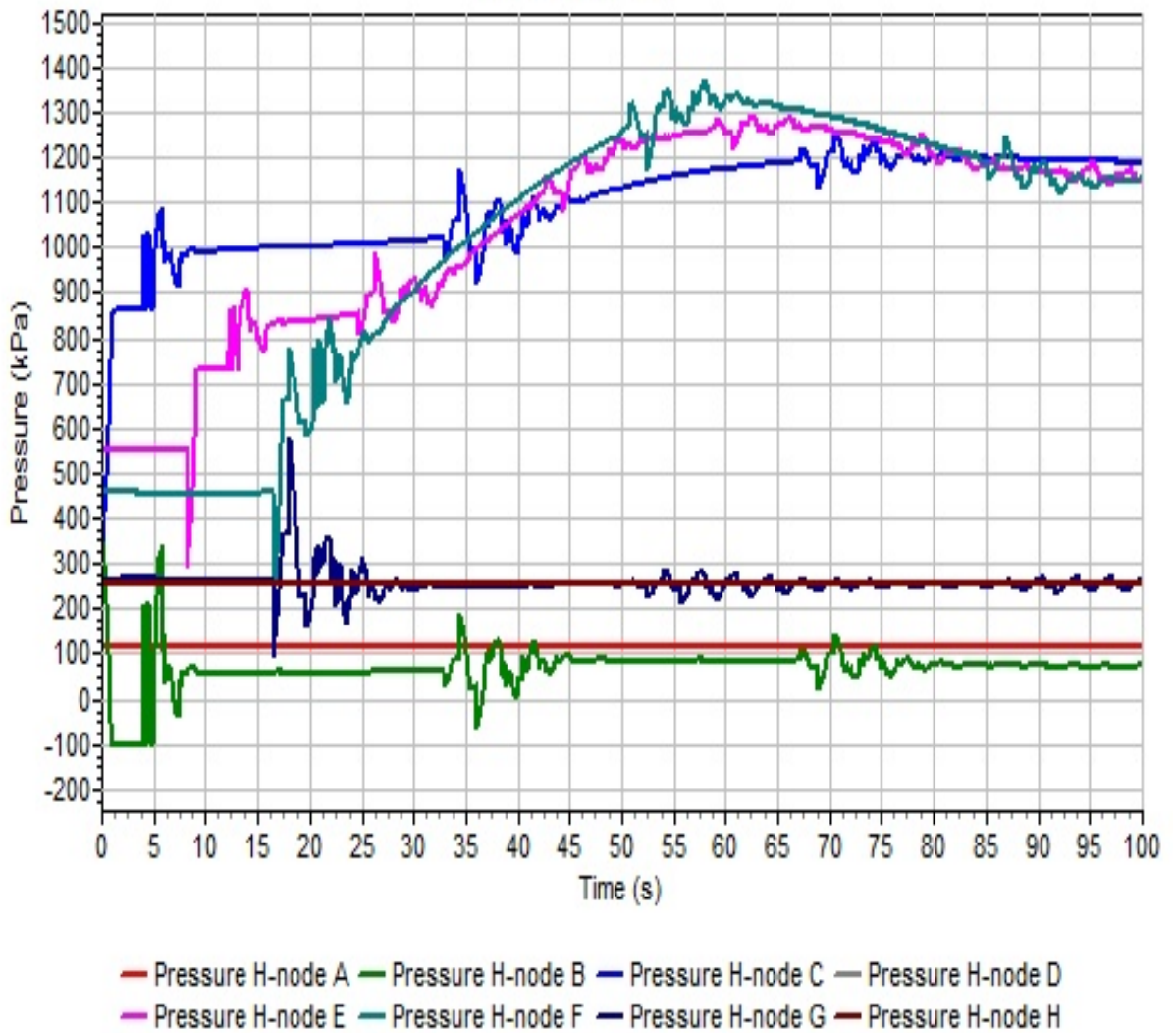
Figure 4.10: Pressure transients at H-nodes for a VCT of 608 s in AGO pipeline

Figure 4.11 depicted the magnitude and behaviours of the cavitations that would be developed due to the development of negative pressures at some nodes. A cavitation voids of magnitude 0.003895 might be developed at nodes B because of the development of negative pressure at these nodes by all the VCTs. The development of this cavitation voids is in agreement with what Gseaa& Dekam (2010) have reported in their research findings.
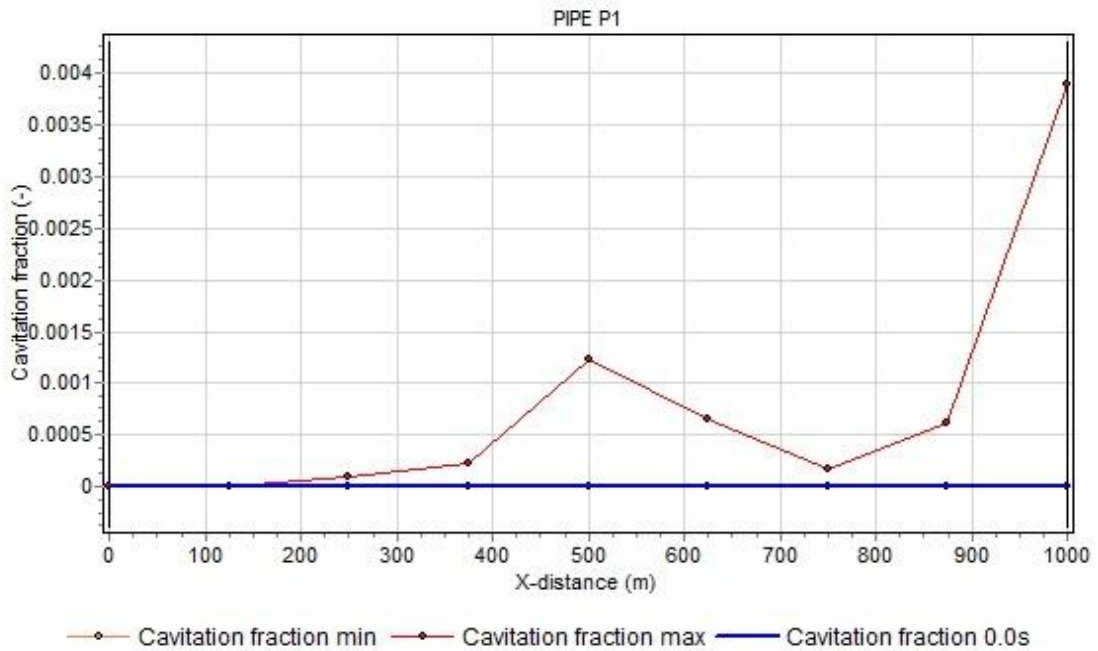
Figure 4.11: Cavitation formed due to sudden valve closure in an AGO pipeline

Figure 4.12 depicts the summary of pressure surges developed in the AGO pipeline according to various VCTs. The Figure showed that the pressure surge decreases with increase in VCT. This could be as a result of the way the flow of the fluid was halted. When a flow is stopped suddenly, the particles of the fluid will start to collide with one another with high forces thereby generating high surges. The pressure surge developed due to VCTs of 76 s to 608 s are below the minimum design pressure range of the pipes at 1,379 kPa. However, the pressure surges developed due to VCTs of 4.75 s to 38 s are above the minimum design pressure of the pipes, but above the design pressure of the nodal sets of 1,035 kPa. The pressure surge dropped from about 1,420 kPa at a VCT of 4.75 s to about 950 kPa at VCTs of 152 s – 608 s. This decrease in pressure surge due to an increase in VCT could be because of a delay in changing the operational status of the flow control device, which in turn also delays the rapid changes in pressure and velocity. At the VCTs of 152 s – 608 s, the magnitude of pressure surges due to sudden valve closure remains almost constant at about 950 kPa. The surge pressure of 950 kPa

is below the maximum allowable operating pressure of the flange of about 1,400 kPa and maximum allowable working pressure of the flange of about 1,050 kPa – 1,260 kPa. According to Carvajal & Bohorquez (2018) a VCT, where the pressure surge effects in a pipeline system is marginal or cannot be reduced further is called marginal time. Hence, VCT range of 152 s and above were considered as marginal VCT for an AGO pipeline with a diameter of 0.3556 m. Valve closure rate range of 0.0006 m/s - 0.0023 m/s was established as the marginal valve closure velocity of a standard 0.3556 m (14 inches) petroleum pipes transporting AGO.
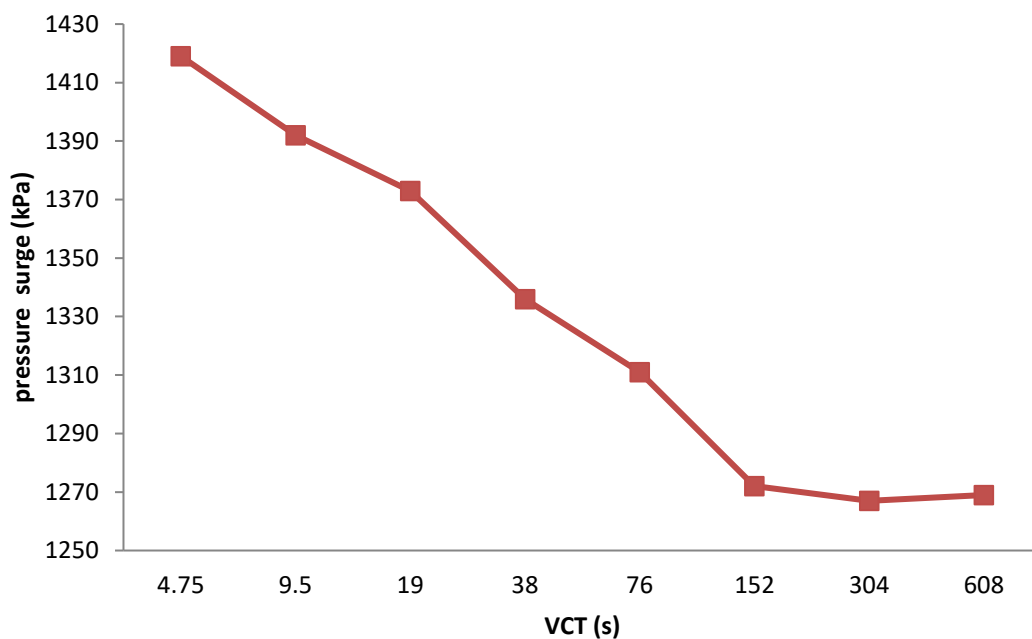
Figure 4.12: Pressure surges at different VCTs in an AGO pipeline

4.2.2.2 *Simulation results of DPK for different VCTs*

The pressure of DPK under normal operating conditions at nodes A, B, C, D, E, F, G, and H are 110.4 kPa, 60 kPa, 915 kPa, 500 kPa, 500 kPa, 500 kPa, 230 kPa, and 210.56 kPa respectively. However, due to the sudden valve closure, the pressure of the fluid

fluctuates between a minimum and maximum pressures before stabilization. Figures 4.13 – 4.20 present results of pressure surges developed due to VCTs of 4.4 s, 8.5 s, 17 s, 34 s, 68 s, 136 s, 272 s, and 544 s respectively in a petroleum pipeline network transporting DPK.

The Figure 4.13 depicts positive and negative pressure surges experienced at the various nodes of the pipeline due to VCT of 4.4 s. The simulation result showed that a peak positive pressure surge of 1,461 kPa and a least negative pressure surge of –99 kPa would be experienced at nodes F and B due to VCT of 4.4 s. The Figure also depicts that the pressure surges fluctuates at various times between maximum and minimum pressure values until stability was established at an operational pressure of about 1,100 kPa.
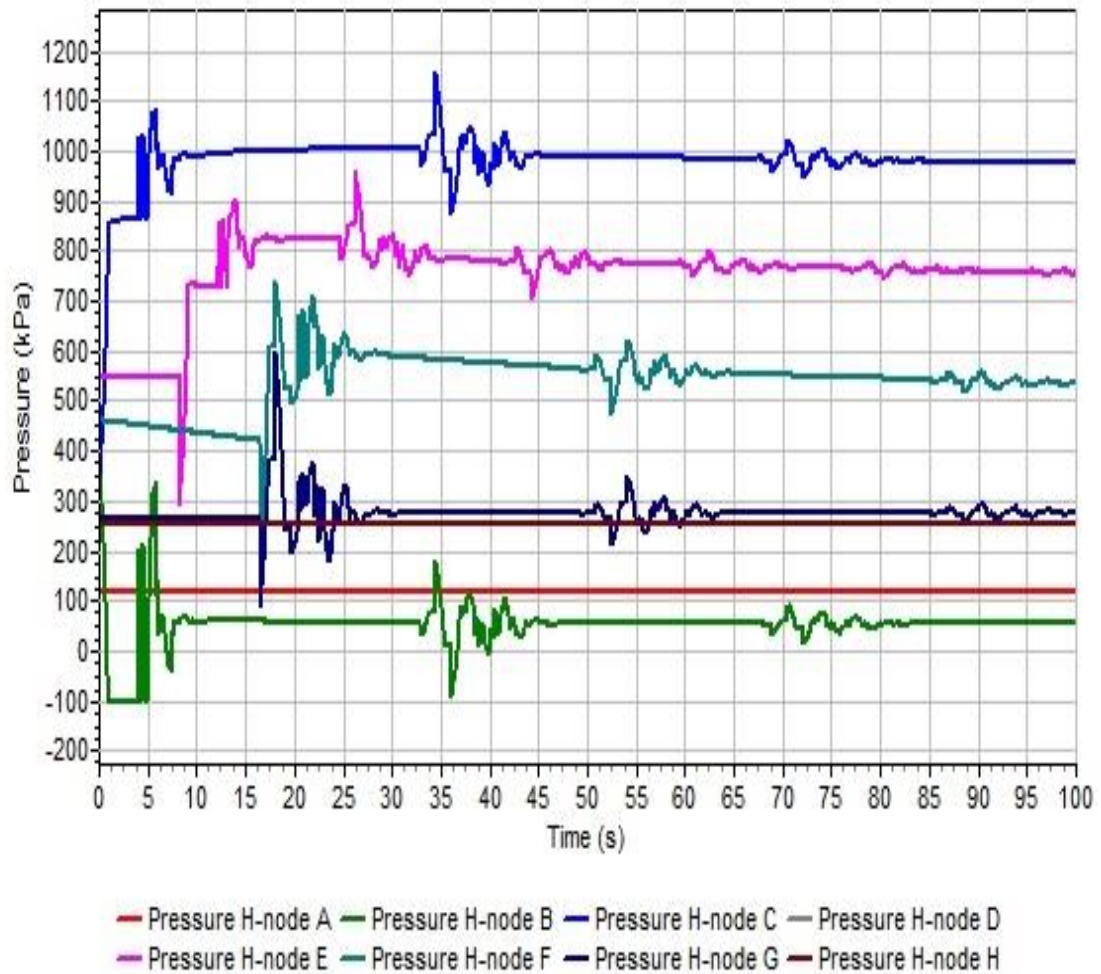

Figure 4.13: Pressure transients at H-nodes for a VCT of 4.38 s in DPK pipeline

The Figure 4.14 depicts positive and negative pressure surges experienced at the various nodes of the pipeline due to VCT of 8.5 s. The simulation result showed that a peak positive pressure surge of 1,456 kPa and a least negative pressure surge of –99 kPa would be experienced at nodes F and B due to VCT of 8.5 s. The Figure also depicts that the pressure surges fluctuates at various times between maximum and minimum pressure values until stability was established at an operational pressure of about 1,100 kPa.
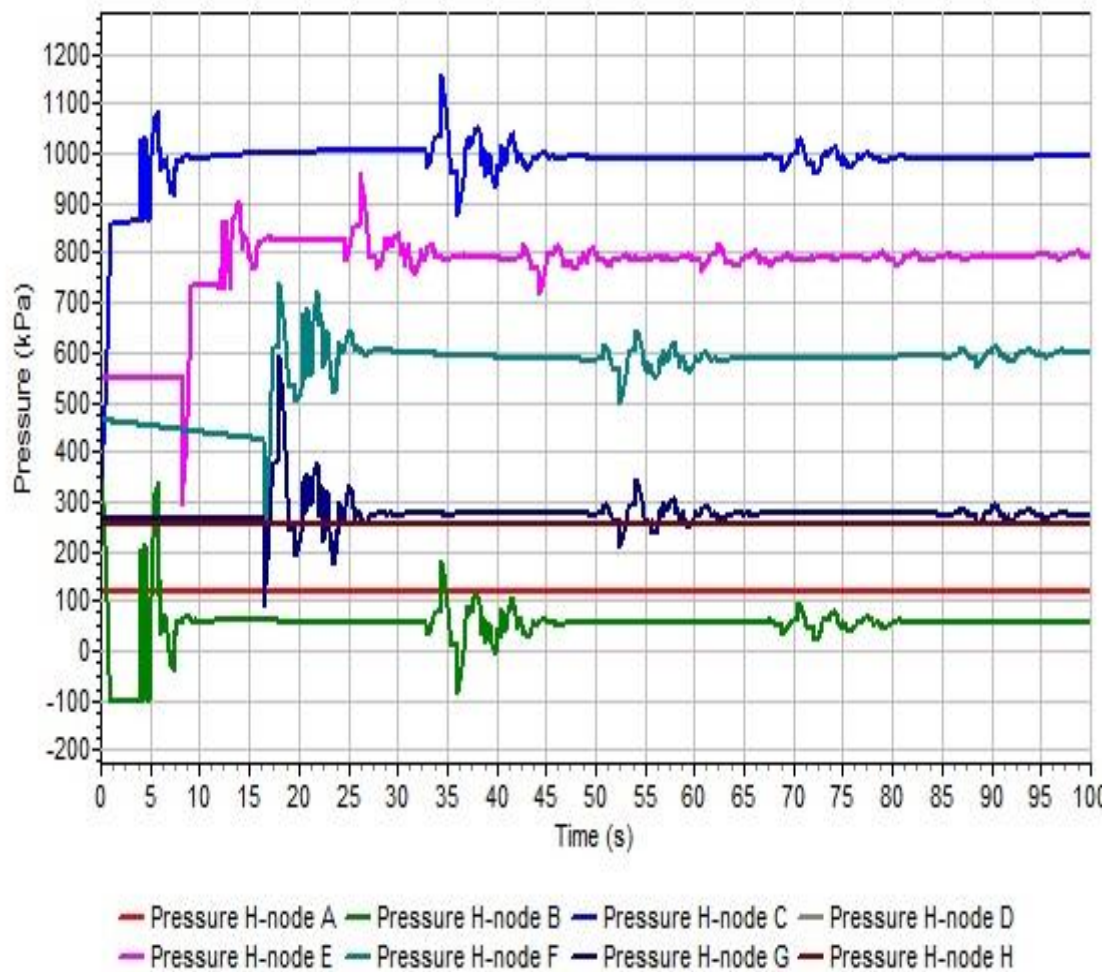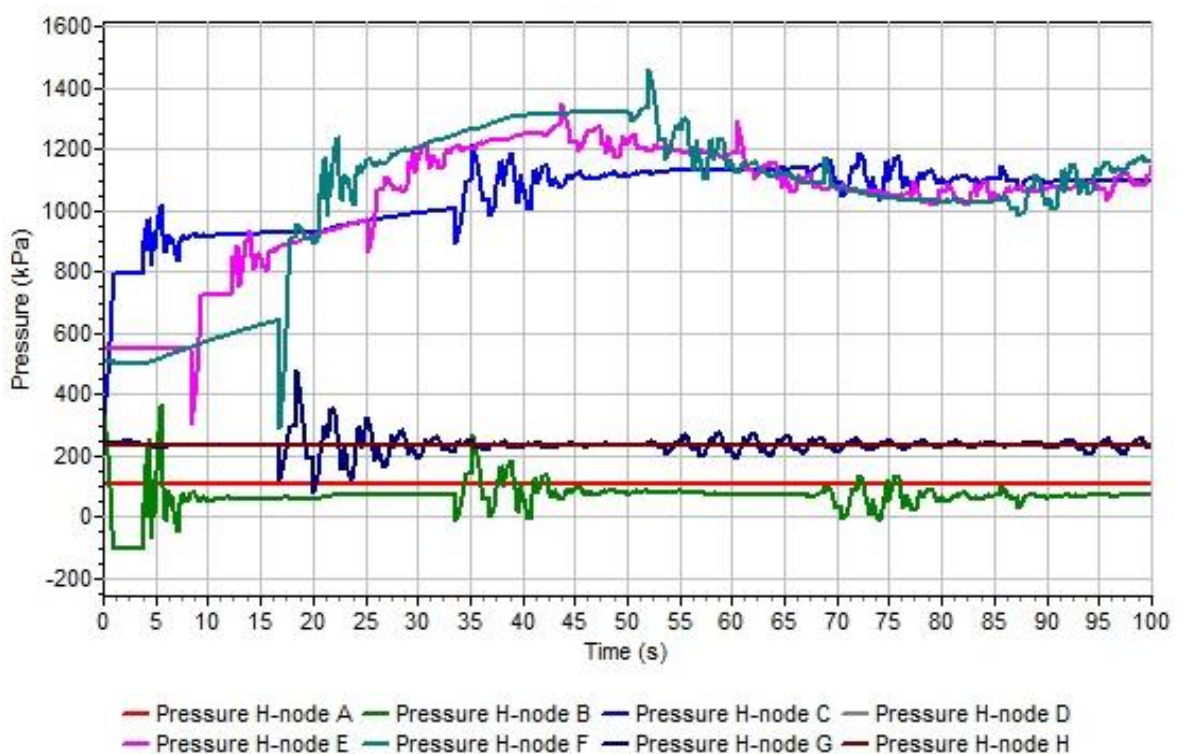

Figure 4.14: Pressure transients at H-nodes for a VCT of 8.5 s in DPK pipeline

The Figure 4.15 depicts positive and negative pressure surges experienced at the various nodes due to VCT of 17 s. The simulation result showed that a peak positive pressure surge of 1,443 kPa and a least negative pressure surge of –99 kPa would be experienced at nodes F and B due to VCT of 17 s. The Figure also depicts that the pressure surges

fluctuates at various times between maximum and minimum pressure values until stability was established at an operational pressure of about 1,100 kPa.
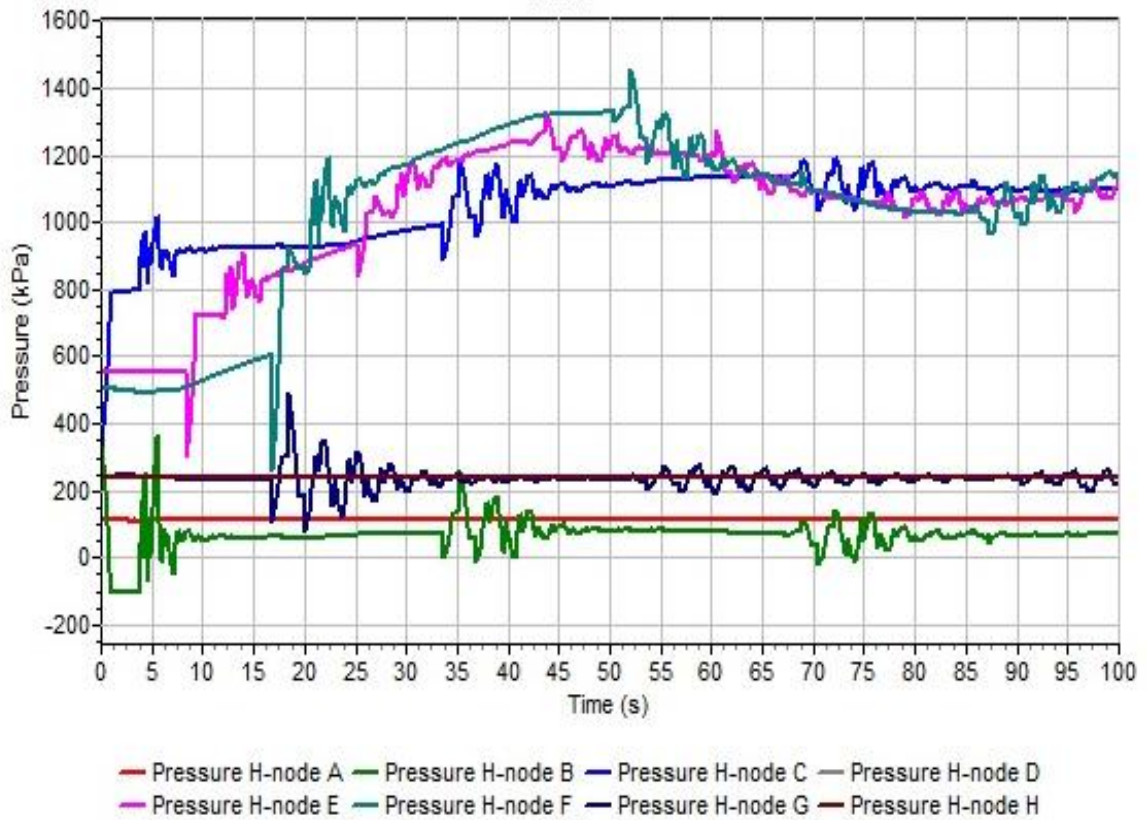
Figure 4.15: Pressure transients at H-nodes for a VCT of 17 s in DPK pipeline

The Figure 4.16 depicts positive and negative pressure surges experienced at the various nodes of the pipeline due to VCT of 34 s. The simulation result showed that a peak positive pressure surge of 1,442 kPa and a least negative pressure surge of –99 kPa would be experienced at nodes F and B due to VCT of 34 s. The Figure also depicts that the pressure surges fluctuates at various times between maximum and minimum pressure values until stability was established at an operational pressure of about 1,100 kPa.
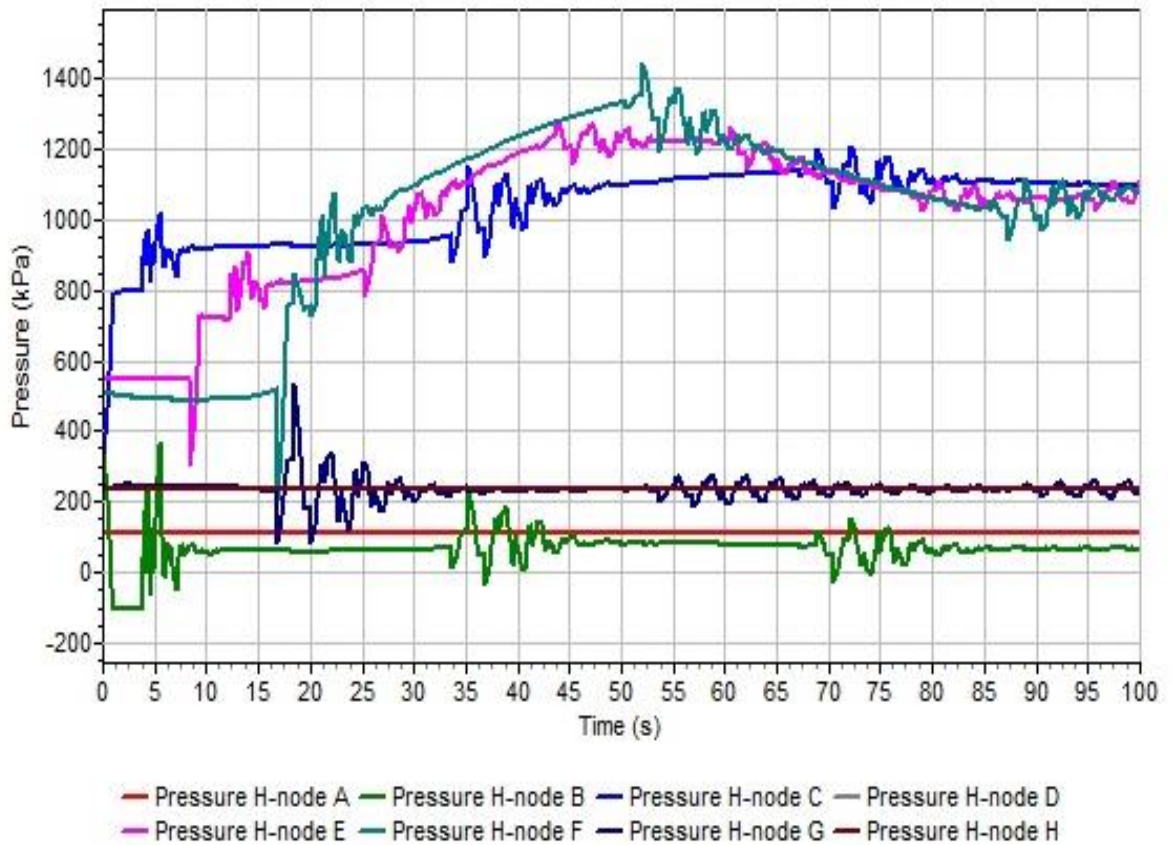
Figure 4.16: Pressure transients at H-nodes for a VCT of 34 s in DPK pipeline

The Figure 4.17 depicts positive and negative pressure surges experienced at the various nodes of the pipeline due to VCT of 68 s. The simulation result showed that a peak positive pressure surge of 1,281 kPa and a least negative pressure surge of –99 kPa would be experienced at nodes F and B due to VCT of 68 s. The Figure also depicts that the pressure surges fluctuates at various times between maximum and minimum pressure values until stability was established at an operational pressure of about 1,100 kPa.

Figure 4.17: Pressure transients at H-nodes for a VCT of 68 s in DPK pipeline

The Figure 4.18 depicts positive and negative pressure surges experienced at the various nodes of the pipeline due to VCT of 136 s. The simulation result showed that a peak positive pressure surge of 1,272 kPa and a least negative pressure surge of –99 kPa would be experienced at nodes F and B due to VCT of 136 s. The Figure also depicts that the pressure surges fluctuates at various times between maximum and minimum pressure values until stability was established at an operational pressure of about 1,100 kPa.

Figure 4.18: Pressure transients at H-nodes for a VCT of 136 s in DPK pipeline

The Figure 4.19 depicts positive and negative pressure surges experienced at the various nodes of the pipeline due to VCT of 272 s. The simulation result showed that a peak positive pressure surge of 1,267 kPa and a least negative pressure surge of –99 kPa would be experienced at nodes F and B due to VCT of 272 s. The Figure also depicts that the pressure surges fluctuates at various times between maximum and minimum pressure values until stability was established at an operational pressure of about 1,100 kPa.

Figure 4.19: Pressure transients at H-nodes for a VCT of 272 s in DPK pipeline

The Figure 4.20 depicts positive and negative pressure surges experienced at the various nodes of the pipeline due to VCT of 544 s. The simulation result showed that a peak positive pressure surge of 1,269 kPa and a least negative pressure surge of –99 kPa would be experienced at nodes F and B due to VCT of 544 s. The Figure also depicts that the pressure surges fluctuates at various times between maximum and minimum pressure values until stability was established at an operational pressure of about 1,100 kPa.
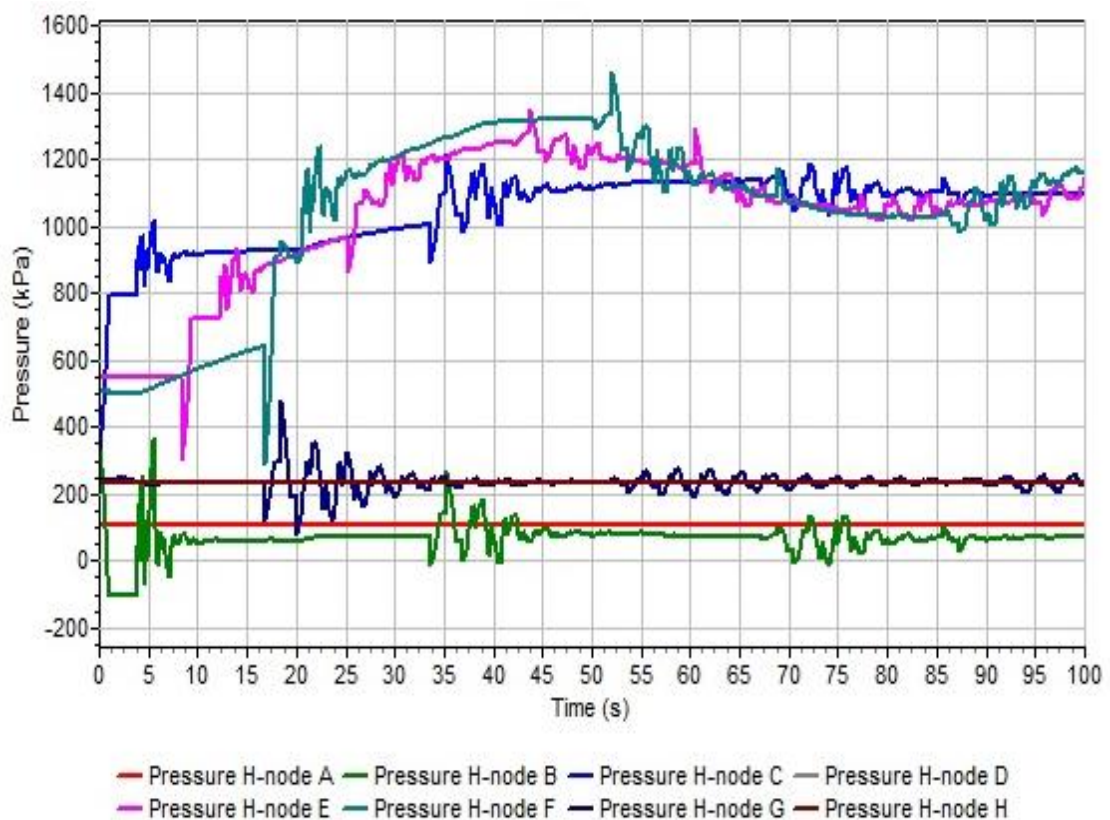
Figure 4.20: Pressure transients at H-nodes for a VCT of 544 s in DPK pipeline

Figure 4.21 depicts the magnitude and behaviour of cavitation voids developed at nodes B for all the VCTs. The development of the negative pressure at node B for all the VCTs investigated might also lead to the formation of cavitations voids of magnitude 0.003143 at that node and along pipe P1 for all the VCTs in a DPK pipeline as shown in Figure 4.21. The development of this cavitation voids is in agreement with what Gseaa& Dekam (2010) have reported in their research findings.
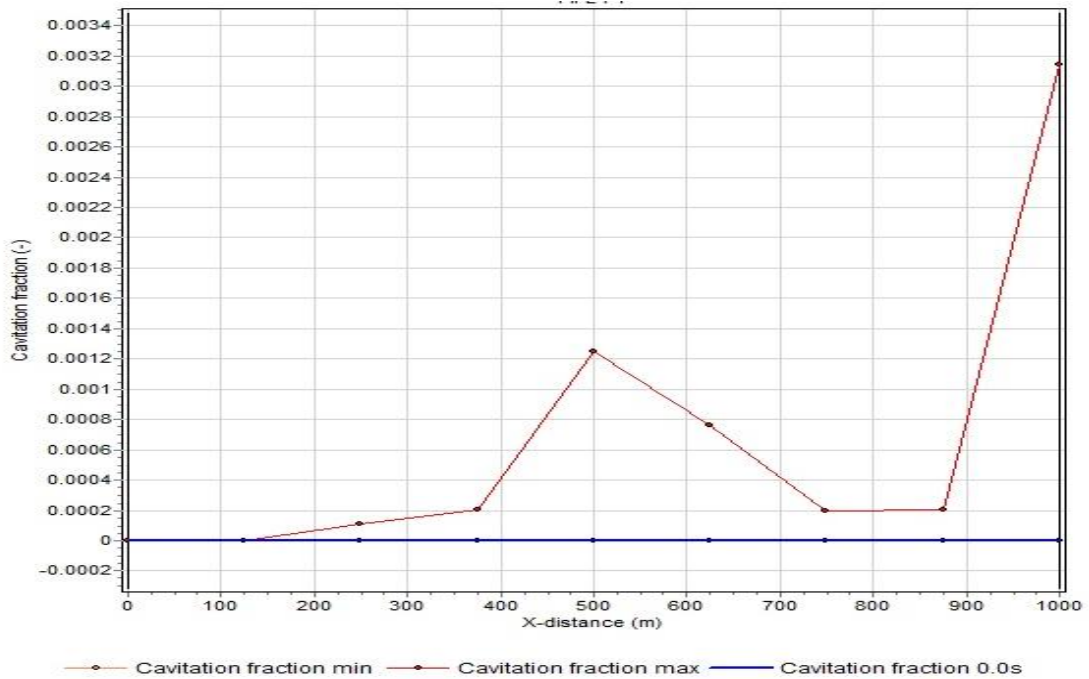
Figure 4.21: Cavitations formed due to sudden valve closure in a DPK pipeline

Figure 4.22 shows the pattern of summary of peaks pressure surges being experienced due to various VCTs in a pipeline transporting DPK. The Figure depicts that the pressure surges decrease as the VCT is increased. The Figures also depicts that peak pressure surges of experienced due to VCTs of 4.4 s, 8.5 s, and 17 s are above the operational pressure of the nodal sets, gaskets and valve sittings at 1,035 kPa and the minimum design pressure of the pipes at 1,379 kPa but below the maximum design pressure of the pipes at 4,400 kPa. The pressure surge dropped from about 1,460 kPa at a VCT of 4.4 s to a pressure surge of about 1,180 kPa at a VCT of 136 s – 544 s. This decrease in pressure surge due to an increase in VCT could be as a result of the delay in changing the operational status of the flow control device which in turn also delays the rapid changes in pressure and velocity. At the VCTs of 136 s – 544 s, the magnitude of pressure surges due to sudden valve closure remains constant at about 1,180 kPa as shown in Figure 4.22, the pressure surge at this node is below the MAOP of the flange

of about 1,400 kPa and within the range of maximum allowable working pressure of the flange of about 1,050 kPa - 1,260 kPa. It can be also observe from Figure 4.22 that as from VCTs of 136 s – 544 s, the pressure surge remains almost constant. Hence, the VCT of 136 s – 544 s were considered as a marginal VCT of a 0.3556 m diameter pipeline transporting DPK. And valve closure rate range of 0.0006 m/s - 0.0025 m/s was established as the marginal valve closure velocity of a standard 0.3556 m (14 inches) petroleum pipes.
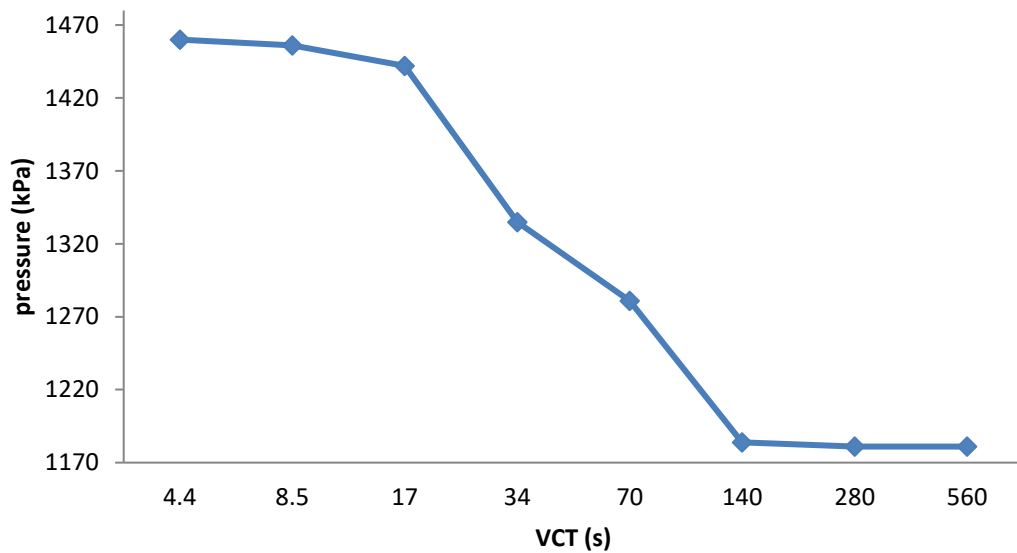
Figure 4.22: Pressure surges at different VCTs in a DPK pipeline

4.2.2.3 *Simulation Result of PMS for different VCTs*

The pressure of PMS under steady-state flow operation conditions at hydraulic nodes A, B, C, D, E, F, G, and H are 98.14 kPa, 57 kPa, 820 kPa, 500 kPa, 500 kPa, 450 kPa, 205 kPa, and 210.56 kPa respectively. Figures 4.23 – 4.30 present results of pressure surges developed due to VCTs of 4.5s, 9 s, 18s, 36s, 72s, 144s, 288, and 576s respectively in a petroleum pipeline network transporting PMS.

Figure 4.23 depicts the development of positive and negative pressure surges at nodes F and B respectively due to VCT of 4.5 s. The simulation result showed that a peak positive pressure surge of 1,321 kPa and a least negative pressure surge of – 52 kPa would be experienced at nodes F and B respectively for a VCT of 4.5 s. The Figure also depicts that the pressure surges fluctuates at various times between maximum and minimum pressure values until stability was established at an operational pressure of about 1,000 kPa.
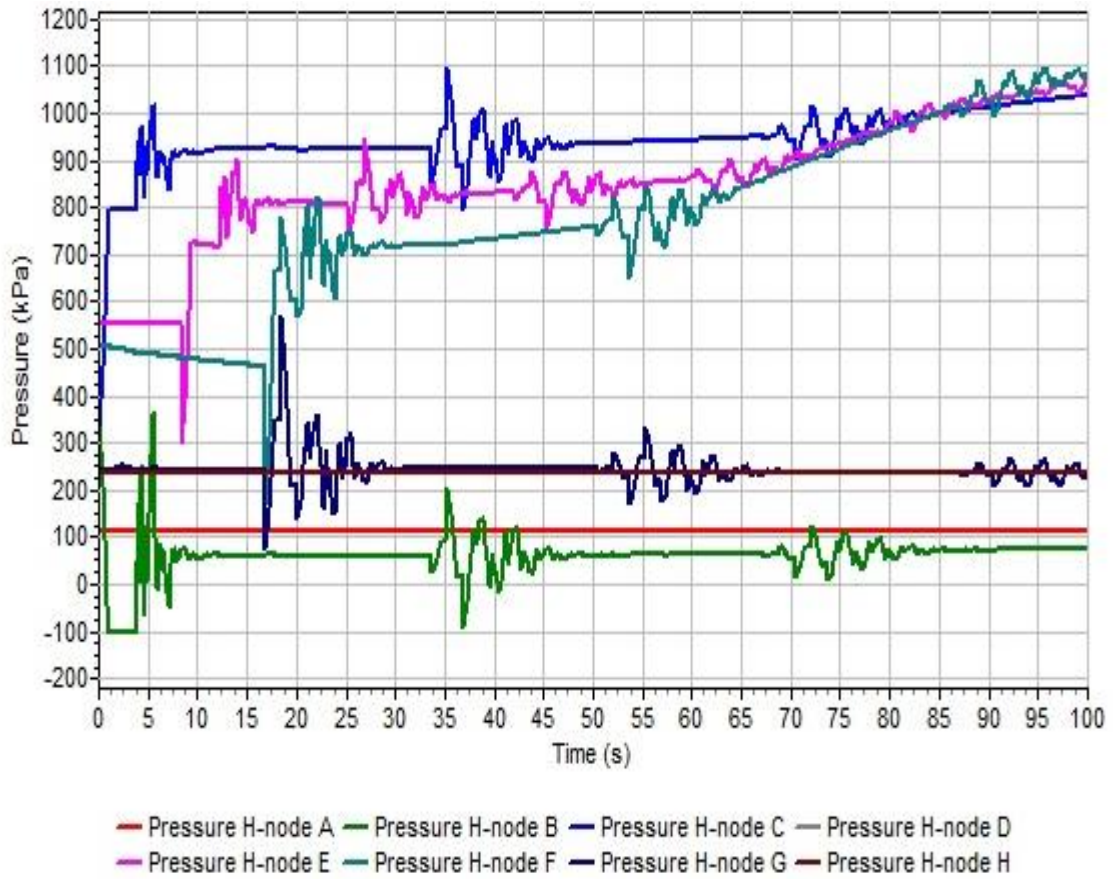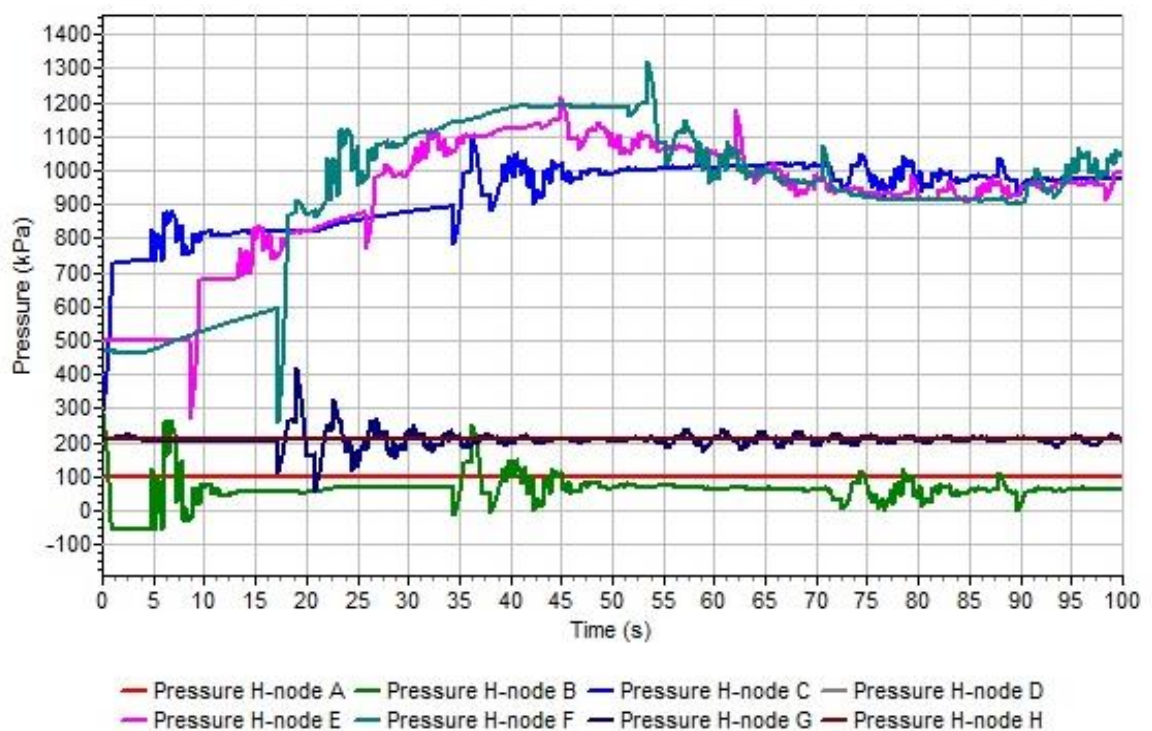

Figure 4.23: Pressure transients at H-nodes for a VCT of 4.5 s in PMS pipeline

Figure 4.24 depicts the development of positive and negative pressure surges at nodes F and B respectively due to VCT of 9 s. The simulation result showed that a peak positive pressure surge of 1,317 kPa and a least negative pressure surge of – 52 kPa would be experienced at nodes F and B respectively for a VCT of 9 s. The Figure also depicts

that the pressure surges fluctuates at various times between maximum and minimum pressure values until stability was established at an operational pressure of about 1,000 kPa.
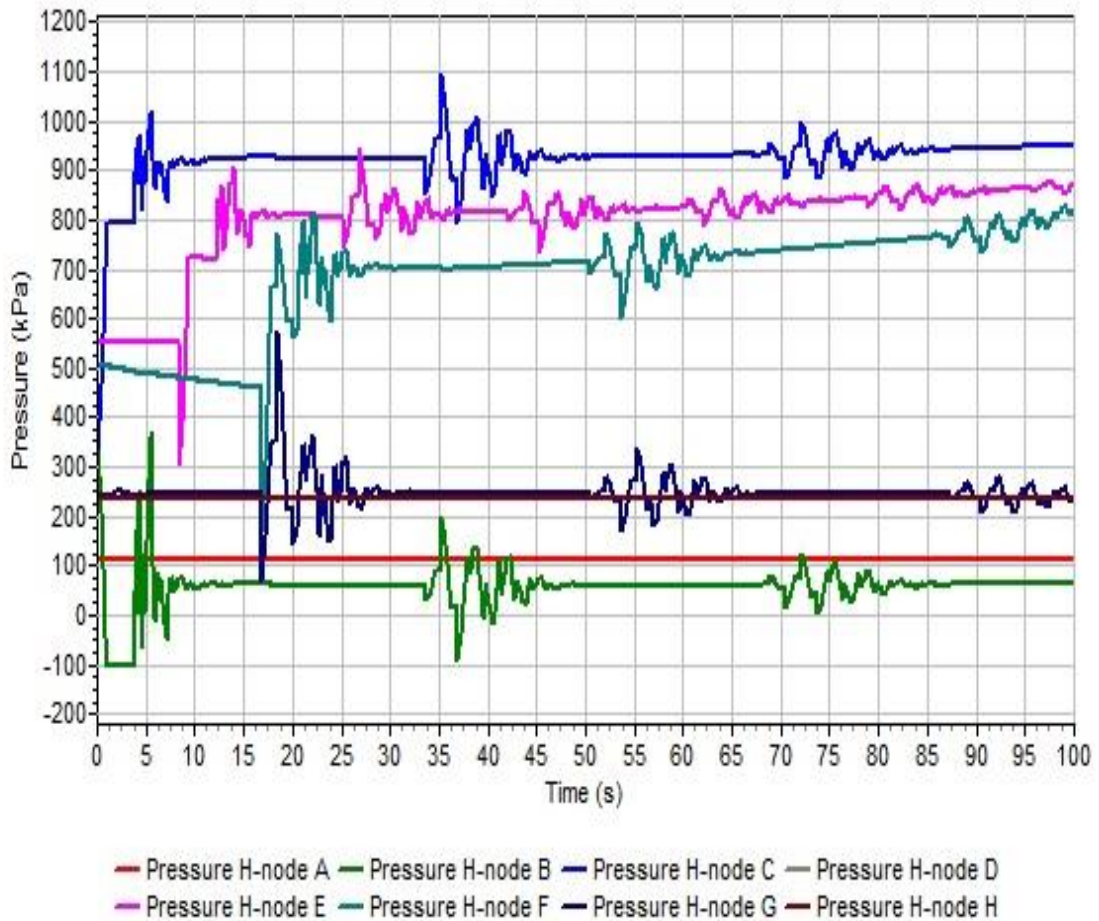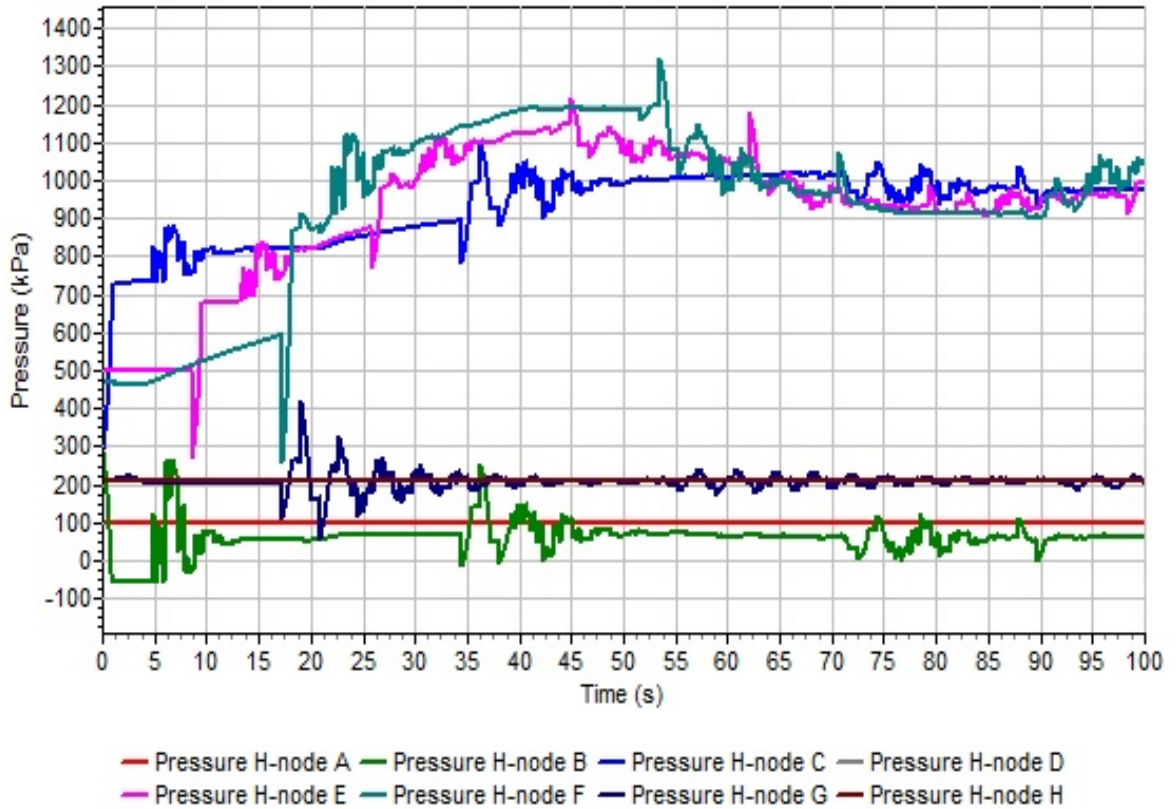

Figure 4.24: Pressure transients at H-nodes for a VCT of 9 s in PMS pipeline

Figure 4.25 depicts the development of positive and negative pressure surges at nodes F and B respectively due to VCT of 18 s. The simulation result showed that a peak positive pressure surge of 1,305 kPa and a least negative pressure surge of – 52 kPa would be experienced at nodes F and B respectively for a VCT of 18 s. The Figure also depicts that the pressure surges fluctuates at various times between maximum and minimum pressure values until stability was established at an operational pressure of about 1,000 kPa.
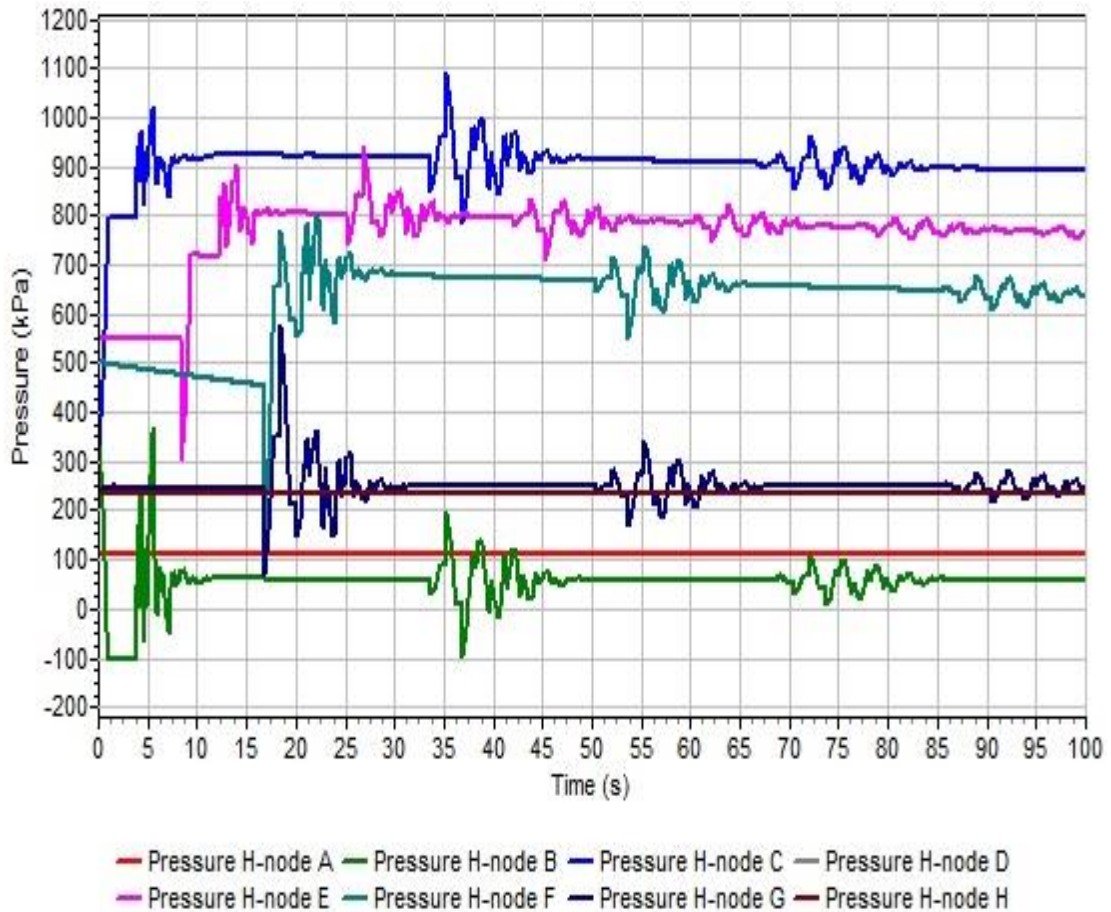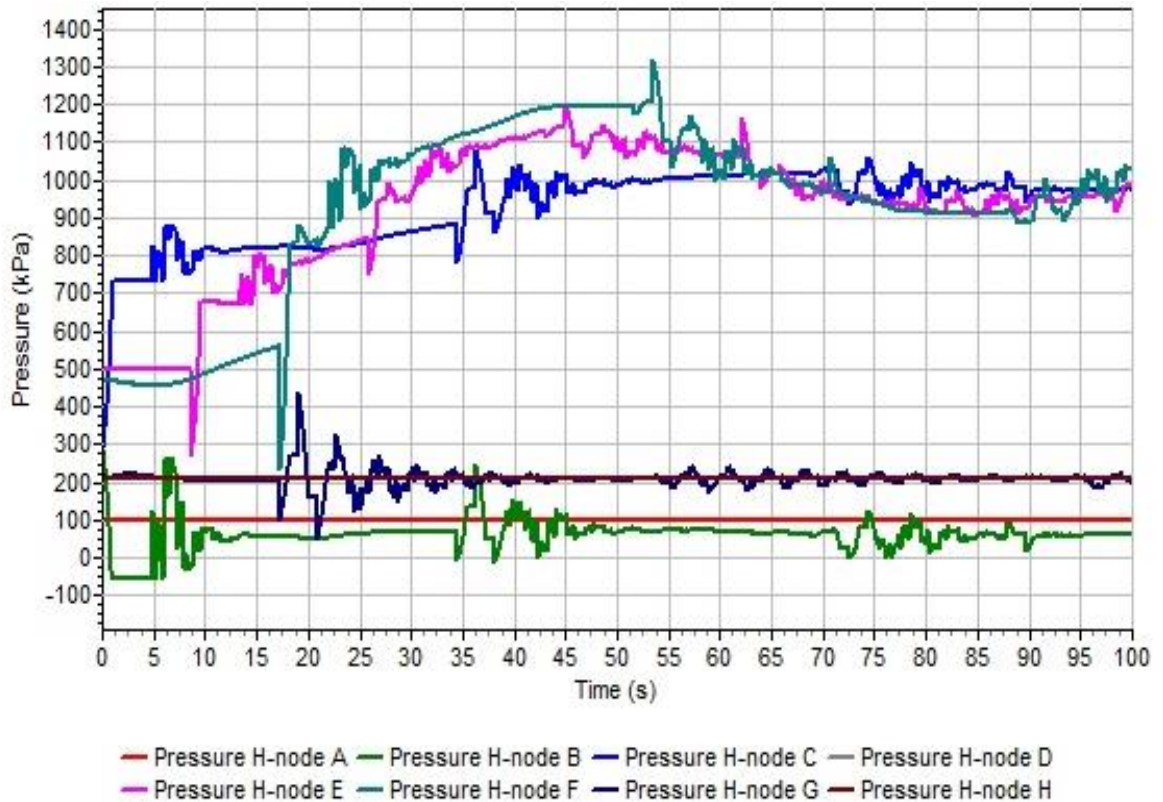
Figure 4.25: Pressure transients at H-nodes for a VCT of 18 s in PMS pipeline

Figure 4.26 depicts the development of positive and negative pressure surges at nodes F and B respectively due to VCT of 36 s. The simulation result showed that a peak positive pressure surge of 1,127 kPa and a least negative pressure surge of – 52 kPa would be experienced at nodes F and B respectively for a VCT of 36 s. The Figure also depicts that the pressure surges fluctuates between maximum and minimum pressure values until stability was established at an operational pressure of about 1,000 kPa.
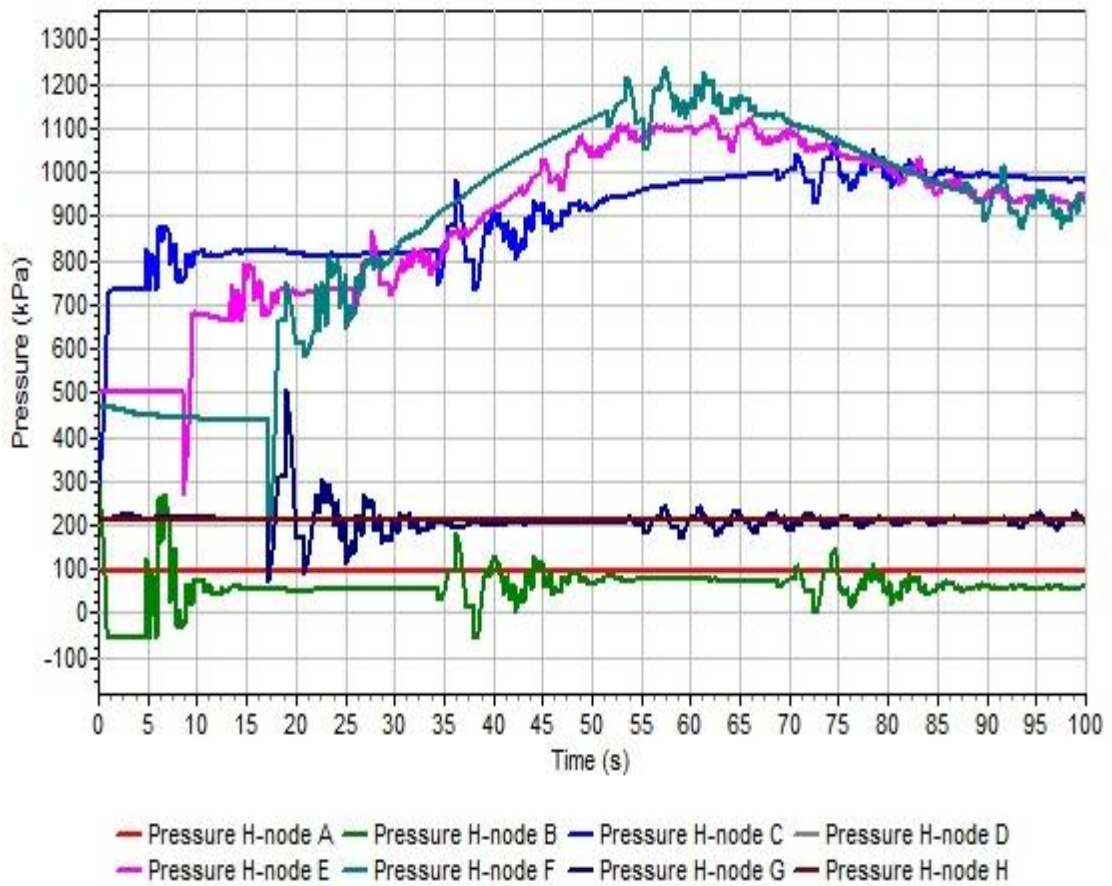
Figure 4.26: Pressure transients at H-nodes for a VCT of 36 s in PMS pipeline

Figure 4.27 depicts the development of positive and negative pressure surges at nodes F and B respectively due to VCT of 72 s. The simulation result showed that a peak positive pressure surge of 1,126 kPa and a least negative pressure surge of – 52 kPa would be experienced at nodes F and B respectively for a VCT of 72 s. The Figure also depicts that the pressure surges fluctuates between maximum and minimum pressure values until stability was established at an operational pressure of about 1,000 kPa.
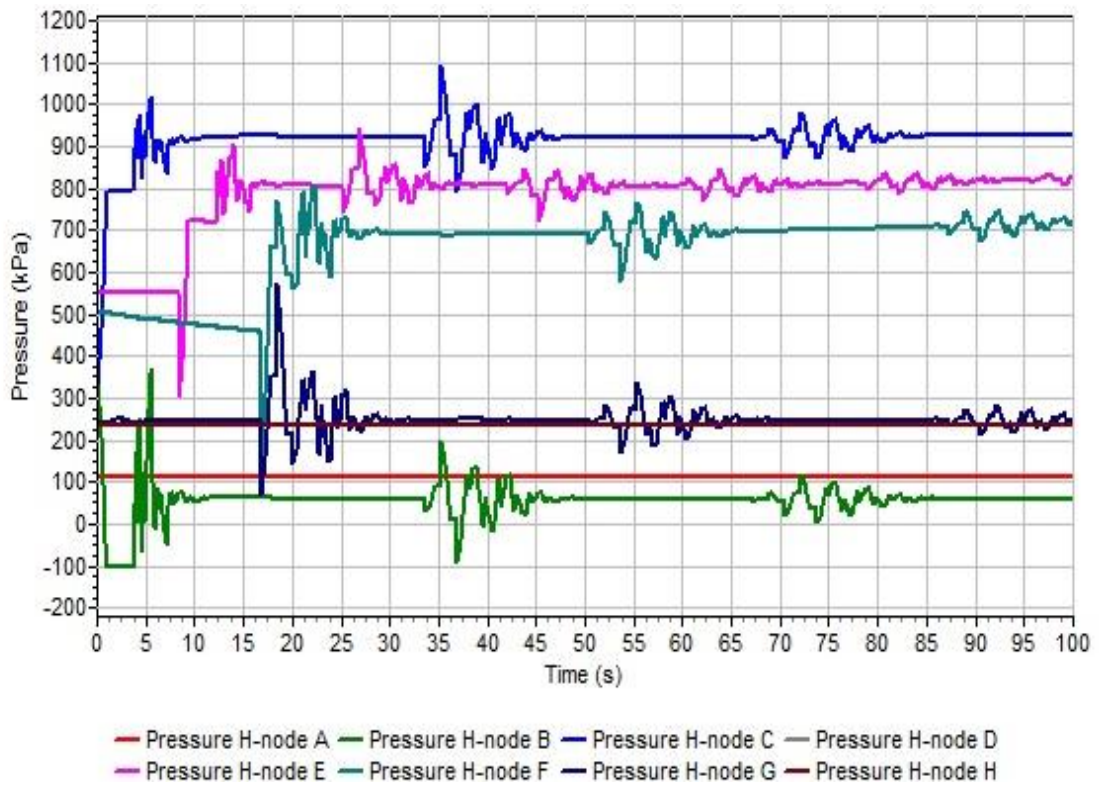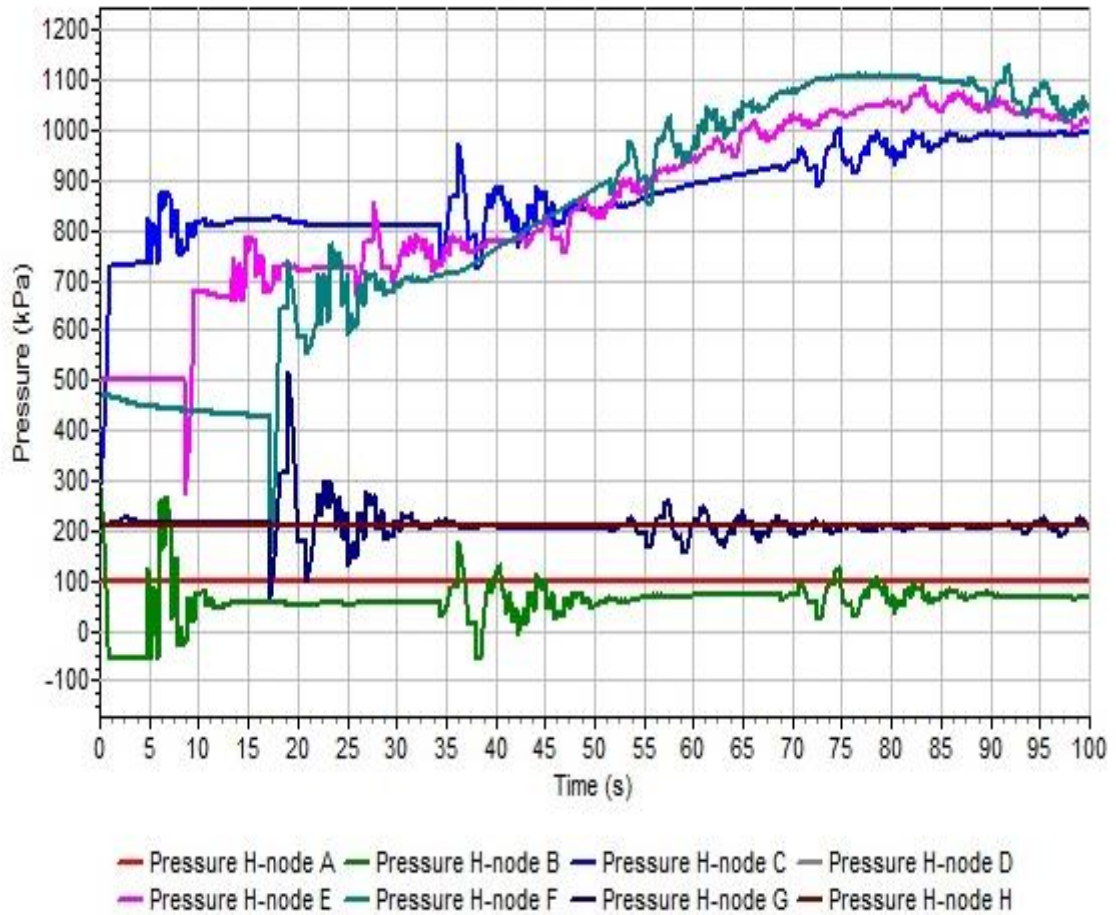
Figure 4.27: Pressure transients at H-nodes for a VCT of 72 s in PMS pipeline

Figure 4.28 depicts the development of positive and negative pressure surges at nodes F and B respectively due to VCT of 144 s. The simulation result showed that a peak positive pressure surge of 1,053 kPa and a least negative pressure surge of – 52 kPa would be experienced at nodes F and B respectively for a VCT of 144 s. The Figure also depicts that the pressure surges fluctuates between maximum and minimum pressure values until stability was established at an operational pressure of about 1,000 kPa.
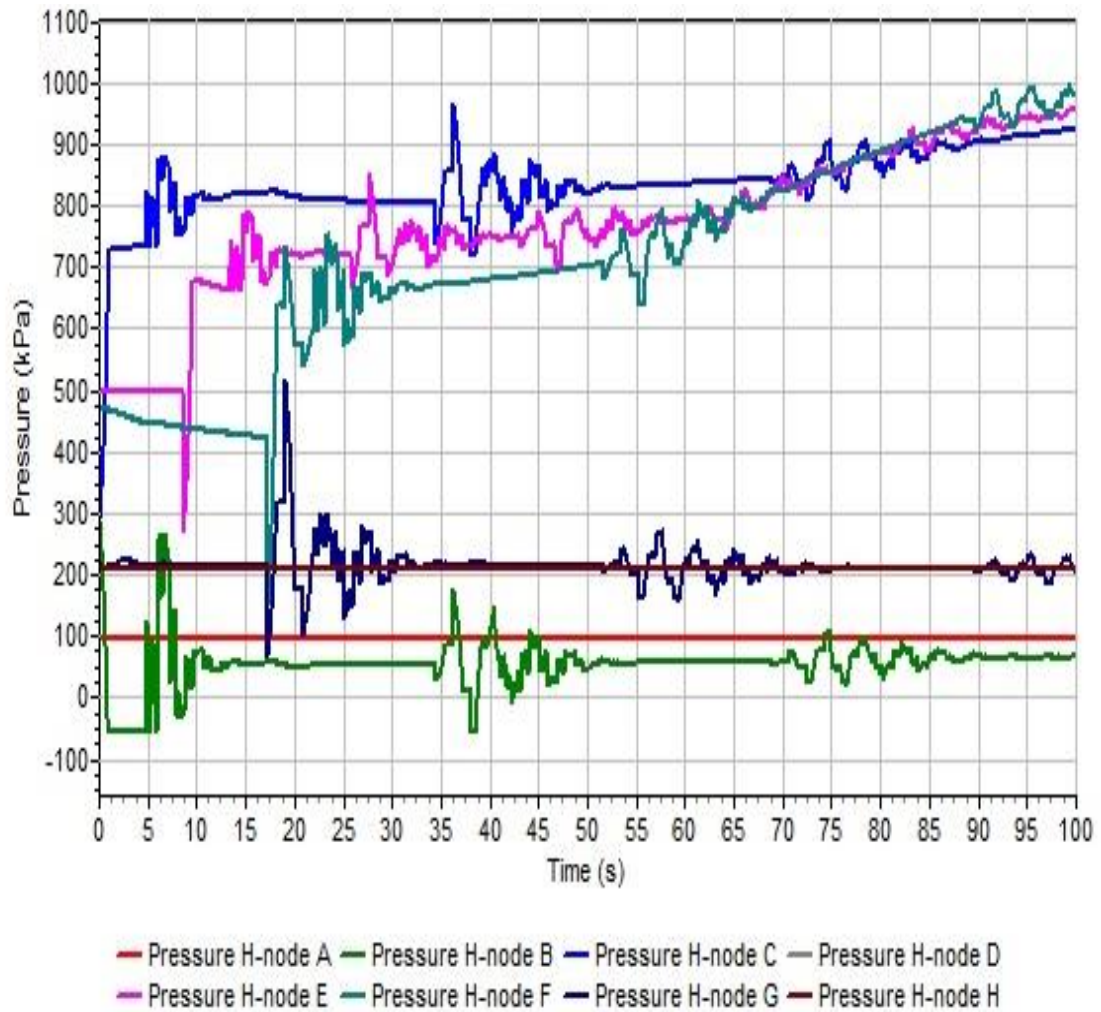
Figure 4.28: Pressure transients at H-nodes for a VCT of 144 s in PMS pipeline

Figure 4.29 depicts the development of positive and negative pressure surges at nodes F and B respectively due to VCT of 288 s. The simulation result showed that a peak positive pressure surge of 1,047 kPa and a least negative pressure surge of – 52 kPa would be experienced at nodes F and B respectively for a VCT of 288 s. The Figure also depicts that the pressure surges fluctuates at various times between maximum and minimum pressure values until stability was established at an operational pressure of about 1,000 kPa.
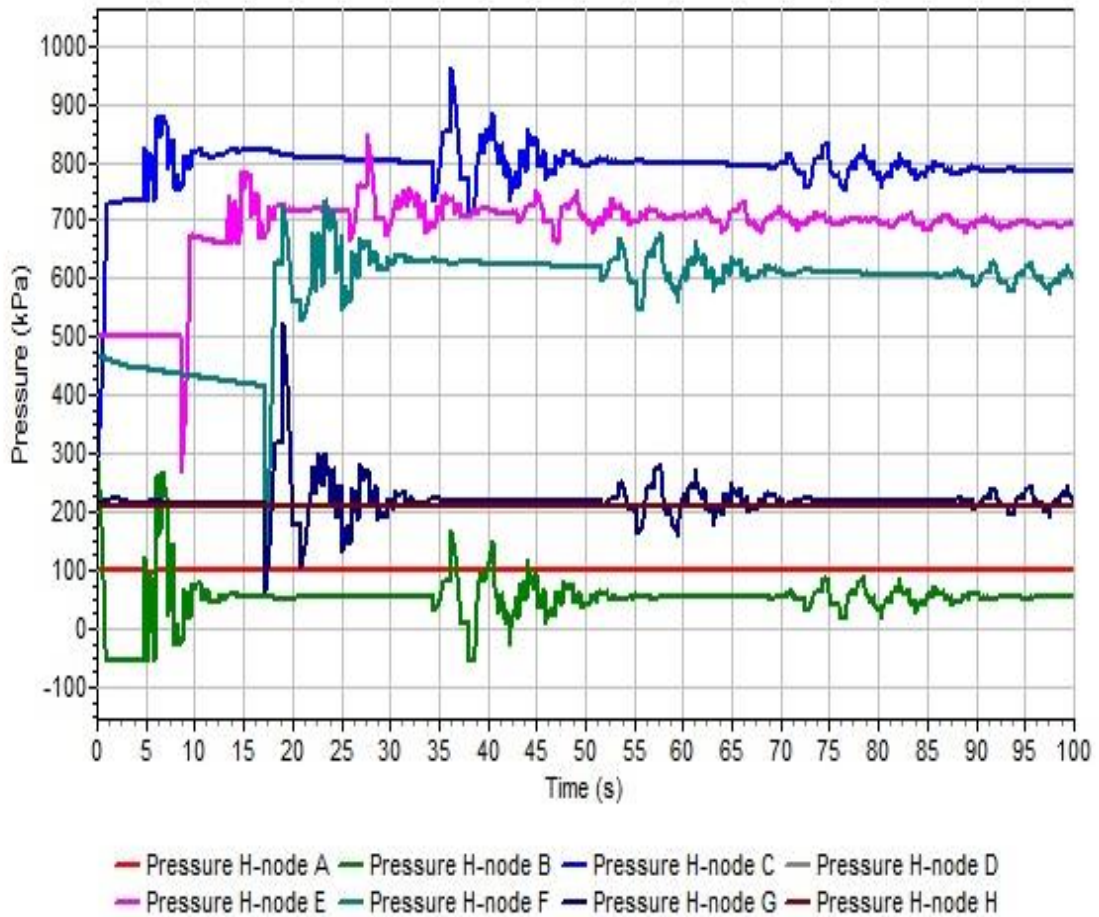
Figure 4.29: Pressure transients at H-nodes for a VCT of 288 s in PMS pipeline

Figure 4.30 depicts the development of positive and negative pressure surges at nodes F and B respectively due to VCT of 576 s. The simulation result showed that a peak positive pressure surge of 1,047 kPa and a least negative pressure surge of – 52 kPa would be experienced at nodes F and B respectively for a VCT of 576 s. The Figure also depicts that the pressure surges fluctuates at various times between maximum and minimum pressure values until stability was established at an operational pressure of about 1,000 kPa.

107
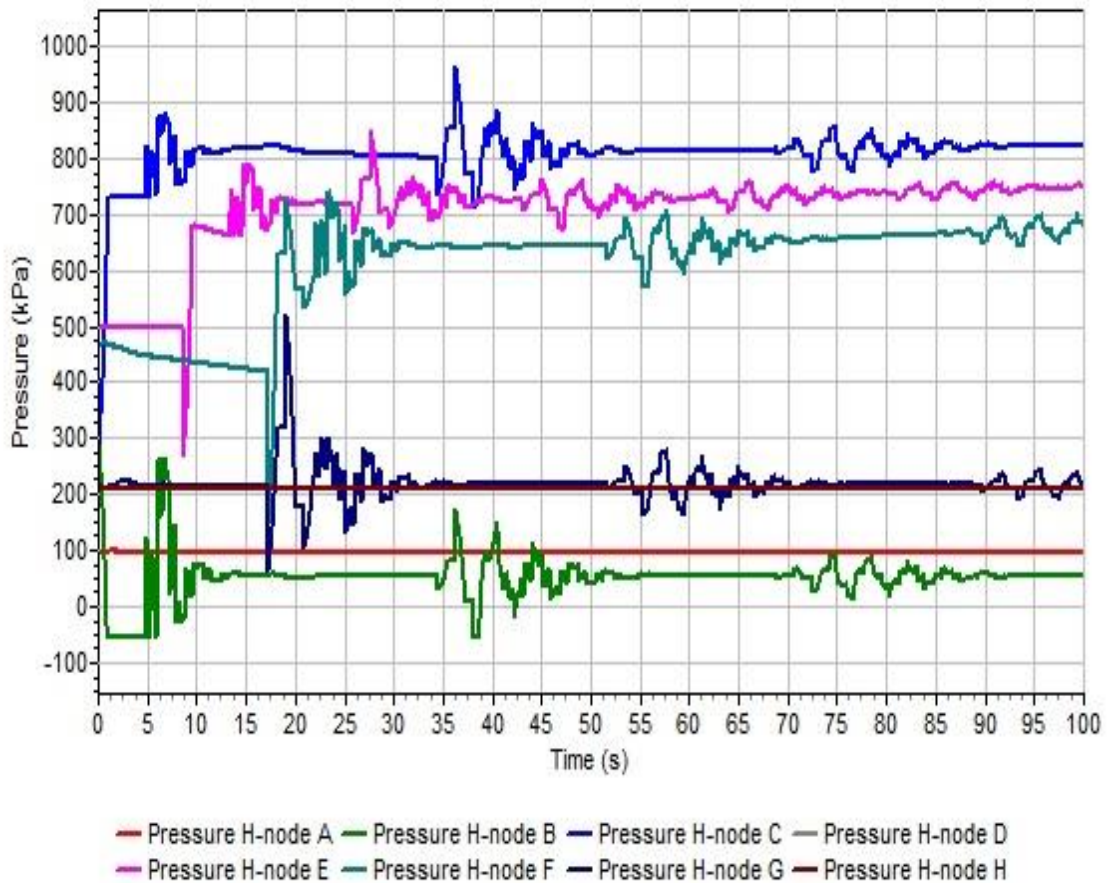
Figure 4.30: Pressure transients at H-nodes for a VCT of 576 s in PMS pipeline

Figure 4.31 depicts the magnitude and behaviour of cavitation voids developed at nodes B for all the VCTs. The development of the negative pressure at node B for all the VCTs investigated might also lead to the formation of cavitations voids of magnitude. The development of negative pressure at node B for all the VCTs used might also lead to the formation of cavitations voids of magnitude 0.007084 at node B and along pipe P1 for all the VCTs for a PMS pipeline as shown in Figure 4.31. The development of this cavitation voids is in agreement with what Gseaa& Dekam (2010) have reported in their research findings.
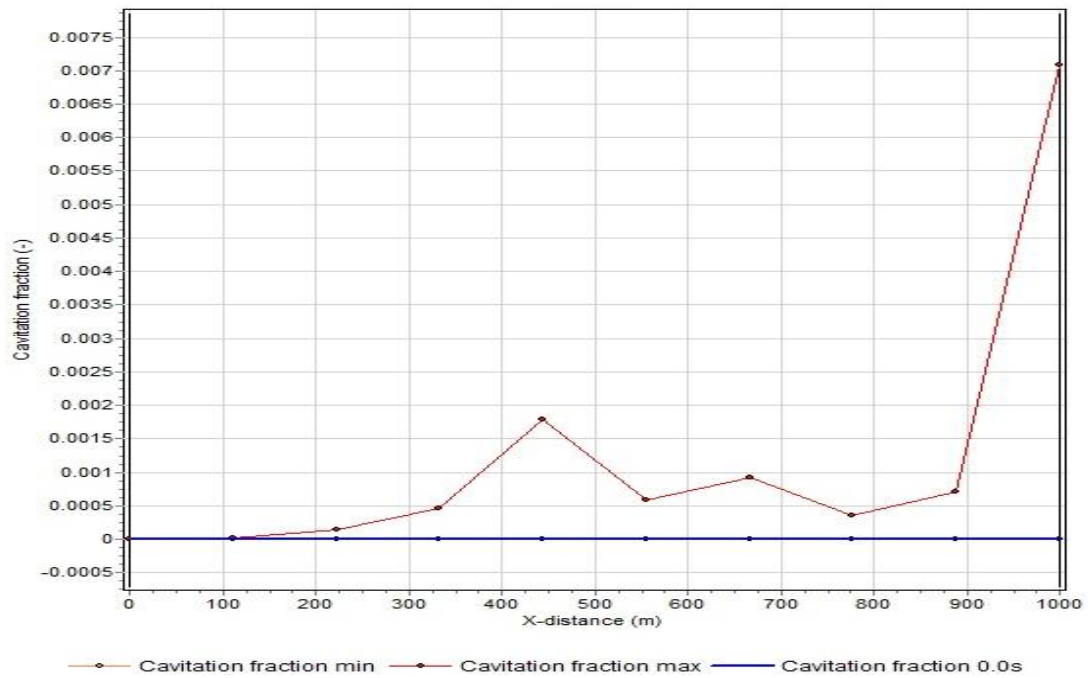
Figure 4.31: Cavitation formed due to sudden valve closure in a PMS pipeline

Figure 4.32 shows the pattern of the summary of peak pressure surges being experienced due to various VCTs in a pipeline transporting PMS. The Figure depicts that the peak pressure surges decrease as the VCT was increased. The Figure also depicts that the highest peak pressure surge of 1321 kPa experienced at F due to the VCTs of 4.5 s is below the design pressure range of 1,379 kPa to 4,400 kPa of the pipes but above the design pressure of the nodal sets at 1,035 kPa. However, the highest peak pressure surge dropped from about 1321 kPa at a VCT of 4.5 s to a pressure surge of about 1,050 kPa at a VCT of 144 s – 576 s. This decrease in pressure surge due to an increase in VCT could be as a result of the delay in changing the operational status of the flow control device which in turn also delays the rapid changes in pressure and velocity. At the VCTs of 140 s – 576 s, the magnitude of pressure surges due to sudden valve closure remains constant at about 1,050 kPa. The peak surge pressure generated is below the MAOP of the flange of about 1,400 kPa and MAOP of the flange of about

1,050 kPa – 1,260 kPa. It can be observed from Figure 4.22, that as from VCTs of 144 s – 544 s, the pressure surge remains almost constant. Therefore, a marginal VCT range of 144 s – 576 s was established for a pipeline transporting PMS. And valve closure rate range of 0.0006 m/s - 0.0025 m/s was established as the marginal valve closure velocity of a standard 0.3556 m (14 inches) petroleum pipes transporting PMS.
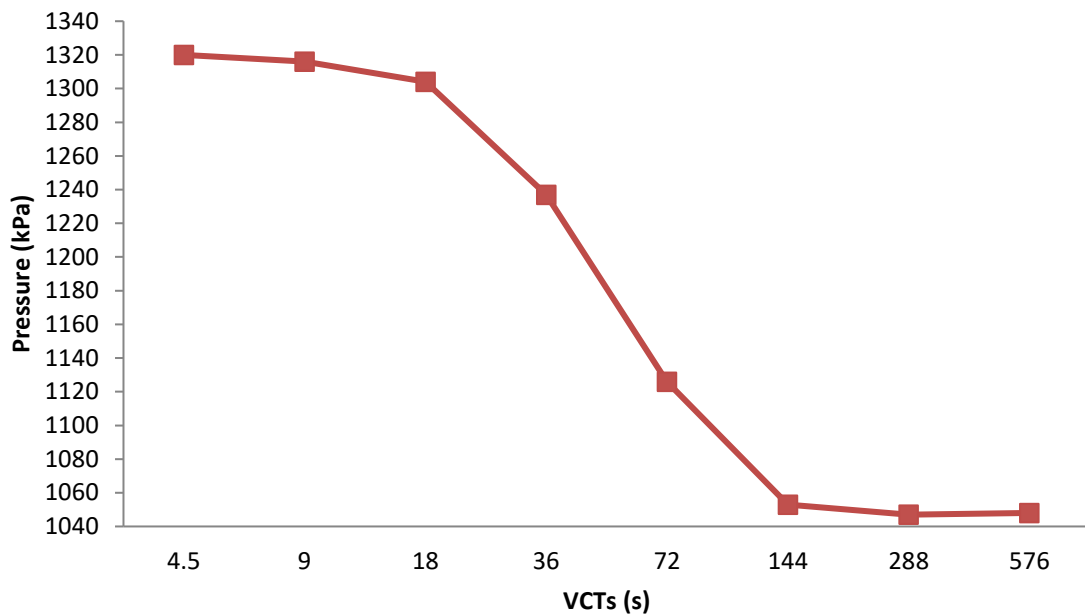
Figure 4.32: Pressure surges at different VCTs in a PMS pipeline

The simulations results obtained because of valve closure for all the fluids carried out in this research work are in agreement with the findings of Twyman (2018), Mylapilli *et al*. (2015) and Simpson & Wu (1997). The authors reported that pressure surges are maximum at nodes just upstream of the flow control valve. And also the results obtained for drop in pressure and development of negative pressure at node B (a node where the fluids were evacuated) due to sudden valve closures are in agreement with what Gseaa& Dekam (2010) have reported in their research findings.

4.2.3 Simulation results for pressure transient due to pump failure

Figures 4.33 to 4.37 presents the pressure transients developed due to abrupt pump failure in a petroleum pipeline transporting AGO, DPK and PMS. The pressure of the fluids under normal operating conditions is 120 kPa, but due to the sudden failure of the pump, the pressure of the fluid in the pipeline starts to fluctuate between a minimum and maximum pressures before attaining stability.

Figure 4.33 depicts the positive and negative pressure surges experienced in a pipeline transporting AGO due to the sudden pump failure. The Figure depicts that a peak positive pressure surge of 640 kPa was recorded at node C. However, a drop in pressure below atmospheric of – 25 kPa, 18 kPa, - 9 kPa, - 8 kPa, 71 kPa, and 70 kPa would be experienced at nodes B, C, D, E, F, and G respectively. These drop in pressure could lead to the development of cavitation and column separation as reported by Gseaa & Dekam, (2010) that when the internal pressure of a filled petroleum pipeline drops to a pressure equal to or lower than the vapour pressure of the petroleum product at certain locations such as nodes, column separation or cavitation will occur. The drop in pressure at node B is also in agreement with what Wan *et al*. (2018) reported. The Figure also depicts that the pressure surges fluctuates at various times between maximum and minimum pressure values until stability was established at an operational pressure of about 260 kPa.
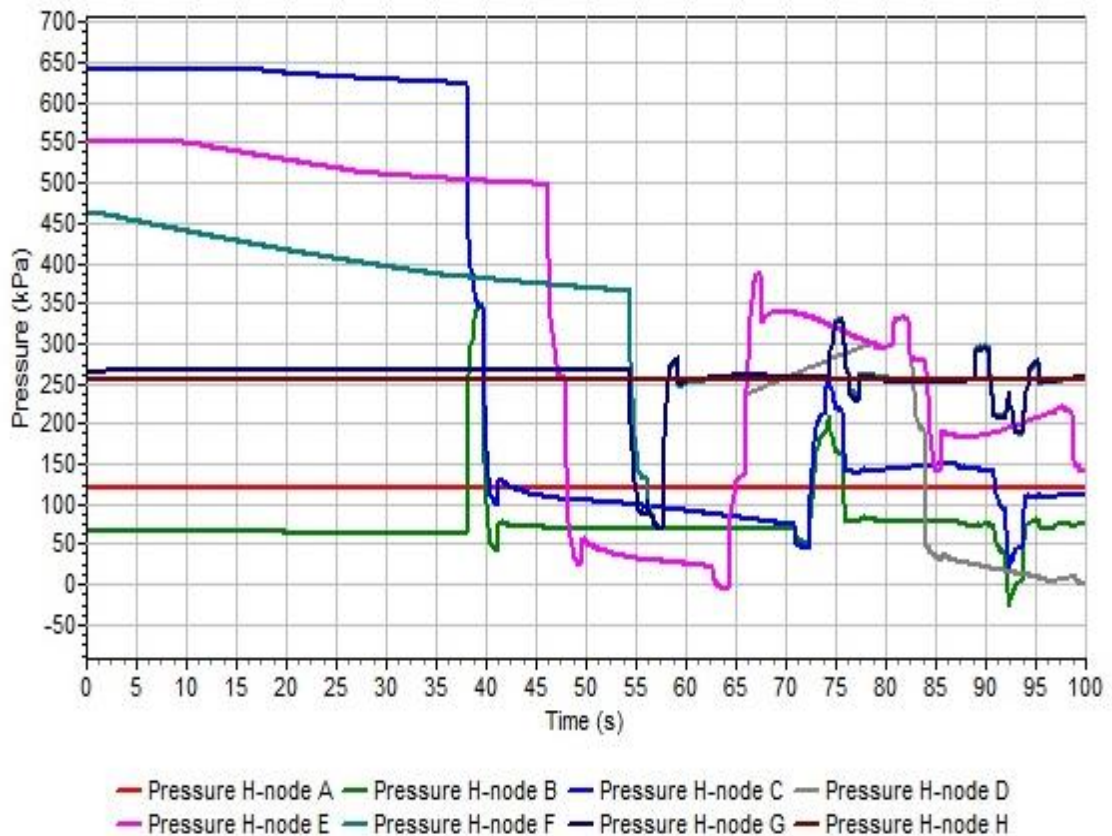
**Figure 4.33:** Pressure Transients Due to Pump Failure in an AGO Pipeline

Figure 4.34 depicts the positive and negative pressure surges experienced in a pipeline transporting DPK due to the sudden pump failure. The Figure depicts that a peak positive pressure surge of 600 kPa was recorded at node C. However, a drop in pressure below atmospheric of – 24 kPa, 17 kPa, -12 kPa, - 12 kPa, 64 kPa, and 63 kPa would be experienced at nodes B, C, D, E, F, and G respectively. These drop in pressure could lead to the development of cavitation and column separation as reported by Gseaa & Dekam, (2010). The Figure also depicts that the pressure surges fluctuates at various times between maximum and minimum pressure values until stability was established at an operational pressure of about 260 kPa.

112
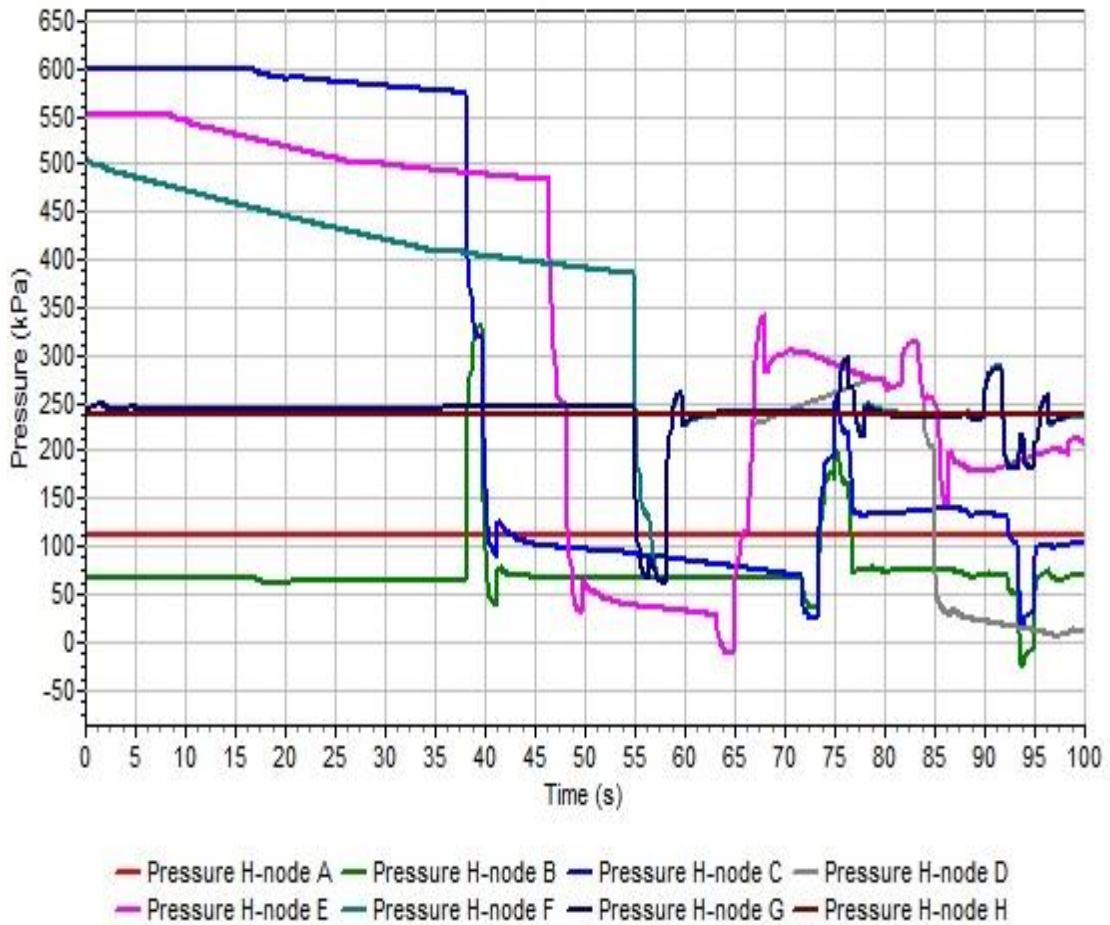
Figure 4.34: Pressure Transients Due to Pump Failure in a DPK Pipeline

Figure 4.35 depicts the positive and negative pressure surges experienced in a pipeline transporting PMS due to the sudden pump failure. The Figure depicts that a peak positive pressure surge of 534 kPa was recorded at node C. However, a drop in pressure below atmospheric of – 21 kPa, 14 kPa, -10 kPa, - 10 kPa, 70 kPa, and 60 kPa would be experienced at nodes B, C, D, E, F, and G respectively. These drop in pressure could lead to the development of cavitation and column separation as reported by Gseaa & Dekam, (2010). The Figure also depicts that the pressure surges fluctuates at various times between maximum and minimum pressure values until stability was established at an operational pressure of about 260 kPa.
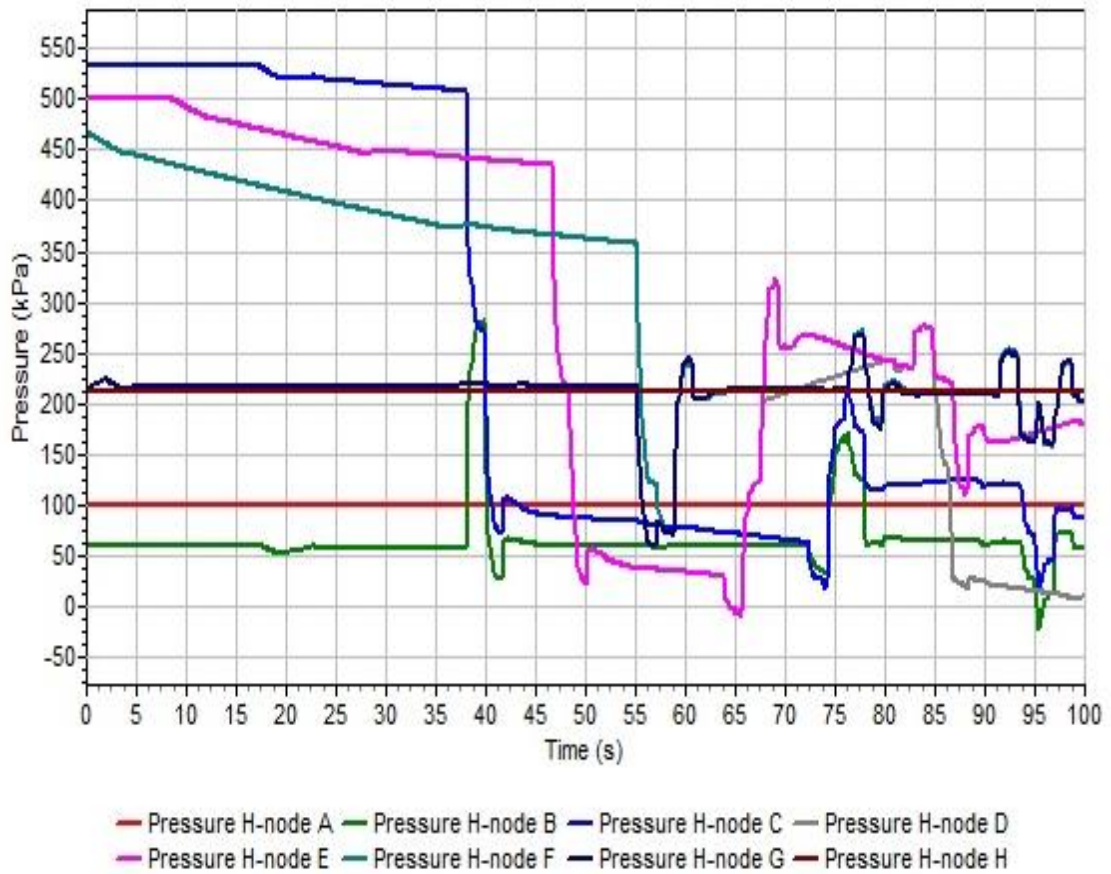
**Figure 4.35:** Pressure Transients Due to Pump Failure in a PMS Pipeline

4.3   Experimental Analysis

Experimental results of HT due to various sudden VCTs in a petroleum pipeline transporting AGO, DPK, and PMS are presented in this section. The results of the experiment are presented in Tables 4.2 to 4.24.

4.3.1   Experimental results of AGO at sudden VCTs

Table 4.1 presents the values of minimum and maximum pressures obtained as a result of experimental investigation of HT due to sudden valve closure in a pipeline transporting AGO for a VCT of 4.75 s. The result of the investigation showed that a peak positive pressure surge of 1,370 kPa and a least pressure of – 90 kPa were

114

recorded at nodes F (node just upstream of the flow control valve) and node B (node just upstream of the pump) for a VCT of 4.75 s. The developed peak positive pressure at node F is above the pressure rating of the nodal sets and may lead to the failure of the nodal sets. Also, the developed negative pressure surge at node B is below the RVP of AGO (0.5 kPa) and may lead to the failure of the node due to the development of cavitation and column separation at that node. The results of the investigation showed that the pressure surge fluctuates between maximum and minimum pressure values before the attainment of stability.

Table 4.1: Pressure surges in an AGO pipeline at 4.75 s VCT

Nodes	T max (s)	T min (s)	P max (kPa)	P min (kPa)
A	5	2	115	115
B	0	0	350	-90
C	18	1	1,247	339
D	12	1	1,235	278
E	1	6	1,232	278
F	2	18	1,370	200
G	0	9	535	105
H	0	0	250	250

Table 4.2 presents the values of minimum and maximum pressure surges obtained as a result of experimental investigation of HT due to sudden valve closure in a pipeline transporting AGO for a VCT of 9.5 s. The result of the experimental investigation

showed that a positive peak pressure surge of 1,361 kPa and a least negative pressure surge of –90 kPa were recorded at nodes F and node B for a VCT of 9.5 s. The developed peak positive pressure at node F is above the pressure rating of the nodal sets and may lead to the failure of the nodal sets. Also, the developed negative pressure surge at node B is below the RVP of AGO (0.5 kPa) and may lead to the failure of the node due to the development of cavitation and column separation at that node. The results of the investigation showed that the pressure surge fluctuates between maximum and minimum pressure values before the attainment of stability.

Table 4.2: Pressure surges in an AGO pipeline at 9.5 s VCT

Nodes	T max	T min	P max	P min
	(s)	(s)	(kPa)	(kPa)
A	2	0	115	115
B	0	1	345	-90
C	17	9	1,191	335
D	1	3	1,180	270
E	1	33	1,182	270
F	2	37	1,361	190
G	4	0	530	105
H	0	2	250	250

Table 4.3 presents the values of minimum and maximum pressures obtained as a result of experimental investigation of HT due to sudden valve closure in a pipeline transporting AGO for a VCT of 19 s. The result showed that a peak pressure surge of

1,340 kPa and a least pressure of – 90 kPa were recorded at nodes F and node B for a VCT of 19 s. The developed peak positive pressure at node F is above the pressure rating of the nodal sets and may lead to the failure of the nodal sets. Also, the developed negative pressure surge at node B is below the RVP of AGO (0.5 kPa) and may lead to the failure of the node due to the development of cavitation and column separation at that node. The results of the investigation showed that the pressure surge fluctuates between maximum and minimum pressure values before the attainment of stability.

Table 4.3: Pressure surges in an AGO pipeline at 19 s VCT

Nodes	T max	T min	P max	P min
	(s)	(s)	(kPa)	(kPa)
A	1	0	115	115
B	16	6	340	-90
C	8	5	1,111	327
D	1	22	1,149	263
E	2	20	1,147	261
F	0	1	1,340	177
G	2	5	521	104
H	0	3	250	250

Table 4.4 presents the values of minimum and maximum pressures obtained as a result of experimental investigation of HT due to sudden valve closure in a pipeline transporting AGO for a VCT of 38 s. The result of the investigation showed that a peak pressure surge of 1,275 kPa and a least negative pressure surge of – 90 kPa were

recorded at nodes F and node B for a VCT of 38 s. The developed peak positive pressure at node F is above the pressure rating of the nodal sets and may lead to the failure of the nodal sets. Also, the developed negative pressure surge at node B is below the RVP of AGO (0.5 kPa) and may lead to the failure of the node due to the development of cavitation and column separation at that node. The results of the investigation showed that the pressure surge fluctuates between maximum and minimum pressure values before the attainment of stability.

Table 4.4: Pressure surges in an AGO pipeline at 38 s VCT

Nodes	T max	T min	P max	P min
	(s)	(s)	(kPa)	(kPa)
A	0	0	115	115
B	12	6	332	-90
C	1	1	955	320
D	1	17	964	245
E	2	17	964	242
F	0	0	1,275	163
G	3	0	518	104
H	0	1	250	250

Table 4.5 presents the values of minimum and maximum pressures obtained as a result of experimental investigation of HT due to sudden valve closure in a pipeline transporting AGO for a VCT of 76 s. The result of the investigation showed that a peak pressure surge of 1,235 kPa and a least negative pressure surge of – 90 kPa were

recorded at nodes F and node B for a VCT of 76 s. The developed peak positive pressure at node F is above the pressure rating of the nodal sets and may lead to the failure of the nodal sets. Also, the developed negative pressure surge at node B is below the RVP of AGO (0.5 kPa) and may lead to the failure of the node due to the development of cavitation and column separation at that node. The results of the investigation showed that the pressure surge fluctuates between maximum and minimum pressure values before the attainment of stability.

Table 4.5: Pressure surges in an AGO pipeline at 76 s VCT

Nodes	T max	T min	P max	P min
	(s)	(s)	(kPa)	(kPa)
A	2	0	115	115
B	8	4	330	-98
C	0	0	888	317
D	1	21	891	241
E	2	1	892	243
F	0	19	1,235	154
G	3	0	508	105
H	1	3	247	245

Table 4.6 presents the values of minimum and maximum pressures obtained as a result of experimental investigation of HT due to sudden valve closure in a pipeline transporting AGO for a VCT of 152 s. The result of the investigation showed that a peak positive pressure surge of 1,130 kPa and a least negative pressure surge of – 90

kPa were recorded at nodes F and node B for a VCT of 152 s. The developed peak positive pressure at node F is above the pressure rating of the nodal sets and may lead to the failure of the nodal sets. Also, the developed negative pressure surge at node B is below the RVP of AGO (0.5 kPa) and may lead to the failure of the node due to the development of cavitation and column separation at that node. The results of the investigation showed that the pressure surge fluctuates between maximum and minimum pressure values before the attainment of stability.

Table 4.6: Pressure surges in an AGO pipeline at 152 s VCT

Nodes	T max	T min	P max	P min
	(s)	(s)	(kPa)	(kPa)
A	0	11	115	115
B	1	3.5	320	-98
C	35	7	880	310
D	26	9	882	234
E	23	11	881	235
F	18	15	1,130	150
G	11	16	500	103
H	10	10	246	244

Table 4.7 presents the values of minimum and maximum pressures obtained as a result of experimental investigation of HT due to sudden valve closure in a pipeline transporting AGO for a VCT of 304 s. The result of the investigation showed that a peak positive pressure surge of 1,105 kPa and a least negative pressure of – 90 kPa were

recorded at nodes F and node B for a VCT of 304 s. The developed peak positive pressure at node F is above the pressure rating of the nodal sets and may lead to the failure of the nodal sets. Also, the developed negative pressure surge at node B is below the RVP of AGO (0.5 kPa) and may lead to the failure of the node due to the development of cavitation and column separation at that node. The results of the investigation showed that the pressure surge fluctuates between maximum and minimum pressure values before the attainment of stability.

Table 4.7: Pressure surges in an AGO pipeline at 304 s VCT

Nodes	T max	T min	P max	P min
	(s)	(s)	(kPa)	(kPa)
A	11	14	115	115
B	1	3.5	320	-98
C	35	7	878	300
D	26	9	880	227
E	23	11	876	227
F	18	15	1,105	144
G	11	16	490	102
H	23	10	240	244

Table 4.8 presents the values of minimum and maximum pressures obtained as a result of experimental investigation of HT due to sudden valve closure in a pipeline transporting AGO for a VCT of 608 s. The result of the investigation showed that a peak positive pressure surge of 1,100 kPa and a least negative pressure of – 90 kPa were

recorded at nodes F and node B for a VCT of 608 s. The developed peak positive

pressure at node F is above the pressure rating of the nodal sets and may lead to the

failure of the nodal sets. Also, the developed negative pressure surge at node B is below

the RVP of AGO (0.5 kPa) and may lead to the failure of the node due to the

development of cavitation and column separation at that node. The results of the

investigation showed that the pressure surge fluctuates between maximum and

minimum pressure values before the attainment of stability.

Table 4.8: Pressure surges in an AGO pipeline at 608 s VCT

Nodes	T max	T min	P max	P min
	(s)	(s)	(kPa)	(kPa)
A	11	14	115	115
B	1	3.5	320	-98
C	35	7	878	300
D	26	9	880	227
E	23	11	876	227
F	18	15	1,100	135
G	11	16	490	102
H	23	10	240	244

Figure 4.36 depicts the summary of the highest pressure surges experienced at nodes F

due to various VCTs in a pipeline transporting AGO and the result showed that as the

rate of VCT is being increased, the pressure surge being developed decreases. This

could be as a result of longer time taken to halt the flow of the fluid and hence the

change in pressure also takes place slowly.
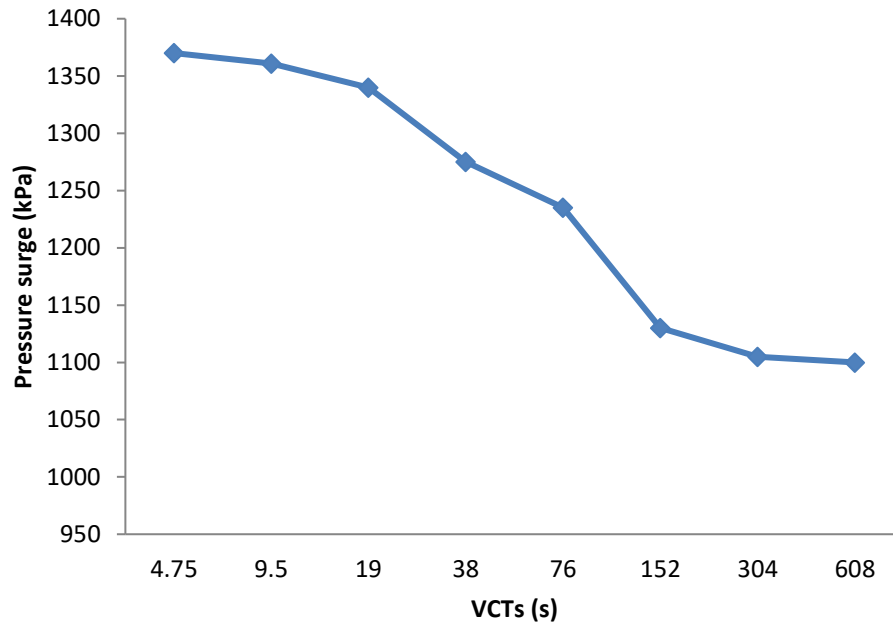
Figure 4.36: Pressure surges due to different VCTs in AGO pipeline

4.3.2 Experimental results of DPK at sudden VCTs

Table 4.9 presents the values of maximum and minimum pressures experienced as a result of VCT of 4.38 s in an experimental investigation of HT due to sudden valve closure in a pipeline transporting DPK. The results of the investigation showed that a peak positive pressure surge of 1,432 kPa and a least negative pressure surge of − 98 kPa were recorded at a nodes F and B respectively for a VCT of 4.38 s. The developed peak positive pressure at node F is above the pressure rating of the nodal sets and may lead to the failure of the nodal sets. Also, the developed negative pressure surge at node B is below the RVP of DPK (1.1 kPa) and may lead to the failure of the node due to the development of cavitation and column separation at that node. The results of the investigation showed that the pressure surge fluctuates between maximum and minimum pressure values before the attainment of stability.

Table 4.9: Pressure surges in a DPK pipeline at 4.38 s VCT

Nodes	T max	T Min	P Max	P Min
	(s)	(s)	(kPa)	(kPa)
A	2	3	105	105
B	0	0	360	-98
C	3	1	1,200	320
D	2	1	1,310	290
E	11	2	1,310	290
F	12	2	1,432	278
G	0	0	467	70
H	4	2	230	230

Table 4.10 presents the values of maximum and minimum pressures experienced as a result of VCT of 8.5 s in an experimental investigation of HT due to sudden valve closure in a pipeline transporting DPK. The results of the investigation showed that a peak positive pressure surge of 1,429 kPa and a least negative pressure surge of – 98 kPa were recorded at a nodes F and B respectively for a VCT of 8.5 s. The developed peak positive pressure at node F is above the pressure rating of the nodal sets and may lead to the failure of the nodal sets. Also, the developed negative pressure surge at node B is below the RVP of DPK (1.1 kPa) and may lead to the failure of the node due to the development of cavitation and column separation at that node. The results of the investigation showed that the pressure surge fluctuates between maximum and minimum pressure values before the attainment of stability.

Table 4.10: Pressure surges in a DPK pipeline at 8.5 s VCT

Nodes	T max	T Min	P Max	P Min
	(s)	(s)	kPa)	(kPa)
A	2	3	105	105
B	0	0	359	-98
C	3	1	1,184	315
D	2	1	1,255	298
E	7	2	1,255	297
F	5	2	1,429	255
G	0	0	460	70
H	4	2	230	230

Table 4.11 presents the values of maximum and minimum pressures experienced as a result of VCT of 17 s in an experimental investigation of HT due to sudden valve closure in a pipeline transporting DPK. The results of the investigation showed that a peak positive pressure surge of 1,400 kPa and a least negative pressure surge of – 98 kPa were recorded at a nodes F and B respectively for a VCT of 17 s. The developed peak positive pressure at node F is above the pressure rating of the nodal sets and may lead to the failure of the nodal sets. Also, the developed negative pressure surge at node B is below the RVP of DPK (1.1 kPa) and may lead to the failure of the node due to the development of cavitation and column separation at that node. The results of the investigation showed that the pressure surge fluctuates between maximum and minimum pressure values before the attainment of stability.

Table 4.11: Pressure surges in a DPK pipeline at 17 s VCT

Nodes	T max	T Min	P Max	P Min
	(s)	(s)	(kPa)	(kPa)
A	2	3	105	105
B	0	0	353	-96
C	3	1	1,170	313
D	2	1	1,191	294
E	11	2	1,190	294
F	12	2	1,400	200
G	0	0	530	70
H	4	2	229	230

Table 4.12 presents the values of maximum and minimum pressures experienced as a result of VCT of 34 s in an experimental investigation of HT due to sudden valve closure in a pipeline transporting DPK. The results of the investigation showed that a peak positive pressure surge of 1,350 kPa and a least negative pressure surge of – 98 kPa were recorded at a nodes F and B respectively for a VCT of 34 s. The developed peak positive pressure at node F is above the pressure rating of the nodal sets and may lead to the failure of the nodal sets. Also, the developed negative pressure surge at node B is below the RVP of DPK (1.1 kPa) and may lead to the failure of the node due to the development of cavitation and column separation at that node. The results of the investigation showed that the pressure surge fluctuates between maximum and minimum pressure values before the attainment of stability.

Table 4.12: Pressure surges in a DPK pipeline at 34 s VCT

Nodes	T max	T Min	P Max	P Min
	(s)	(s)	(kPa)	(kPa)
A	3	1	105	105
B	0	2	350	-96
C	3	1	1,139	305
D	2	1	1,147	290
E	9	4	1,145	290
F	12	2	1,350	165
G	0	0	529	68
H	1	2	230	230

Table 4.13 presents the values of maximum and minimum pressures experienced as a result of VCT of 68 s in an experimental investigation of HT due to sudden valve closure in a pipeline transporting DPK. The results of the investigation showed that a peak positive pressure surge of 1,257 kPa and a least negative pressure surge of – 98 kPa were recorded at a nodes F and B respectively for a VCT of 68 s. The developed peak positive pressure at node F is above the pressure rating of the nodal sets and may lead to the failure of the nodal sets. Also, the developed negative pressure surge at node B is below the RVP of DPK (1.1 kPa) and may lead to the failure of the node due to the development of cavitation and column separation at that node. The results of the investigation showed that the pressure surge fluctuates between maximum and minimum pressure values before the attainment of stability.

Table 4.13: Pressure surges in a DPK pipeline at 68 s VCT

Nodes	T max	T min	P max	P min
	(s)	(s)	(kPa)	(kPa)
A	2	3	104	103
B	0	0	348	-95
C	1	2	961	300
D	2	1	970	286
E	4	2	971	286
F	7	2	1,257	162
G	0	0	525	68
H	4	2	230	225

Table 4.14 presents the values of maximum and minimum pressures experienced as a result of VCT of 136 s in an experimental investigation of HT due to sudden valve closure in a pipeline transporting DPK. The results of the investigation showed that a peak positive pressure surge of 1,250 kPa and a least negative pressure surge of – 98 kPa were recorded at a nodes F and B respectively for a VCT of 136 s. The developed peak positive pressure at node F is above the pressure rating of the nodal sets and may lead to the failure of the nodal sets. Also, the developed negative pressure surge at node B is below the RVP of DPK (1.1 kPa) and may lead to the failure of the node due to the development of cavitation and column separation at that node. The results of the investigation showed that the pressure surge fluctuates between maximum and minimum pressure values before the attainment of stability.

Table 4.14: Pressure surges in a DPK pipeline at 136 s VCT

Nodes	T max	T min	P max	P min
	(s)	(s)	(kPa)	(kPa)
A	2	3	104	103
B	0	0	348	-95
C	1	2	961	300
D	2	1	970	286
E	4	2	971	286
F	7	2	1,250	162
G	0	0	525	68
H	4	2	230	225

Table 4.15 presents the values of maximum and minimum pressures experienced as a result of VCT of 272 s in an experimental investigation of HT due to sudden valve closure in a pipeline transporting DPK. The results of the investigation showed that a peak positive pressure surge of 1235 kPa and a least negative pressure surge of – 98 kPa were recorded at a nodes F and B respectively for a VCT of 272 s. The developed peak positive pressure at node F is above the pressure rating of the nodal sets and may lead to the failure of the nodal sets. Also, the developed negative pressure surge at node B is below the RVP of DPK (1.1 kPa) and may lead to the failure of the node due to the development of cavitation and column separation at that node. The results of the investigation showed that the pressure surge fluctuates between maximum and

minimum pressure values before the attainment of stability.

Table 4.15: Pressure surges in a DPK pipeline at 272 s VCT

Nodes	T max (s)	T min (s)	max (kPa)	Min (kPa)
A	5	12	104	104
B	6	35	340	-95
C	35	1	950	270
D	20	7	921	270
E	19	9	920	280
F	20	19	1,235	160
G	18	17	514	70
H	9	5	228	225

Table 4.16 presents the values of maximum and minimum pressures experienced as a result of VCT of 544 s in an experimental investigation of HT due to sudden valve closure in a pipeline transporting DPK. The results of the investigation showed that a peak positive pressure surge of 1,230 kPa and a least negative pressure surge of – 98 kPa were recorded at a nodes F and B respectively for a VCT of 544 s. The developed peak positive pressure at node F is above the pressure rating of the nodal sets and may lead to the failure of the nodal sets. Also, the developed negative pressure surge at node B is below the RVP of DPK (1.1 kPa) and may lead to the failure of the node due to the development of cavitation and column separation at that node. The results of the investigation showed that the pressure surge fluctuates between maximum and minimum pressure values before the attainment of stability.

Table 4.16: Pressure surges in a DPK pipeline at 544 s VCT

Nodes	T max (s)	T min (s)	max (kPa)	Min (kPa)
A	5	12	104	104
B	6	35	340	-95
C	35	1	950	270
D	20	7	921	270
E	19	9	920	280
F	20	19	1,230	160
G	18	17	514	70
H	9	5	228	225

Figure 4.37 depicts the summary of the peak pressure surges experienced at node F due to various VCTs and the result showed that as the rate of VCT is being increased, the pressure surge being developed decreases. This could be as a result of longer time taken to halt the flow of the fluid and hence the change in pressure also takes place slowly.
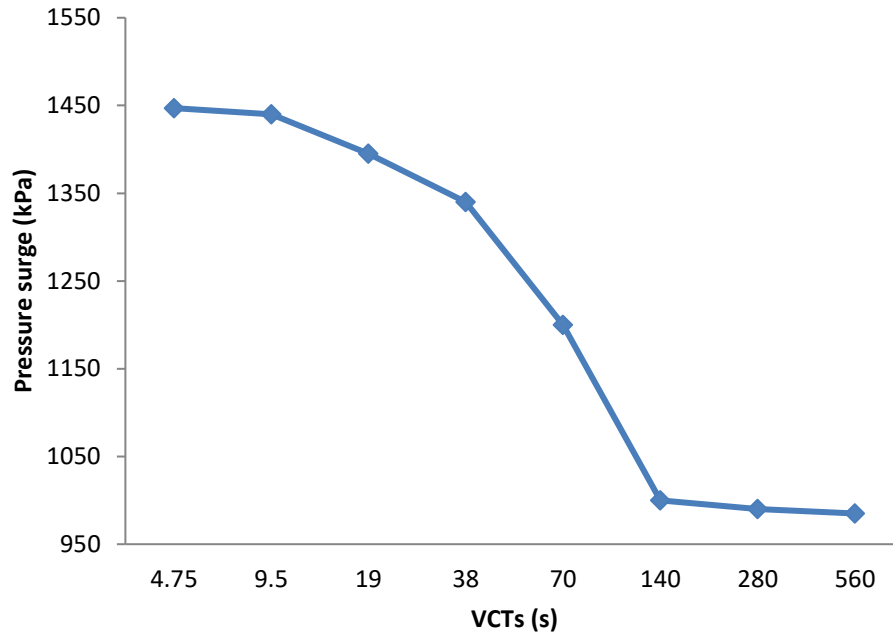
Figure 4.37: Pressure surges due to different VCTs in a DPK pipeline

4.3.3 Experimental results of PMS at sudden VCTs

Table 4.17 presents the values of maximum and minimum pressures experienced as a result of VCT of 4.5 s in an experimental investigation of HT due to sudden valve closure in a pipeline transporting PMS. The results of the investigation showed that a peak positive pressure surge of 1,310 kPa and a least negative pressure surge of – 50 kPa were recorded at a nodes F and B respectively for a VCT of 4.5 s. The developed peak positive pressure surge at node F is above the pressure rating of the nodal sets and may lead to the failure of the nodal sets. Also, the developed negative pressure surge at node B is below the RVP of PMS (48 kPa) and may lead to the failure of the node due to the development of cavitation and column separation at that node. The results of the investigation showed that the pressure surge fluctuates between maximum and minimum pressure values before the attainment of stability.

132

Table 4.17: Pressure surges in a PMS pipeline at 4.5 s VCT

Nodes	T max	T min	P max	P min
	(s)	(s)	(kPa)	(kPa)
A	1	2	98	98
B	4	0	290	-50
C	16	7	1,100	285
D	14	0	1,185	270
E	1	36	1,187	268
F	1	32	1,310	250
G	0	0	417	55
H	3	5	210	210

Table 4.18 presents the values of maximum and minimum pressures experienced as a result of VCT of 9 s in an experimental investigation of HT due to sudden valve closure in a pipeline transporting PMS. The results of the investigation showed that a peak positive pressure surge of 1,300 kPa and a least negative pressure surge of – 50 kPa were recorded at a nodes F and B respectively for a VCT of 9 s. The developed peak positive pressure surge at node F is above the pressure rating of the nodal sets and may lead to the failure of the nodal sets. Also, the developed negative pressure surge at node B is below the RVP of PMS (48 kPa) and may lead to the failure of the node due to the development of cavitation and column separation at that node. The results of the investigation showed that the pressure surge fluctuates between maximum and minimum pressure values before the attainment of stability.

Table 4.18: Pressure surges in a PMS pipeline at 9 s VCT

Nodes	T max	T min	P max	P min
	(s)	(s)	(kPa)	(kPa)
A	1	2	98	98
B	0	0	278	-50
C	23	12	1,003	272
D	45	1	1,105	262
E	1	36	1,100	262
F	1	32	1,300	238
G	0	0	410	51
H	2	2	210	207

Table 4.19 presents the values of maximum and minimum pressures experienced as a result of VCT of 18 s in an experimental investigation of HT due to sudden valve closure in a pipeline transporting PMS. The results of the investigation showed that a peak positive pressure surge of 1,285 kPa and a least negative pressure surge of – 50 kPa were recorded at a nodes F and B respectively for a VCT of 18 s. The developed peak positive pressure surge at node F is above the pressure rating of the nodal sets and may lead to the failure of the nodal sets. Also, the developed negative pressure surge at node B is below the RVP of PMS (48 kPa) and may lead to the failure of the node due to the development of cavitation and column separation at that node. The results of the investigation showed that the pressure surge fluctuates between maximum and minimum pressure values before the attainment of stability.

Table 4.19: Pressure surges in a PMS pipeline at 18 s VCT

Nodes	T max	T min	P max	P min
	(s)	(s)	(kPa)	(kPa)
A	2	1	98	98
B	0	0	262	-50
C	2	1	981	262
D	4	1	992	251
E	32	23	992	250
F	1	35	1,285	221
G	0	0	400	50
H	2	1	210	210

Table 4.20 presents the values of maximum and minimum pressures experienced as a result of VCT of 36 s in an experimental investigation of HT due to sudden valve closure in a pipeline transporting PMS. The results of the investigation showed that a peak positive pressure surge of 1,230 kPa and a least negative pressure surge of – 50 kPa were recorded at a nodes F and B respectively for a VCT of 36 s. The developed peak positive pressure surge at node F is above the pressure rating of the nodal sets and may lead to the failure of the nodal sets. Also, the developed negative pressure surge at node B is below the RVP of PMS (48 kPa) and may lead to the failure of the node due to the development of cavitation and column separation at that node. The results of the investigation showed that the pressure surge fluctuates between maximum and minimum pressure values before the attainment of stability.

Table 4.20: Pressure surges in a PMS pipeline at 36 s VCT

Nodes	T max (s)	T min (s)	P max (kPa)	P min (kPa)
A	0	0	98	96
B	4	1	255	-48
C	1	75	976	253
D	9	63	950	247
E	9	63	950	247
F	17	57	1,230	216
G	17	19	382	49
H	0	0	210	208

Table 4.21 presents the values of maximum and minimum pressures experienced as a result of VCT of 72 s in an experimental investigation of HT due to sudden valve closure in a pipeline transporting PMS. The results of the investigation showed that a peak positive pressure surge of 1,100 kPa and a least negative pressure surge of – 50 kPa were recorded at a nodes F and B respectively for a VCT of 72 s. The developed peak positive pressure surge at node F is above the pressure rating of the nodal sets and may lead to the failure of the nodal sets. Also, the developed negative pressure surge at node B is below the RVP of PMS (48 kPa) and may lead to the failure of the node due to the development of cavitation and column separation at that node. The results of the investigation showed that the pressure surge fluctuates between maximum and minimum pressure values before the attainment of stability.

Table 4.21: Pressure surges in a PMS pipeline at 72 s VCT

Nodes	T max	T min	P max	P min
	(s)	(s)	(kPa)	(kPa)
A	0	0	97	97
B	38	10	250	-50
C	1	18	961	248
D	9	8	985	242
E	7	17	985	239
F	17	10	1,100	208
G	17	19	371	50
H	0	0	210	210

Table 4.22 presents the values of maximum and minimum pressures experienced as a result of VCT of 144 s in an experimental investigation of HT due to sudden valve closure in a pipeline transporting PMS. The results of the investigation showed that a peak positive pressure surge of 1,035 kPa and a least negative pressure surge of – 50 kPa were recorded at a nodes F and B respectively for a VCT of 144 s. The developed peak positive pressure surge at node F is above the pressure rating of the nodal sets and may lead to the failure of the nodal sets. Also, the developed negative pressure surge at node B is below the RVP of PMS (48 kPa) and may lead to the failure of the node due to the development of cavitation and column separation at that node. The results of the investigation showed that the pressure surge fluctuates between maximum and minimum pressure values before the attainment of stability.

Table 4.22: Pressure surges in a PMS pipeline at 144 s VCT

Nodes	T max (s)	T min (s)	max (kPa)	min (kPa)
A	5	9	98	98
B	10	34	245	-50
C	30	6	996	240
D	69	8	954	238
E	67	9	953	238
F	78	17	1,035	205
G	20	17	370	50
H	11	2	210	210

Table 4.23 presents the values of maximum and minimum pressures experienced as a result of VCT of 288 s in an experimental investigation of HT due to sudden valve closure in a pipeline transporting PMS. The results of the investigation showed that a peak positive pressure surge of 1,020 kPa and a least negative pressure surge of – 50 kPa were recorded at a nodes F and B respectively for a VCT of 288 s. The developed peak positive pressure surge at node F is above the pressure rating of the nodal sets and may lead to the failure of the nodal sets. Also, the developed negative pressure surge at node B is below the RVP of PMS (48 kPa) and may lead to the failure of the node due to the development of cavitation and column separation at that node. The results of the investigation showed that the pressure surge fluctuates between maximum and minimum pressure values before the attainment of stability.

Table 4.23: Pressure surges in a PMS pipeline at 288 s VCT

Nodes	T max (s)	T min (s)	max (kPa)	Min (kPa)
A	10	4	97	98
B	11	7	240	-50
C	30	10	958	240
D	21	9	845	235
E	23	9	845	234
F	20	15	1,020	150
G	19	20	369	52
H	7	9	210	212

Table 4.24 presents the values of maximum and minimum pressures experienced as a result of VCT of 576 s in an experimental investigation of HT due to sudden valve closure in a pipeline transporting PMS. The results of the investigation showed that a peak positive pressure surge of 1,005 kPa and a least negative pressure surge of – 50 kPa were recorded at a nodes F and B respectively for a VCT of 576 s. The developed peak positive pressure surge at node F is above the pressure rating of the nodal sets and may lead to the failure of the nodal sets. Also, the developed negative pressure surge at node B is below the RVP of PMS (48 kPa) and may lead to the failure of the node due to the development of cavitation and column separation at that node. The results of the investigation showed that the pressure surge fluctuates between maximum and minimum pressure values before the attainment of stability.

Table 4.24: Pressure surges in a PMS pipeline at 576 s VCT

Nodes	T max (s)	T min (s)	max (kPa)	Min (kPa)
A	11	8	99	97
B	10	5	236	-48
C	36	10	945	235
D	29	9	839	231
E	27	9	836	230
F	20	19	1,005	141
G	17	18	370	53
H	7	5	209	211

Figure 4.38 depicts the summary of the positive peak pressure surges experienced at node F due to various VCTs and the result showed that as the rate of VCT is been increased, the pressure surge been developed decreases. This could be as a result of longer time taken to halt the flow of the fluid and hence the change in pressure also takes place slowly.
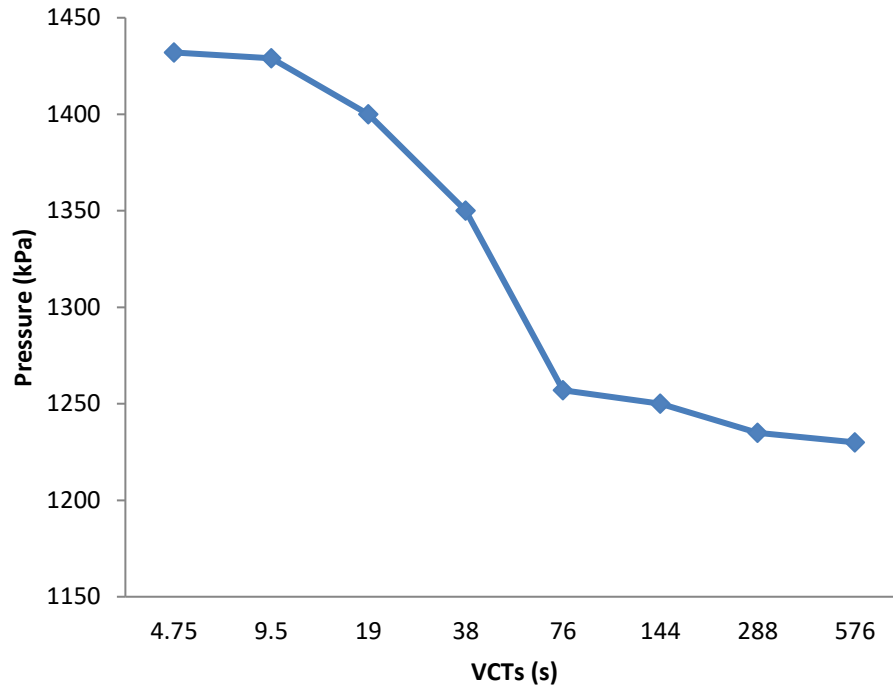
Figure 4.38: Pressure surges due to different VCTs in a PMS pipeline

4.3.4   Experimental results for pump failure

Figure 4.39 depicts the pressures surges for AGO in a pipeline due to pump failure. The result showed that negative pressure surges of about – 24 kPa, - 7 kPa and -4 kPa were recorded at nodes B, D, and E respectively. The pressure surges developed at these nodes are below the RVP of the AGO of about 0.5 kPa and therefore, it leads to the occurrence of cavitation at these nodes and the pipes in general. Because according to Cucit *et al.* (2018) cavitation or vacuum conditions come into being as a result of a drop in pressure below atmospheric or below the vapour pressure of the fluid been transported.
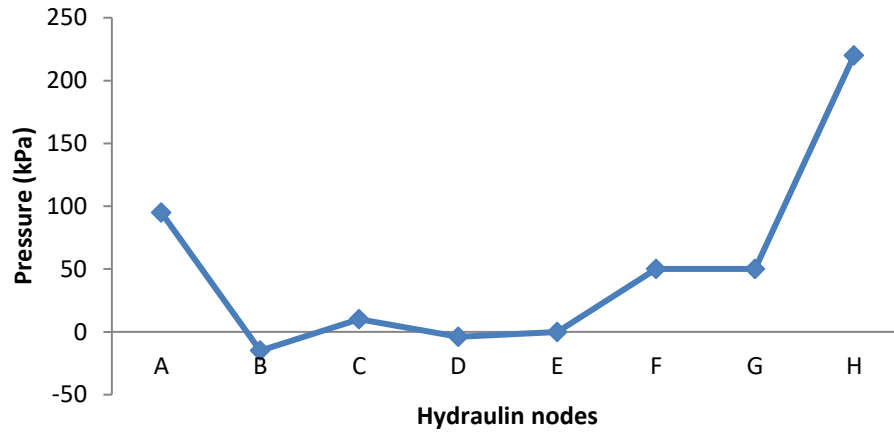
Figure 4.39: Pressure surges due to pump failure in an AGO pipeline

Figure 4.40 depicts the pressures surges for DPK in a pipeline due to pump failure. The result showed that negative pressures of about – 24 kPa, - 11 kPa and -4 kPa were recorded at nodes B, D, and E respectively. The pressure surges developed at these nodes are below the vapour pressure of the DPK of about 1.1 kPa and therefore, it leads to the occurrence of cavitation at these nodes.
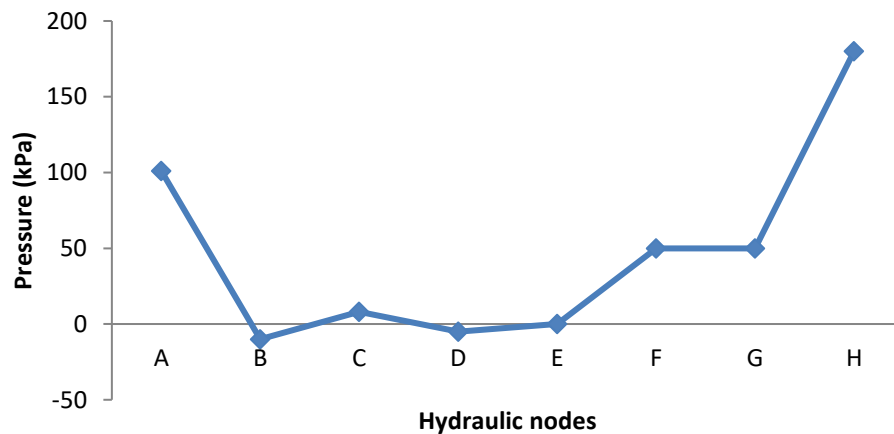

Figure 4.40: Pressure surges due to pump failure in a DPK pipeline

Figure 4.41 depicts the pressures surges for PMS in a pipeline due to pump failure. The result showed that negative pressures of about – 21 kPa, - 10 kPa and -4 kPa were

recorded at nodes B, D, and E respectively. The pressure surges developed at these nodes are below the vapour pressure of the DPK of about 48 kPa and therefore, it leads to the occurrence of cavitation at these nodes.
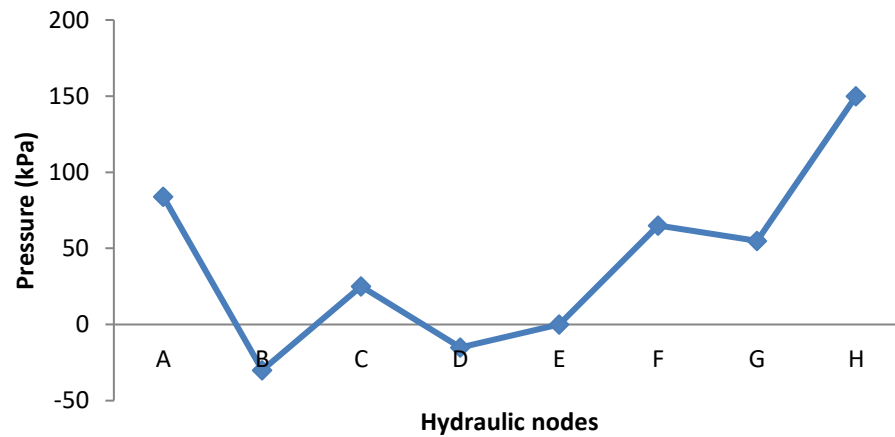
Figure 4.41: Pressure surges due to pump failure in a PMS pipeline

4.4   Validation of Results

4.4.1 Comparison of simulation and experimental pressure surges due to sudden valve closures

Figures 4.42 shows the comparison of results of simulation and experimental pressure surges obtained for AGO in this research. The simulation and experimental results are having the same pattern under nearly all the conditions and the average error difference between the two set of the results is around 3% - 5% as such they are in good agreement with one another despite having some little differences due to environmental and operational factors.

Figure 4.42: Comparison of pressure surges of simulation and experiments in anAGO pipeline due to sudden valve closure

Figure 4.43 shows the comparison of simulation and experimental results of pressure surges due to sudden valve closures in a pipeline transporting DPK. The simulation and experimental results are having the same pattern under nearly all the conditions and the average percentage error between the two set of the results is around 5% as such they are in good agreement with one another despite having some little differences due to environmental and operational factors.

Figure 4.43: Comparison of pressure surges of simulation and experiments in a DPK pipeline due to sudden valve closure

Figure 4.44 shows the comparison of simulation and experimental results of pressure surges due to sudden valve closures in a pipeline transporting PMS. The simulation and experimental results are having the same pattern under nearly all the conditions and the average error difference between the two set of the results is around 3% - 5% as such they are in good agreement with one another despite having some little differences due to environmental and operational factors.
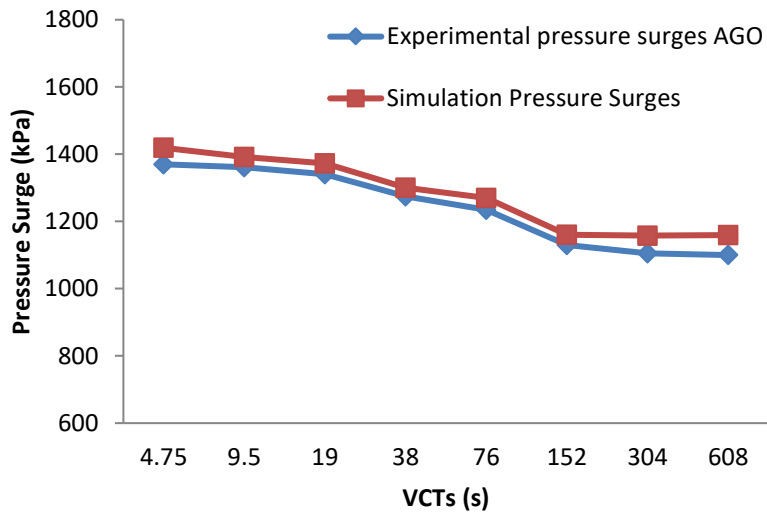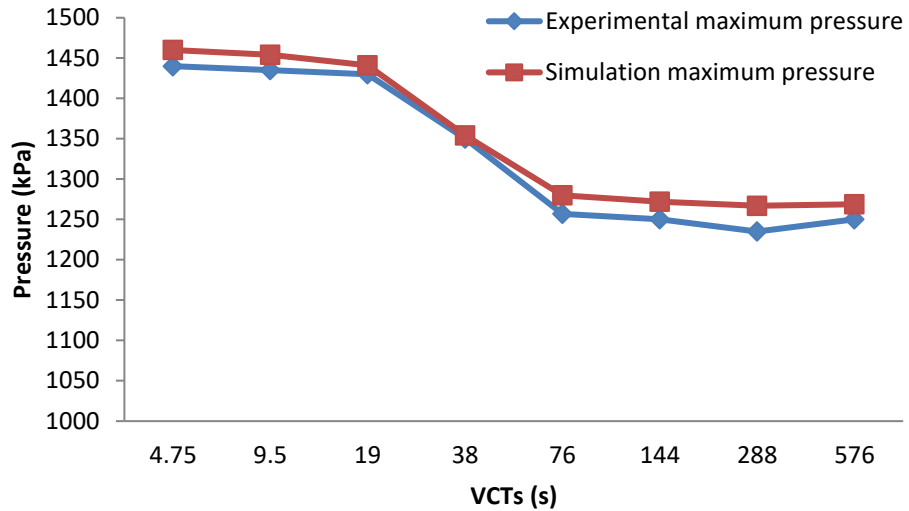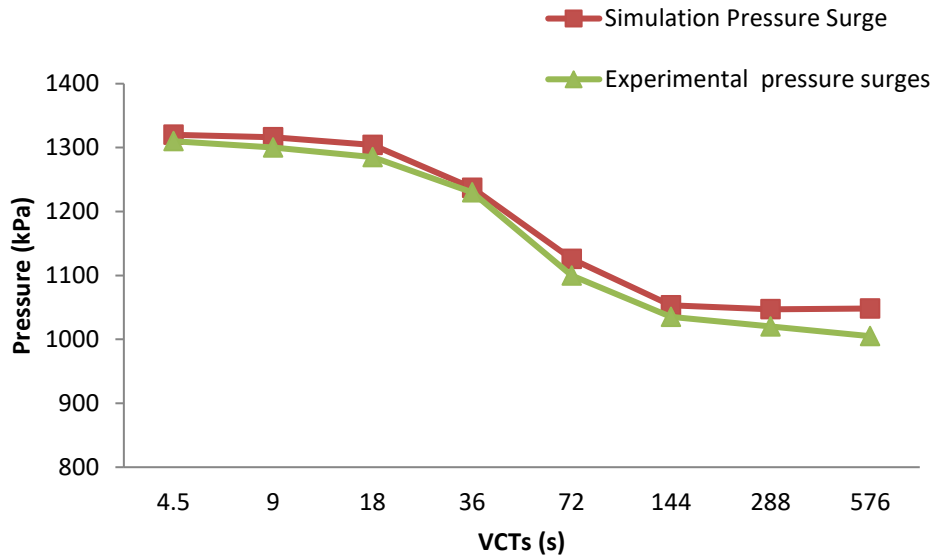
Figure 4.44: Comparison of pressure surges of simulation and experiments in PMS pipelines due to sudden valve closure

4.4.2 Comparison of simulation and experimental pressure surges due to sudden pump failure

Figure 4.45 depicts the behaviours of the pressure surge for both simulation and experimental analysis in an AGO pipeline due to pump failure. From the Figures, it can be deduced that the values of pressure surges presented are in good agreement up to about 95% - 97% between the simulated results and the experimental results with an error difference of about 3% - 5%.
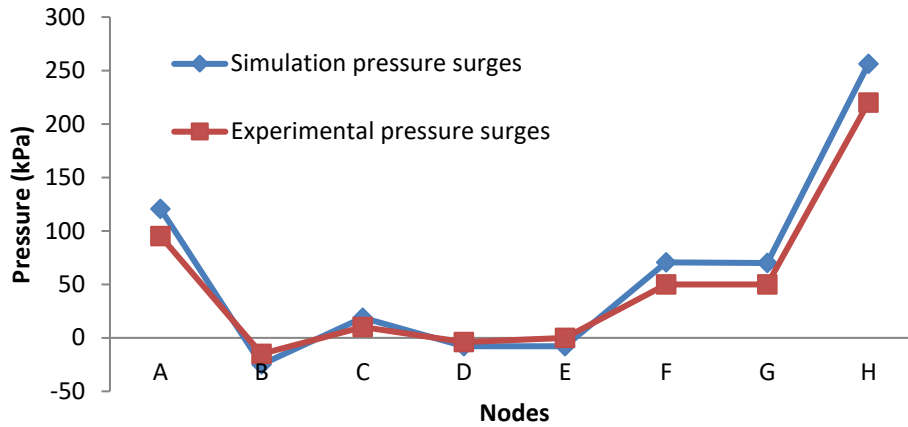
Figure 4.45: Comparison of pressure surges of simulation and experiments in AGO pipelines due to pump failure

Figure 4.46 depicts the behaviours of the pressure surge for both simulation and experimental analysis in a DPK pipeline due to pump failure. From the Figures, it can be deduced that the values of pressure surges presented are in good agreement up to about 98% between the simulated results and the experimental results with an error difference of about 2%.
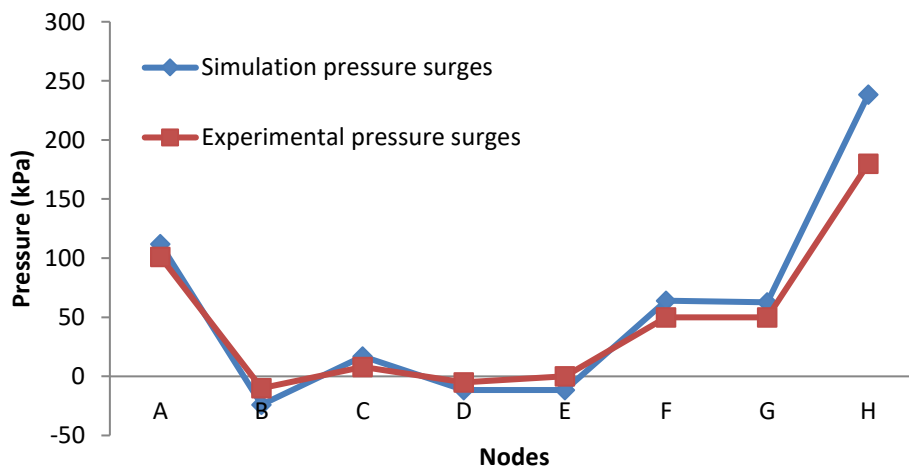
Figure 4.46: Comparison of pressure surges of simulation and experiments in a DPK pipeline due to pump failure

Figure 4.47 depicts the behaviours of the pressure surge for both simulation and experimental analysis in a PMS pipeline due to pump failure. From the Figures, it can be deduced that the values of pressure surges presented are in good agreement with one another with about 3% error difference between the simulated results and the experimental results.
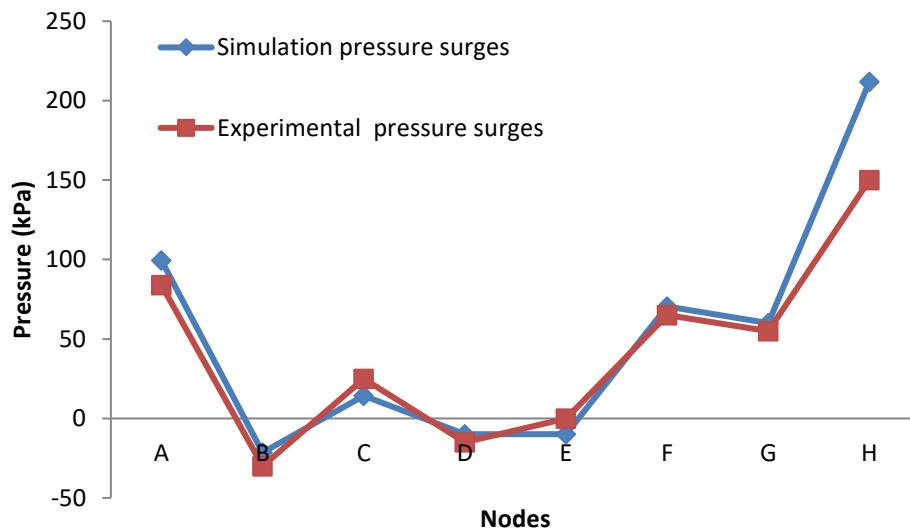

Figure 4.47: Comparison of pressure surges of simulation and experiments in PMS pipelines due to pump failure

CHAPTER FIVE

5.0   CONCLUSION AND RECOMMENDATIONS

5.1   Conclusion

In this research, problems associated with HT were presented to point out the numerous issues connected to its causes prevention and control procedures. Analytical, numerical, and experimental methods were used in this research to investigate HT. The following conclusions were reached from this research work:

The pressure and velocity heads at the nodes of a petroleum pipeline transporting refined petroleum products namely AGO, DPK, and PMS was carried out. The results showed that all the fluid under study exhibits the same nature of pressure head with node C (a node just upstream of the pump) having the highest pressure heads among all the nodes. The pressure heads at the node C are as follows; AGO has 0.117034 m, DPK has 0.115151 m and PMS has 0.107164 m. It was observed that pressure heads are high at points where more pressure or energy is added to the flowing fluid and low at points where fluid is extracted as is the case at node B. The research also found that that the velocity head in the pipeline network is reducing along the downstream side of the network. Node A experiences the highest velocity heads by all the fluid while node H records the least. Among the fluids, DPK has the highest velocity head at all the nodes, followed by PMS then AGO.

The effects of HT (pressure surges) due to sudden valve closure were investigated in this research. The nature of the responses of AGO, DPK, and PMS to the sudden valve closures showed that the magnitude of the surge decreases as a result of increase in VCTs

The effects of hydraulic transient due to abrupt pump failure were also investigated in this research work. The nature of the responses of AGO, DPK, and PMS to the abrupt pump failure at the various hydraulic nodes showed that all the fluids showed similar responses to the pump failure. The pressure of the fluids at all the nodes fluctuates between positive and negative pressures before stabilizing. Negative pressures would be experienced at nodes B, D and. The negative pressures developed at these nodes is below atmospheric pressure and below the RVP of the fluids being transported, hence the formation of cavitation voids and column separations at these nodes as well as along the pipes.

The simulated results were validated with experimental results and the result of the validation showed that there were significant agreement of up to about 95% with an average error difference of around 5% between the simulated and the experimental results.

5.2   Recommendations

The research recommends that surge tank should be installed at nodes where the rise in pressure are high and fluctuating in order stabilise and maintain the appropriate operating pressure of the pipeline. Also, vents are to be installed at nodes where the pressure of the pipeline drops below atmospheric or below the vapour pressure of the fluid being transported.

The pressure rating of a pipeline should be taken from the pressure rating of the nodal sets because of their lower pressure ratings compared to the pressure ratings of other components of the pipeline network.

5.3   Contributions to Knowledge

The thesis revealed that, in order to avoid hydraulic transient, a marginal valve closure rate (MVCR) ranging from 0.0006 m/s to 0.0025 m/s is safe for a standard pipe size of 0.3556m (14") with the flow of Automotive Gas Oil (AGO), Dual Purpose Kerosene (DPK) and Premium Motor Spirit (PMS). The pressure heads of 0.117034 m, 0.115151 m, and 0.107164 m occurs at the node just immediately after the pump for Automotive Gas Oil (AGO), Dual Purpose Kerosene (DPK) and Premium Motor Spirit (PMS) respectively which indicates that the node just immediately after the pump experiences more load due to weight of the fluids. The thesis also revealed that velocity head reduces along the downstream side of the network. The fluid particles at the nodes upstream of the pump require more energy to move down the downstream during steady state flow condition. The results of the simulation analysis showed that worst case scenarios due to the sudden valve closures are the development of excessively high positive pressure and negative pressure of 1419kPa, -98kPa (AGO), 1461kPa, -99kPa (DPK) and 1321kPa, -52kPa (DPK) experienced at the node just before the flow control valve (node F) and the node just before the pump (node B) respectively against an operating pressure of 1034kPa of the nodal sets. In addition, the worst-case scenario experienced for pump failure is drop in pressure below atmospheric and below the vapour pressure of the fluids being transported at nodes just before the pump and the nodes just before and after the non-return valve for all the fluids. Hence,the formation of cavitation and column separation at these nodes.

REFERENCES

Abuiziah, I., Oulhaj, A., Sebari, K., & Ouazar, D. (2013). Simulating flow transients in conveying pipeline systems by rigid column and full elastic methods : pump combined with air chamber. *International Journal of Mechanical and Mechatronics Engineering*, *7*(12), 2391–2397.

Abuiziah, I., Oulhaj, A., Sebari, K., & Ouazar, D. (2014). Comparative study on status and development of transient flow analysis including simple surge tank. International Journal of Civil and Environmental Engineering, *8*(2), 228–237.

Abukhousa, E., Al-jaroodi, J., Lazarova-molnar, S., & Mohamed, N. (2014). Simulation and modeling efforts to support decision making in healthcare supply chain management. *The Scientific World Journal*, 1–16, doi.org/10.1155/2014/354246.

Achebe, C. H., Nneke, U. C., & Anisiji, O. E. (2012). Analysis of oil pipeline failures in the oil and gas industries in the Niger Delta area of Nigeria. *Proceedings of the International MultiConference of Engineers and Computer Scientist*, *II*(1), 1–6.

Adamkowski, A., Henclik, S., Janicki, W., & Lewandowski, M. (2016). The influence of pipeline supports stiffness onto the water hammer run. *International Symposium on Transport Phenomena and Dynamics of Rotating Machinery*, 1–8.

Adamu, A. A. (2017). Software for natural gas pipeline design and simulation (GASPISIM). *Global Journal of Engineering Research*, *15*, 47–62. doi.org/10.4314/gjer.v15i1.6

Adeyemi, L. O. (2020). The political ecology of oil pipeline vandalism in Nigeria. International Journal of Research and Innovation in Social Science , 4(5), 239-245

Agho, N., Mailabari, S. K., Omorodion, I. H., Ariavie, G. O., & Sadjere, G. E. (2017). Design construction and testing of a petroleum product storage tank 10 million litre capacity. *European Journal of Engineering Research and Science*, *2*(3), 1–6. doi.org/10.24018/ejers.2017.2.3.308

Aibada, N., Manickam, R., Gupta, K. K., & Raichurkar, P. (2017). Review on various gaskets based on the materials , their characteristics and applications. *International Journal on Textile Engineering and Processes*, *3*(1), 1–8.

Akpan, P. U., Jones, S., Eke, M. N., & Yeung, H. (2015). Modelling and transient simulation of water flow in pipelines using WANDA Transient software. *Ain Shams Engineering Journal*, 1–10, doi.org/10.1016/j.asej.2015.09.006

Al-Muntasser, O., & Dekam, E.I. (2019). WANDA Transient Flow Analysis; 2.8 m Diameter "Tarhunah-Abu-Ziyyan" Water Pipeline. Retrieved on December 20, 2021 from https://www.researchgate.net/publication/331743049

Ammar, H. T. (2014). Water hammer modeling and analysis for khobar-dammam water

transmission ring line. (Master of Engineering Thesis of King Fahd University of Petroleum and Minerals. Retrieved on December 26, 2021 from https://eprints.kfupm.edu.sa/id/eprint/139203/1/199940370_MS_Thesis.pdf

Aroh, K.N. Ubong I.U.,Eze, CL., Harry, I.M.& A. E. G. (2010). Oil spill incidents and pipeline vandalization in Nigeria : Impact on public health and negation to attainment of Millenniu goal, doi.org/10.1108/09653561011022

Arsham, H. (n. d). Systems Simulation: The Shortest Route to applications. Retrieved on December 19, 2021 from http://home.ubalt.edu/ntsbarsh/simulation/sim.htm

B16.5 (2013). Pipe flanges and flanged fittings NPS. In *American Society of Mechanical Engineers*. Retrieved on December 26, 2021 from https://www.amazon.com/Pipe-Flanges-Flanged-Fittings-Standard/dp/0791834913

Barker, G. (2018). *The Engineer's guide to plant layout and piping design for the oil and gas industries*(pp. 9–71). Gulf Professional Publishing. doi.org/10.1016/B978-0-12-814653-8.00002-3

Barros, R. M., Tiago Filho, G. L., Dos Santos, I. F. S., & Da Silva, F. G. B. (2014). Case studies for solving the Saint-Venant equations using the method of characteristics : pipeline hydraulic transients and discharge propagation. *27th Symposium on Hydraulic Machinery and Systems*, *22*, 1–11, doi.org/10.1088/1755-1315/22/4/042019

Beckman, K., Grewal, G., & Christensen, K. (2009). ASME B31.3 Process piping guide. In *LANL Engineering Standards Manual PD342* (No. 2; Section D2, pp. 1–168). Retrieved on December 26, 2021 from https://engstandards.lanl.gov/esm/pressure_safety/process_piping_guide_R2.pdf

Bergant, A., Karadži, U., & Tijsseling, A. S. (2018). Developments in multiple-valve pipeline column separation control. *Journal of Physics: Conference Series*, *813*(1). doi.org/10.1088/1742-6596/813/1/012015

Bhatia, A. (n.d-a). *Control Valve Basics : Sizing and Selection* (Issue 877). Retrieved on December 26, 2021 from http://docplayer.net/187929621-Control-valve-basics-sizing-selection-quick-book-by-a-bhatia.html

Bhatia, A. (n.d-b). *Process Piping Fundamentals , Codes and Standards Credit : 5 PDH*. *877*. Retrieved on December 26, 2021 from https://www.academia.edu/39245950/Process_Piping_Fundamentals_Codes_and_Standards_Credit_5_PDH

Bhattarai, K. P., Zhou, J., Palikhe, S., & Pandey, K. P. (2019). Numerical modeling and hydraulic optimization of a surge tank using particle swarm optimization. *Water*, *11*(715), 1–19.doi.org/10.3390/w11040715

Carlsson, J. (2016). *Water* hammer phenomenon analysis using the method of characteristics and direct measurements using a " stripped " electromagnetic flow

meter, (Master of Science Thesis, Royal Institute of Technology, Stockholm, Sweden). Retrieved on December 26, 2021 fromhttp://www.diva-portal.org/smash/get/diva2:981316/

Carmona-Paredes, R. B., Autrique, R., & Rodal-Canales, E. (2019). A new method to calculate hydraulic transients in HDPE pipes using the standard solid model to represent the HDPE viscoelastic behaviour. *29th IAHR Symposium on Hydraulic Machinery and Systems, Conference Series: Earth and Environmental Science*, *240*. doi.org/10.1088/1755-1315/240/5/052020

Carvajal, J. D.,& Bohorquez, J. (2018). Estimation of marginal time in water distribution systems for valve closure considering transient flow effects. Retrieved on December 26, 2021 from http*//ojs.library.queensu.ca/index.php/wdsa-ccw/article/view/12324*

Chaichan, M. T.,& Al-zubaidi, D. S. M. (2015). Control of hydraulic transients in the water piping system in Badra–pumping station No. 5. *Al-Nahrain University, College of Engineering Journal*, *18*(2), 229–239.

Chandra, S., & Dutta, H. (2014). *Guidelines for integrity assessment of cross country pipelines oil industry safety directorate*. Retrieved on December 26, 2021 from https://www.oisd.gov.in/Image/GetDocumentAttachmentByID?documentID=136

Chuka, C. E., Freedom, I. H.,& Anthony, U. O. (2016). Transient model-based leak detection and localization technique for crude.*Saudi Journal of Engineering and Technology*, *1*(2), 37–48, doi.org/10.21276/sjeat.2016.1.2.2

Cucit, V., Burlon, F., Fenu, G., Furlanetto, R., Pellegrino, A.,& Simonato, M. (2018). A control system for preventing cavitation of centrifugal pumps. *73rd Conference of the Italian Thermal Machines Engineering Association, Pisa, Italy*, 12–14.DOI: 10.1016/j.egypro.2018.08.074

Curl, H., & O'Donnell, K (1977). Chemical and physical properties of refined petroleum products, Retrieved from https://repository.library.noaa.gov/view/noaa /11031/noaa_11031_DS1.pdf on 26/12/2021.

Dawidowicz, J. (2018). Evaluation of a pressure head and pressure zones in water distribution systems by artificial neural networks. *Neural Computing and Applications*, *30*(8), 2531–2538. doi.org/10.1007/s00521-017-2844-8

Dawotola, A. (2012). Risk based maintenance of petroleum pipelines. (Doctoral dissertation, Technische Universiteit Delft).DOI:10.4233/UUID:288ED504-60E4-4E47-8E73-203EC5984A45

Delgado, J. N. G. B. (2013). Hydraulic transients in pumping systems – numerical modelling and experimental analysis. (Master of science thesis, Instituto Superior Técnico).Retrieved on December 26, 2021 from http://www.civil.ist.utl.pt/~didia/FCT2014_ARIETE/17_MasterThesis_JDelgado_ 2013.pdf

DPR (2007). Guidelines and procedures for the design, construction, operation and maintenance of oil and gas pipeline systems in Nigeria.Retrieved on December 26, 2021 fromhttps://dpr.gov.ng/wp-content/uploads/2018/03/pipeline-guidelines.pdf

Duan, H. F. (2017). Transient flow analysis and utilization in urban water supply systems. *Journal of Hydroinformatics*, *2*(1), 10–13. https://doi.org/10.19080/CERJ.2017.02.555576

Economides, M., & Kappos, L. (n.d.). Petroleum *pipeline network optimization. exergy, energy system analysis and optimization*, *II*, 1–7. Retrieved on December 26, 2021 from https://www.eolss.net/Sample-Chapters/C08/E3-19-03-09.pdf

Egbe, J., Ewa, D., Ettah, E., Bassey, G., & Nsifik, E. (2017). An investigation of the gathering system options for a hypothetical field with uniformly distributed production wells. *Journal of Civil & Environmental Engineering*, *7*(1), 1–7. doi.org/10.4172/2165-784X.100

El-Turki, A. (2013). *Modeling of hydraulic transients in closed conduits*. (Master of Science, Colorado State University Fort Collins, Colorado). Retrieved on October 20, 2018 from https://mountainscholar.org/bitstream/handle/10217/80235

Elbashir, M. A. M., Oduro, S., & Amoah, K. (2007). *Hydraulic transient in a pipeline, using computer model to calculate and simulate transient*. Lund University. Retrieved on October 20, 2021 from https://lup.lub.lu.se/student-papers/search/publication/1324026.

Gambit-Group (n. d). Gamspir spiral woundgaskets. Retrieved on December 17, 2021 fromhttps://gambitgi.eu/en/produkty/seals/gamspirr-spiral-wound-gaskets.html

Garcia-hernandez, A., Wilcox, M., & Moore, T. (2010). Hydraulic modelling and simulation of pumping systems. *Proceedings of the Twenty-Sixth International Pump Users Symposium*, 8. doi.org/10.21423/R1CP90

Garg, R. K., & Kumar, A. (2018). *Analysis of hydraulic transients in a reservoir-valve-pipeline arrangement by using method of characteristics (MOC)*. Retrieved on October 20, 2018 from https://www.researchgate.net/publication/324311451

Ghidaoui, M. S., Zhao, M., Mcinnis, D. A., & Axworthy, D. H. (2005). A review of water hammer theory and practice. *Applied Mechanics Reviews*, *58*, 49–76. doi.org/10.1115/1.1828050

Gómez, A. M. (2018). *Physical aspects of air in pipe systems, including its effect on pipeline flow capacity and surge pressure (water hammer)*, (Master's Thesis, Aalborg University). Retrieved on July 6, 2021 from https://projekter.aau.dk/projekter/files/281295911

Gseaa, F. S., & Dekam, E. I. (2010). Pressure transient in pipe networks; simulation and analysis. *Journal of Engineering Research (Al-Fateh University)*, *14*, 40–52.

Retrieved on December 26, 2021 from https://www.researchgate.net/publication/286921637_Pressure_Transient_in_pipe_Networks_Simulation_and_Analysis

Han, C. J., Zhang, H., & Zhang, J. (2016). Failure pressure analysis of the pipe with inner corrosion defects by FEM. *International Journal of Electrochemical Science*, *11*, 5046–5062. doi.org/10.20964/2016.06.6

Henclik, S. (2015). A numerical approach to the standard model of water hammer with fluid-structure interaction. *Theoretical, Journal of Mechanics, Applied*, *53*(3), 543–555. doi.org/10.15632/jtam-pl.53.3.543.

Himr , D., Haban, V., Hudec, M., & Pavlík, V. (2017). Experimental investigation of the check valve behaviour when the flow is reversing, Web of Conferences 143, 02036. DOI: 10.1051/epjconf/201714302036

Hirani, A. A., & Kiran, C. U. (2013). CFD Simulation and analysis of fluid flow parameters within a y-shaped branched pipe. *Journal of Mechanical and Civil Engineering*, *10*(1), 31–34. Doi:10.9790/1684-1013134

Huijzer, L. (2018). *Improving the solution method in wanda*. TU Delft. Retrived on October 10, 2020 from http://ta.twi.tudelft.nl/nw/users/vuik/numanal/huijzer_presentation1.pdf

Inno-bi solution (n. d). Definition for surge analysis. Retrieved on December 17, 2021 from http://www.inno-bi.net/wp/definitions-for-surge-analysis?

Jablonska, J., & Kozubkova, M. (2017). Experimental measurements and mathematical modeling of static and dynamic characteristics of water flow in a long pipe. *Conf. Series: Materials Science and Engineering*, *223*, 1–8. doi.org/10.1088/1757-899X/233/1/012013

Jalut, Q. H., & Ikheneifer, A. A. (2010). Mathematical simulation for transient flow in pipes under potential water hammer. *Diyala Journal of Engineering Sciences, First Engineering Scientific Conference*, *1*, 222–236. Retrieved on December 26, 2021 fromhttps://dengs.iraqjournals.com/pdf_39570_009dccb4ad20fe457a5aa4d378cdf

James, S. (2012). Characteristics of centrifugal pump. Retrieved on December 19, 2021 from https://www.pumpsandsystems.com/characteristics-centrifugal

Jaya, A., & Kolmetz, K. (2014). Fluid flow hydraulic liquid surge (process engineering equipment design guideline). Retrieved on December 26, 2021 fromhttps://www.researchgate.net/publication/339926486_fluid_flow_hydraulic_liquid_surge_Kolmetz_Handbook_of_Process_Equipment_Design

Jayakumar, R., Meenakshi, T., & Sivakumar, R. (2014). CFD analysis of transient flow in transverse corrugated pipes, 5th International Congress on Computational Mechanics and Simulation, 10-13 December 2014, India. DOI: 10.3850/978-981-09-1139-3_065

156

Jiang, D., Ren, C., Zhao, T., & Cao, W. (2018). Pressure transient model of water-hydraulic pipelines with cavitation. *App/. Sci.*, *8*(388), 1–14. doi.org/10.3390/app8030388

Jiang, D., Lu, Q., Liu, Y., & Zhao, D. (2019). Study on pressure transients in low pressure water-hydraulic pipelines. Institute of Electrical and Electronics Engineers *Access*, *7*, 80561-80569. doi:10.1109/access.2019.2923100

J-Gold (n. d.). Dual purpose kerosene (DPK). Retrieved on December 17, 2021 fromhttp://www.jgoldpet.com/services/dual-purpose-kerosene on 17/12/2021

Jones, C., Shorts, M., Pollock, M., Raty, G., Miskell, C., Bisset, D., Raimer, M., Norton, C., Frisard, R., Boyd, M., Petrunich, P., Azibert, H., Sheffield, L., Hasha, B., Drago, J., & Mahoney, P. (2017). *Gasket handbook*. Retrieved on December 26, 2021 from https://www.fluidsealing.com/publication-downloads/FSA%20Gasket%

Kelemen, N., Keil, B., Mielke, R., Davidenko, G., & Gardner, J. (2011). Performance of gasket joints in steel pressure pipes. *Pipelines: A Sound Conduit for Sharing Solutions ASCE*, *919*, 1278–1287.doi.org/10.1061/41187(420)117

Kiefner, J. F., & Rosenfeld, M. J. (2012). The role of pipeline age in pipeline safety. Retrieved on June 6, 2021 from https://www.ingaa.org/file.aspx?id=19307

Kim, H. (2012). *Numerical and experimental study on dynamics of unsteady pipe flow involving (Doctoral dissertation, Univaersity of Southern California)*. Retrieved on December 12, 2017 from http://digitallibrary.usc.edu/digital/collection/p15799coll3/id/116209

Kolmetz, K., Chan, J. H., Mulyandasari, V., Kolmetz, K., & Sari, R. M. (2020). Instrumentation control valve selection, sizing and trouble shooing: handbook of process equipment design (No. 4). Retrived on December 26, 2021 from Https://www.academia.edu/40639301/

Kothandaraman, C. P., & Rudramoorthy, R. (2007). *basic fluid mechanics* (Second Edi). New Age International (P) Limited, Publishers. Retrieved on December 26, 2021 from https://www.amazon.com/Fluid-Mechanics-Machinery-Rudramoorthy-Kothandaraman/dp/B01LX6KCHA

Lahane, S., Patil, R., Mahajan, R., & Palve, K. (2015). Analysis of water hammering in pipeline and its CFD simulation. *International Journal of Engineering Technology, Management and Applied Sciences*, *3*(5), 250–255.

Larock, B. E., Jeppson, R. W., & Watters, G. Z. (2000). Hydraulics *of Pipeline Systems* (Eds.); first). CRC Press LLC, 2000 N.W. Corporate Blvd., Boca Raton, Florida 33431. Retrieved on December 24, 2018 from https://www.academia.edu/31765037/Hydraulics_of_Pipeline_Systems

Lebele-alawa, B. T., & Oparadike, F. E. (2015). Pressure surge dependence on valve

operations in a pipeline loading system. *Engineering*, *7*, 322–330. doi.org/10.4236/eng.2015.76028

Lee, J. (2015). Hydraulic transients in service lines. *International Journal of Hydraulic Engineering*, *4*(2), 31–36. doi.org/10.5923/j.ijhe.20150402.02

Li, X. Z. W., & He, Z. L. H. (2015). *Reliability analysis of aged natural gas pipelines based on utility theory*. *35*(2), 193–203. Retrieved on December 26, 2021 from https://hrcak.srce.hr/139386

Malppan, P. J., & Sumam, K. S. (2015). Pipe burst risk assessment using transient analysis in surge 2000. *Aquatic Procedia*, *4*(Icwrcoe), 747–754. doi.org/10.1016/j.aqpro.2015.02.157

Maryono, A., Kurniawan, S. A, Alatas, M., Akhita, A. M. R., & Wicaksono, A. B. (2013). Experimental Study of Water Hammer Phenomena in Drinking Water Pipeline Distribution Using Video Camera Method, International Journal of Scientific & Engineering Research, 4(2),

Metallic-steel (2018). Flange, Metallicsteel (2018). Flange. Retrieved on December 20, 2021 from https://www.metallicsteel.com/flange.html

Miriti, M. M., & Osiemo, M. C. (2012). *Pumping system design for petroleum industry in line with vision 2030 (From Mombasa to Nairobi)*. University of Nairobi. Retrieved on December 26, 2021 from https://www.scribd.com/document/438631760/pumping-system-design-pdf

Moran, S. (2016). Pump sizing: bridging the gap between theory and practice. *American Institute of Chemical Engineers*7. Retrieved on December 26, 2021 from www.aiche.org/resources/publications/cep/2016/december/pump-sizing/

Muhammad, A. B., Nasir, A., Ayo, S. A., & Ige, B. (2019). Hydraulic transient analysis in fluid pipeline : A review.*Journal of Science, Technology and Education*, *7*(4), 291–299.

Mylapilli, L. K. (2015). *Hydraulic and surge analysis in a pipeline network using pipeline studio*. International Journal of Engineering Research & Technology, *4*(2), 41–48.

Naik, U., & Shreenivas, B. D. (2015). Water hammering effects in pipe system and dynamic stress prediction. *International Journal of Emerging Research in Management and Technology*, *4*(6), 236–243.

Natgas (2013). The transportation of natural gas. Retrieved on December 17, 2021 fromhttp://naturalgas.org/naturalgas/transport/

Nerella, R., & Rathnam, E. V. (2015). Fluid transients and wave propagation in pressurized conduits due to valve closure. *Procedia Engineering*, *127*, 1158–1164. doi.org/10.1016/j.proeng.2015.11.454

Nikodijević, M., Stamenković, Ž., Petrović, J., & Kocić, M. (2018). Valve selection for the purpose of reducing the water hammer effect in a pressurized pipeline. working and living environmental protec*tion*, *15*(3), 217–227. doi.org/https://doi.org/10.22190/FUWLEP1803217N

Nnadi, U., El-hassan, Z., Smyth, D., & Mooney, J. (2007). Lack of proper safety management systems in nigeria oil and gas pipelines. *Hazards*, *24*(159), 1–10.

Okoli, A. C., & Orinya, S. (2013). Pipeline Vandalism and Nigeria's National Security, Global Journal of Human Social Science Political Science, 13(5), 66-75

Olenev, N. N. (n.d.). modeling and simulation techniques. *Systems Analysis And Modeling of Integrated World Systems*, *I*, 1–9. Retrieved on December 26, 2021 from https://www.eolss.net/Sample-Chapters/C15/E1-26-05-04.pdf

Olugboji, O. A. (2011). Development of an Impact Monitoring System for Petroleum Pipelines. *Assumption University Journals Thailand*, *15*(2), 115–120.

Oluwole, M. S., & Ojekunle, J. A. (2016). Perceived environmental impact of refined petroleum products transportation and distribution: case of Kaduna City, Nigeria. *FUTA Journal of Management and Technology*, *1*(2), 112–122.

Ox-science (2020). Stopwatch: definition, types and uses. Retrieved on December 26, 2021 from https://www.astopwatch.co.uk/products/index.

Oyedeko, K. F. K., & Balogun, H. . (2015). Modeling and simulation of a leak detection for oil and gas pipelines via transient model : a case study of the Niger Delta. *Journal of Energy Technologies and Policy*, *5*(1), 16–28.

Oyinloye, M. A., Oladosu, B. L., & Olamiju, I. O. (2017). pipeline right-of-way encroachment in Arepo , Nigeria. *The Journal of Transport and Land Use*, *10*(1), 715–724. doi.org/10.5198/jtlu.2017.1217

Pearson, J. (2021). Pressure rating table for carbon steel pipe. Retrieved on December 17, 2021 from www.dpr-guidelines-n-procedures-for-the-design-construction-operation/

Pharris, T. C., & Kolpa, R. L. (2007). Overview of the design, construction, and operation of interstate liquid petroleum pipelines. doi.org/10.2172/925387

Profound-Energy (2018). Automotive gas oil ago (AGO) Retrieved on December 17, 2021 fromhttp://www.profundenergy.com/automotive-gas-oil-ago/

Pullinger, M. G. (2011). E*valuating hydraulic transient analysis techniques in pumped-storage hydropower systems*. (Master of science thesis, Murdoch University). Retrieved on December 26, 2021 from https://core.ac.uk/download/pdf/11236318.pdf

Puntorieri, P., Calabria, R., Barbaro, G., Calabria, R., Fiamma, V., & Calabria, R., (2017). Experimental study of the transient flow with cavitation in a copper pipe system. *International Journal of Civil Engineering and Technology*, *8*(9), 1035–1041.

Ques10 (n. d). What are the advantages and disadvantages of finite element method. Retrieved on December 20, 2021 fromhttps://www.ques10.com/p/23381/what-are-the-advantages-and-disadvantages-of-finit/

Radulj, D. (2010). *Assessing the hydraulic transient performance of water and wastewater systems using field and numerical modelling data*. (Master of applied science thesis, University of Toronto). Retrieved on October 10, 2019 from https://tspace.library.utoronto.ca/bitstream/1807/24625/6/Radulj_thesis.pdf

Rajput, R. K. (2013). *Fluid mechanics and hydraulic machines*. Retrieved on December 26, 2021 fromwww.schandpublishing.com/books/tech-professional/mechanical-engineering/a-textbook-fluid-mechanics-hydraulic-machines/9789385401374/

Rathore, V., Ahmad, Z., & Kashyap, D. (2015). Modeling of transient flow in pipes with dynamic friction modelling of transient flow in pipes with dynamic friction. *20th International Conference on Hydraulics, Water Resources and River Engineering, Roorkee, Indi*. Retrieved on December 26, 2021 from https://www.researchgate.net/publication/317340890

Rezaei, H., Ryan, B., & Stoianov, I. (2015). Pipe failure analysis and impact of dynamic hydraulic conditions in water supply networks. *Procedia Engineering*, *119*, 253–262. doi.org/10.1016/j.proeng.2015.08.883

Rikstad, L. (2016). *Design of a test rig for investigations of flow transient*, (Masters thesis, Norwegian University of Science and Technology. Retrieved on December 20, 2019 from http://hdl.handle.net/11250/2402302

Rodriguez, G., & Pavel, B. (2016). A rational methodology for detailed pipeline transient hydraulic analysis. *Proceedings of the 2012, 9th International Pipeline Conference*, 1–8. Retrieved on October 10, 2020 fromhttp://proceedings.asmedigitalcollection.asme.org/

Rukthong, W., Piumsomboon, P., Weerapakkaroon, W., & Chalermsinsuwan, B. (2016). Computational fluid dynamics simulation of a crude oil transport pipeline : effect of crude oil properties. *Engineering Journal*, *20*(3), 145–154. doi.org/10.4186/ej.2016.20.3.145

Salmanzadeh, M. (2013). Numerical method for modeling transient flow in distribution systems. *International Journal of Computer Science and Network Security*, *13*(1), 72–78.

Samanody, M. El, & Noaman, A. S. (2017). Design and study of floating roofs for oil storage tanks. *Mechanics and Mechanical Engineering*, *21*(1), 117–136.

Sani, D. A., Shahabi, H., Ahmad, B. A., Mirmokrigharehveran, S., & Ahmad, B. Bin. (2016). Application of geographic information system technology in controlling pipeline vandalism of oil and gas industry. *Research Journal of Information Technology*, *8*(1–2), 39–46. doi.org/10.3923/rjit.2016.39.46

Satterfield, Z. (2013). Reading centrifugal pump curves. *National Environmental Services Centre*, *12*(1), 2–5.

Shani, T., & Gupta, T. (2017). Hydraulic transient flow analysis using MOC method. *International Journal of Innovative Research in Science, Engineering and Technology*, *6*(7), 14812–14827. doi.org/10.15680/IJIRSET.2017.0607323

Simão, M., Mora-rodriguez, J., & Ramos, H. M. (2015). Mechanical interaction in pressurized pipe systems: experiments and numerical models. *Water*, *7*, 6321–6350. doi.org/10.3390/w7116321

Simão, M., Mora, J., & Ramos, H. M. (2014). Dynamic behaviour of a pipe system under unsteady flow and structure vibration. *V Conferência Nacional de Mecânica Dos Fluidos, Termodinâmica E Energia MEFTE 2014, 11–12 Setembro 2014, Porto, Portugal*, 11–12. Corpus ID: 42295990

Simpson, A. R., & Wu, Z. Y. (1997). Computer modelling of hydraulic transients in pipe networks and the associated design criteria. *International Congress on Modelling and Simulation*, Modelling and Simulation Society of Australia, Hobart, Tasmania, Australia. Retrieved on March 21, 2020 from https://www.researchgate.net/publication/256097818

Singh, B. P., Mehta, H. C., Mishra, S. S., Gupta, A. K., Kanal, P. ., Vijh, L. K., Bhatli, V. K., Bhutda, R. K., Chakraborty, U. K., Jagdish, V., Thakkar, P., Rao, N., Gupta, D., Nandi, K. C., Agrawal, R., Mishra, A., & Adhikari, D. K. (2012). *Storage and handling of petroleum products at depots and terminals* (Vol. 1). Retrieved on December 26, 2021 from https://pdfslide.net/documents/storage-handling-of-petroleum-products-at-depots-and-terminals.html

Smith, M. (n. d.). Useful information on pipe velocity. Retrieved on December 18, 2021 fromwww.michael-smith-engineers.co.uk/resources/useful-info/pipe-velocity

Sousa, C. A., & Romero, O. J. (2017). Influence of oil leakage in the pressure and flow rate behaviors in pipeline. *Latin American Journal of Energy Research*, *4*(1), 17–29. doi.org/10.21712/lajer.2017.v4.n1.p17-29

Starczewska, D., Collins, R., & Boxall, J. (2016). Occurrence of transients in water distribution networks. *13th Computer Control for Water Industry Conference, 119*, 1473–1482. doi.org/10.1016/j.proeng.2016.01.001

Stewart, M. (2016). Piping system components. In *surface production operations*(1st ed., Issue 3, pp. 193–300). doi.org/10.1016/B978-0-12-814653-8.00002-3

Subani, N., & Amin, N. (2015). Analysis of water hammer with different closing valve laws on transient flow of hydrogen-natural gas mixture. *Hindawi Publishing Corporation, Abstract and Applied Analysis*, doi.org/10.1155/2015/510675

Sutton, I. (2017). Gate valves. in *plant design and operations* (Second Edi, pp. 165–195). Gulf Professional Publishing. doi.org/10.1016/s1369-7021(02)01271-3

Tukker, M. (2012). WANDA validation report, Deltares, Delft Hydraulics Project. Retrieved on December 19, 2021 from http:///Users/User/Downloads/Wanda%20Validation%20report% 202012.pdf

TotalEnergies (n. d.). Fuel for petrol engines. Retrieved on December 17, 2021 fromhttps://www.total.com.ng/fuels-petrol-engines

Twyman, J. (2018). *Water hammer in a pipe network due to a fast valve closure.* Revista Ingeniería de Construcción *33*, 193–200. Rerrieved on March 26, 2021 from https://scielo.conicyt.cl/pdf/ric/v33n2/en_0718-5073-ric-33-02-00193.pdf

Tycoon (n. d). Piping solution: API underground piping. Retrieved on December 17, 2021 from https://www.oilandgaspipingmaterials.com/

Urbanowicz, K. (2017). Modern modelling of water hammer. *Polish Maritime Research*, *24*(3), 68–77.Doi: 10.1515/pomr-2017-0091

Victor, T. B., & Shi-yi, Z. (2015). A New approach in pressure transient analysis part i : improved diagnosis of flow regimes in oil and gas wells. *Journal of Petroleum & Environmental Biotechnology*, *6*(5), 1–17. doi.org/10.4172/2157-7463

Vtorushinaa, A. N., Anishchenko, Y. V., & Nikonova, E. D. (2017). Risk assessment of oil pipeline accidents in special climatic conditions. *all-russian research-to-practice conference "ecology and safety in the technosphere" IOP Conf. Series: Earth and Environmental Science*, *66*, 1–8, doi.org/10.1088/1755-1315/

Waltrich, P. J., Hughes, R. Tyagi, M., Kam, S., Williams, W., Cavalcanti de Sousa, P., Zulqarnain, M., Atheus, W.L., & Capovilla, M.S. (2016) Experimental Investigation of Two-Phase Flows in Large-Diameter Pipes and Evaluation of Flow Models Applied to Worst-Case-Discharge Calculations. Retrieved on December 19, 2021 from https://www.boem.gov/interim-report-lsu

Wan, W., Zhang, B., & Chen, X. (2018). Investigation on water hammer control of centrifugal pumps in water supply pipeline systems, Energies, *12*(108). doi:10.3390/en12010108

WANDA 4.2 (2013) User Manual: Deltares (the former WL | Delft Hydraulics), Delft, The Netherlands. Retrieved on December 20, 2021 fromhttps://www.deltares.nl/en/software/wanda/

Wang, R., Wang, Z., Wang, X., Yang, H., & Sun, J. (2014). Water hammer assessment techniques for water distribution systems. *Procedia Engineering*, *70*, 1717–1725,

/doi.org/10.1016/j.proeng.2014.02.189

Wéber, R., & Hős, C. (2018). Experimental and numerical analysis of hydraulic transients in the presence of air valve. Periodica Polytechnica Mechanical Engineering, 62(1), 1–9., doi.org/10.3311/PPme.10336

Wood, S. L. (2011). *Modeling of pipeline transients : modified method of characteristics*.(Master of science thesis, Florida International University) https://doi.org/10.25148/etd.FI11080807

Woodford, C. (2020). *Valves*. Retrieved on December 20, 2021 from https://www.explainthatstuff.com/valves.html

Yang, B., Deng, J., Liu, K., & Ye, F. (2017). Theory analysis and cfd simulation of the pressure wave generator. *Chemical Engineering Transaction*, *61*, 481–486. https://doi.org/10.3303/CET1761078

Yin, C., & Mckay, A. (2018). Introduction to modeling and simulation techniques. *The 8th International Symposium on Computational Intelligence and Industrial Applications*, 1–7. Retrieved on October 10, 2021 from https://eprints.whiterose.ac.uk/135646/

Yousif, S. A., & Kalaf, A. N. (2017). Experimental investigation of the dynamics of laboratory simple surge tank. *Basrah Journal for Engineering Sciences*, *17*(2), 38–42.

Zhang, Z. (2016). Transient flows in a pipe system with pump shut- down and the simultaneous closing of a spherical valve. *28th Symposium on Hydraulic Machinery and Systems Conference Series: Earth and Environmental Science*, *49*, 1–11. doi.org/10.1088/1755-1315/49/5/052001

Zhu, J., & Zhang, X.H. (n. d.). A case study of time step validation strategy and convergence method for oscillation numerical simulation in a heat transfer process. Retrieved on December 26, 2021 from https://www.sci-en-tech.co/ICCM2016 /PDFs/1402-6192-1-PB.pdf